AD-A045 999 ARMY ENGINEER WATERWAYS EXPERIMENT STATION VICKSBURG MISS F/G 19/4
EFFECTS OF INSTRUMENT CANISTER PLACEMENT CONDITIONS ON GROUND S--ETC(U)
SEP 77 J K INGRAM, M B FORD

UNCLASSIFIED WES-TR-N-77-5 NL

1 OF 2
AD
A045999

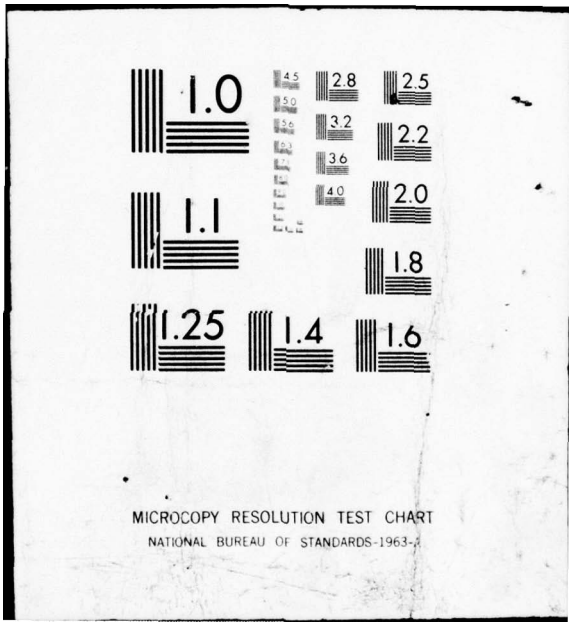
1.0
1.1
1.25
1.4
1.6
1.8
2.0
2.2
2.5
2.8
3.2
3.6
4.0
4.5
5.0
5.6
MICROCOPY RESOLUTION TEST CHART
NATIONAL BUREAU OF STANDARDS-1963-A

WES TR N-77-5

EFFECTS OF INSTRUMENT CANISTER PLACEMENT CONDITIONS ON GROUND SHOCK MEASUREMENTS

Weapons Effects Laboratory
U. S. Army Engineer Waterways Experiment Station
P. O. Box 631
Vicksburg, Mississippi 39180

September 1977

Final Report

THIS WORK SPONSORED BY THE DEFENSE NUCLEAR AGENCY UNDER DNA SUBTASK L11CAXSX352, WORK UNIT 50.

Prepared for

Director
DEFENSE NUCLEAR AGENCY
Washington, D. C. 20305

Unclassified

SECURITY CLASSIFICATION OF THIS PAGE (When Data Entered)

REPORT DOCUMENTATION PAGE

READ INSTRUCTIONS BEFORE COMPLETING FORM

1. REPORT NUMBER

2. GOVT ACCESSION NO.

3. RECIPIENT'S CATALOG NUMBER

4. TITLE (and Subtitle)

EFFECTS OF INSTRUMENT CANISTER PLACEMENT CONDITIONS ON GROUND SHOCK MEASUREMENTS.

5. TYPE OF REPORT & PERIOD COVERED

Final report. 1973-1975,

6. PERFORMING ORG. REPORT NUMBER

Technical Report N-77-5

7. AUTHOR(s)

J. K. Ingram
M. B. Ford

8. CONTRACT OR GRANT NUMBER(s)

9. PERFORMING ORGANIZATION NAME AND ADDRESS

U. S. Army Engineer Waterways Experiment Station
Weapons Effects Laboratory
P. O. Box 631, Vicksburg, Mississippi 39180

10. PROGRAM ELEMENT, PROJECT, TASK AREA & WORK UNIT NUMBERS

See Block 18

11. CONTROLLING OFFICE NAME AND ADDRESS

Defense Nuclear Agency
Washington, D. C. 20305

12. REPORT DATE

September 1977

13. NUMBER OF PAGES

99

14. MONITORING AGENCY NAME & ADDRESS (if different from Controlling Office)

142p.

15. SECURITY CLASS. (of this report)

Unclassified

15a. DECLASSIFICATION/DOWNGRADING SCHEDULE

16. DISTRIBUTION STATEMENT (of this Report)

Approved for public release; distribution unlimited.

WES-TR-N-77-5

17. DISTRIBUTION STATEMENT (of the abstract entered in Block 20, if different from Report)

18. SUPPLEMENTARY NOTES

This research was sponsored by the Defense Nuclear Agency under Subtask L11CAXSX352, "Development of Field Instrumentation," Work Unit 50, "Canister-Backfill-Medium Interaction."

19. KEY WORDS (Continue on reverse side if necessary and identify by block number)

Backfills
Ground shock measurement
Measuring instruments
Wave propagation

20. ABSTRACT (Continue on reverse side if necessary and identify by block number)

A combined analytical/experimental study entitled "Canister-Backfill-Medium Interaction" (CBMI) was conducted to investigate the effects of backfilling procedures on the response of ground motion instruments located in instrumentation boreholes during wave propagation experiments. The experimental portion was conducted by the U. S. Army Engineer Waterways Experiment Station (WES) and is reported herein. A companion analytical study was

(Continued)

over

DD FORM 1 JAN 73 1473 EDITION OF 1 NOV 65 IS OBSOLETE

Unclassified

SECURITY CLASSIFICATION OF THIS PAGE (When Data Entered)

038100

LB

20. ABSTRACT (Continued).

conducted by Agbabian Associates (AA), El Segundo, California. The analytical study attempted to calculate the measured motion-time histories by use of input load functions and material properties data. Results of the analytical effort are discussed in a separate report published by AA.

The CBMI study addressed only one-dimensional wave propagation (end-loaded specimens), which simulated only the superseismic region for explosions detonated on a half-space (field test condition).

All wave propagation tests were conducted in the WES Small Blast Load Generator (SBLG), a 4-foot-diameter stacked-ring loading device. The test chamber was 6 feet high for all tests. The interior of the device was filled with soillike grout representing a free-field material. Motion and stress instruments were installed at several depths in the material during placement. A number of specimens were constructed and a control test was conducted on two specimens without boreholes. A 5-inch-diameter by 5.5-foot-deep axial borehole located in the center of the free-field material was then instrumented at depths corresponding to those of instruments placed in the free field, then backfilled with select soillike grout. An effort was made to maintain constant material properties for each free-field specimen constructed. The material strength (constrained secant modulus) of the borehole filler was varied from 0.05 to 2 times that of the free field. Dynamic airblast pressures of approximately 250 psi were applied to the top of each test specimen.

Earlier tests in the SBLG involving a study of the effects of instrument borehole backfilling procedures on stress measurements were used as a point of departure for the CBMI study.

Results from the CBMI study are summarized as follows:

1. A strong bond between the instrument canister and the free field assures vertical particle velocity response that is essentially insensitive to large impedance mismatches between the borehole filler "soil" and the free field; vertical displacement, being a derived quantity, will also be within reasonable bounds.

2. Good vertical motion response can be expected over a range of borehole to free-field stiffness ratios between 0.05 and 1.

3. The use of a very stiff borehole filler in soils is not recommended. It is desirable to use borehole backfill materials of equal or slightly less stiffness than the free-field material when measuring accelerations. A stiffer backfill will allow the shock wave in the borehole to outrun the free-field wave due to the faster propagation velocity of the stiffer material, which can adversely affect the acceleration response.

4. Stress measurements are far more sensitive to material property mismatches than are particle motion measurements. Hence, not only must the impedance characteristics of the backfill and free-field materials be closely matched, but intimate contact must be assured between the sensing surfaces of the stress gage and the embedment material.

PREFACE

This study was conducted by the Weapons Effects Laboratory (WEL) of the U. S. Army Engineer Waterways Experiment Station (WES) under the sponsorship of the Defense Nuclear Agency (DNA), Subtask L11CAXSX352, "Development of Field Instrumentation," Work Unit 50, "Canister-Backfill-Medium Interaction." This study was conducted during the period 1973 through 1975.

A companion analytical study was conducted by Agbabian Associates (AA), El Segundo, California, under DNA Contract No. DNA001-74-C-0100-P00001. The analytical study attempted to calculate the measured motion-time histories by use of input load functions and material properties data. Results of the analytical effort are discussed in a separate report published by AA.

Principal investigators were Messrs. J. G. Wallace, formerly of Phenomenology and Effects Division (PED), WEL, during the planning and test phases of the study, and J. K. Ingram, PED, during the analysis and reporting phases. Mr. M. B. Ford, PED, was the associate investigator for the entire study.

Special recognition is extended to Dr. J. S. Zelasko and Dr. J. E. Windham, Soils and Pavements Laboratory, WES, for development and evaluation of the artificial soils used throughout this study; Messrs. W. M. Gay, PED, and C. M. Wright, formerly of PED, who constructed the test specimens and installed the gages; Mr. J. T. Brogan and Mrs. D. W. McAlpin, PED, who processed all experimental test data; and Messrs. N. J. Lavecchia, Jr., F. P. Leake, E. L. Sadler, and S. Bell, Instrumentation Services Division, WES, for instrumentation calibration and assembly and data acquisition.

The study was conducted under the general supervision of Messrs. W. J. Flathau, Chief, WEL; L. F. Ingram, Chief, PED; and J. D. Day, Test Instrumentation Development Program Manager.

COL G. H. Hilt, CE, and COL J. L. Cannon, CE, were Directors of WES during the conduct of this study and the preparation and publication of this report. Mr. F. R. Brown was Technical Director.

CONTENTS

CONVERSION FACTORS, U. S. CUSTOMARY TO METRIC (SI) UNITS OF MEASUREMENT

U. S. customary units of measurement used in this report can be converted to metric (SI) units as follows:

Multiply	By	To Obtain
inches	2.54	centimetres
feet	0.3048	metres
pounds (mass)	0.4535924	kilograms
tons (2000 lb)	907.1847	kilograms
pounds (mass) per cubic foot	16.01846	kilograms per cubic metre
pounds (force) per square inch	6.894757	kilopascals
kips per square inch	6.894757	megapascals
feet per second	0.3048	metres per second
degrees (angle)	0.01745329	radians

EFFECTS OF INSTRUMENT CANISTER PLACEMENT CONDITIONS
ON GROUND SHOCK MEASUREMENTS

CHAPTER 1

INTRODUCTION

1.1 BACKGROUND

During the past two decades, numerous high-explosive field tests have been conducted. Each of these tests was usually instrumented with a large number of motion and stress gages to record transient ground shock. Generally, because of economic reasons, several gages were placed in a borehole. Because no standards for placement of these instruments existed, techniques used to couple these gages to the ground usually differed between tests.

Prior to 1968, little research had been done to determine the adequacy of methods used for coupling ground shock instruments to the local free field, i.e., the qualitative effects of material property (compressibility and strength) mismatches between instrument borehole backfill and the in situ material.

A laboratory experimental study was conducted at the U. S. Army Engineer Waterways Experiment Station (WES) in 1968-70 to investigate instrument placement effects on dynamic stress measurements in soils. This study is described briefly in Appendix A and in more detail in Reference 1. In summary, peak stress was found to be highly sensitive to placement conditions, i.e., impedance matching of the instrument borehole backfill material to the free-field materials is critical for meaningful stress measurements. For even moderate impedance mismatches, strain discontinuities (and consequently stress redistribution) will occur across the borehole/free-field interfaces. The technique developed as a result of this study (and out of necessity for field stress gage placement) was to place the instruments in small boreholes and try to match the backfill properties to those of the free field.

1.2 OBJECTIVES AND BACKGROUND FOR PRESENT STUDY

1.2.1 Experimental

The Canister-Backfill-Medium Interaction (CBMI) study was designed to investigate experimentally the relative effects of earth and backfill properties on the response of ground motion instruments. The degree of mismatch between backfill and free field was intended to span a range of field conditions.

Out of economic considerations and a desire for material uniformity and reproducibility, "artificial soils" (grouts) were used for the CBMI study. Laboratory stress-strain and strength tests were conducted on the various grouts to provide a basis for quantitatively defining material mismatches as well as to support the calculational analysis described in Section 1.2.2. Laboratory analysis of the artificial soils has pointed out several undesirable characteristics of these materials (see Section B.5.5).

1.2.2 Analytical

A calculational study performed by Agbabian Associates (AA), El Segundo, California, has paralleled and supported the CBMI experimental program. The results of the AA study, which includes comparison of calculated motions and stresses with the directly measured WES data, are documented in References 2 and 3. Only the WES experimental phase of the CBMI study is discussed in this report.

1.3 APPROACH

The Small Blast Load Generator (SBLG), a 4-foot-diameter,[1] variable-height, end-loading test chamber, was used for the CBMI experiments (Reference 4). All tests were dynamic. A single explosive-induced air overpressure level was used (nominally 250 psi). Five

[1] A table of factors for converting U. S. customary units of measurement to metric (SI) units is found on page 5.

gage placement conditions (free-field/borehole configurations) were evaluated:

1. Uniform material specimen, well instrumented; no borehole
2. Property-matching borehole filler
3. Soft uniform borehole (soft relative to free-field material)
4. Soft borehole, but instrument canisters locally locked to free-field material with hard grout
5. Stiff uniform borehole

1.4 SCOPE

This report deals primarily with the initial loading pulse because of undesirable and complicated wave interactions due to boundary conditions imposed by the loading device. Material stiffness (i.e., constrained secant modulus), rather than strength, was selected as the primary material property parameter to characterize the various artificial soils because the SBLG experiments are primarily one-dimensional wave propagation tests. A range of borehole filler material to free-field stiffness ratios from approximately 0.05 to 2 were studied. Particle velocity was the primary measurement standard, although both acceleration and velocity were measured in certain tests. Stresses were measured only in the free field.

1.5 BACKGROUND STUDY

An earlier SBLG study, referred to herein as the background study (Appendix A and Reference 1), involved the investigation of five stress gage placement conditions ranging from a uniform remolded clay as the specimen was constructed layer by layer through the use of a clay-matching artificial soil borehole to a sand-filled borehole placed in a remolded clay free-field specimen. One test involved using a soft artificial soil material to backfill a borehole in a stiff artificial soil free-field specimen. The primary objective of the background study was to quantify the effects of extremes in stress gage placement; a subsidiary objective was to develop a satisfactory artificial soil for potential use as a field borehole filler in clayey type soils. The

desirability of artificial soil for use in field gage placement is described by Zelasko and Perry[3] and discussed in Appendix D of this report.

1.6 CBMI TESTS

The CBMI study was intended to quantify the effects of placement conditions on motion instrument response, with borehole material to free-field material stiffness ratios ranging from about 0.05 to 2.0. For this study, stiffness is defined as the constrained secant modulus of a given material taken at the 20 percent overstress level, i.e., approximately 300 psi (the dynamic test loadings were nominally 250 psi; hence, all secant moduli were taken at approximately 300 psi).

The nature of the SBLG test facility (References 4 and 5) is such that only a very narrow portion of a field loading environment could be modeled, i.e., all boreholes were end-loaded at 0-degree impingement angle, a situation approximating the near-surface, close-in, super-seismic airblast regime (Figure 1.1 and Reference 6). Because the specimens were end-loaded, the maximum effect of the backfill (borehole) material was obtained. In actual field practice, only a small number of gages would experience this loading condition; the bulk of the gages would be in regions where oblique shock wave impingements occurred (Figure 1.1). The SBLG has several other limitations: (1) the effects of boundary conditions, e.g., complicated reflections from the sidewalls and base and dynamic sidewall friction effect, have not been completely resolved; (2) the experiment is not perfectly free of chamber venting time restrictions (a quasi-static gas loading condition is established shortly after the initial air pressure peak occurs), which does not allow for formation of the relief wave associated with explosion-induced airblast in the field; and (3) only shallow depth effects can be studied.

1.7 TEST FACILITIES

Fourteen CBMI tests were conducted using five basic free-field

---

[2] J. S. Zelasko and E. B. Perry, unpublished data.

specimens. For each specimen, the SBLG was equipped with a sidewall-friction-reducing greased rubber liner (References 4 and 5), Figure 1.2.

Dynamic surface loads were applied axially to the test specimens by detonating Primacord explosive in a special top firing chamber. This blast load was transmitted to the top of the test specimen through a neoprene membrane that prevented the explosive gases from entering the specimen and generating undesired pore pressures.

1.8 DATA ACQUISITION

Acceleration, particle velocity, and stress gages were used to sense the transient phenomena. Electronic recordings were then manipulated to obtain computer-generated acceleration-, velocity-, displacement-, and stress-time plots. All gage output signals were conditioned, amplified, and calibrated through direct-current operational amplifiers, and dually recorded on galvanometer oscillographs and FM magnetic tapes. The oscillograms were used for "quick-look" data assessments while the tapes were converted to digital format for processing through the computer.

1.9 LABORATORY MATERIAL PROPERTY TESTING SUPPORT

Various static and dynamic laboratory material property tests were conducted on most of the artificial soil materials employed for the CBMI study. These tests were performed in the WES Soil Dynamics Division (SDD) Test Facility. Constitutive property analyses were performed subsequently for selected experiments in order to develop appropriate inputs for AA's calculational analyses; these efforts are summarized in Appendix D.

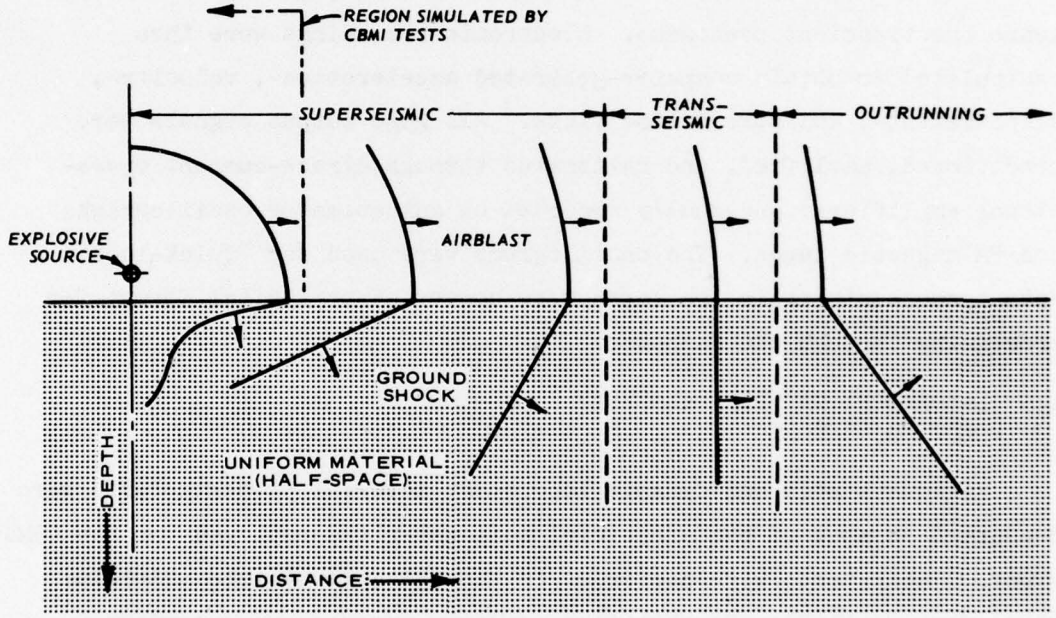

Figure 1.1 Idealized airblast-induced ground shock profile.

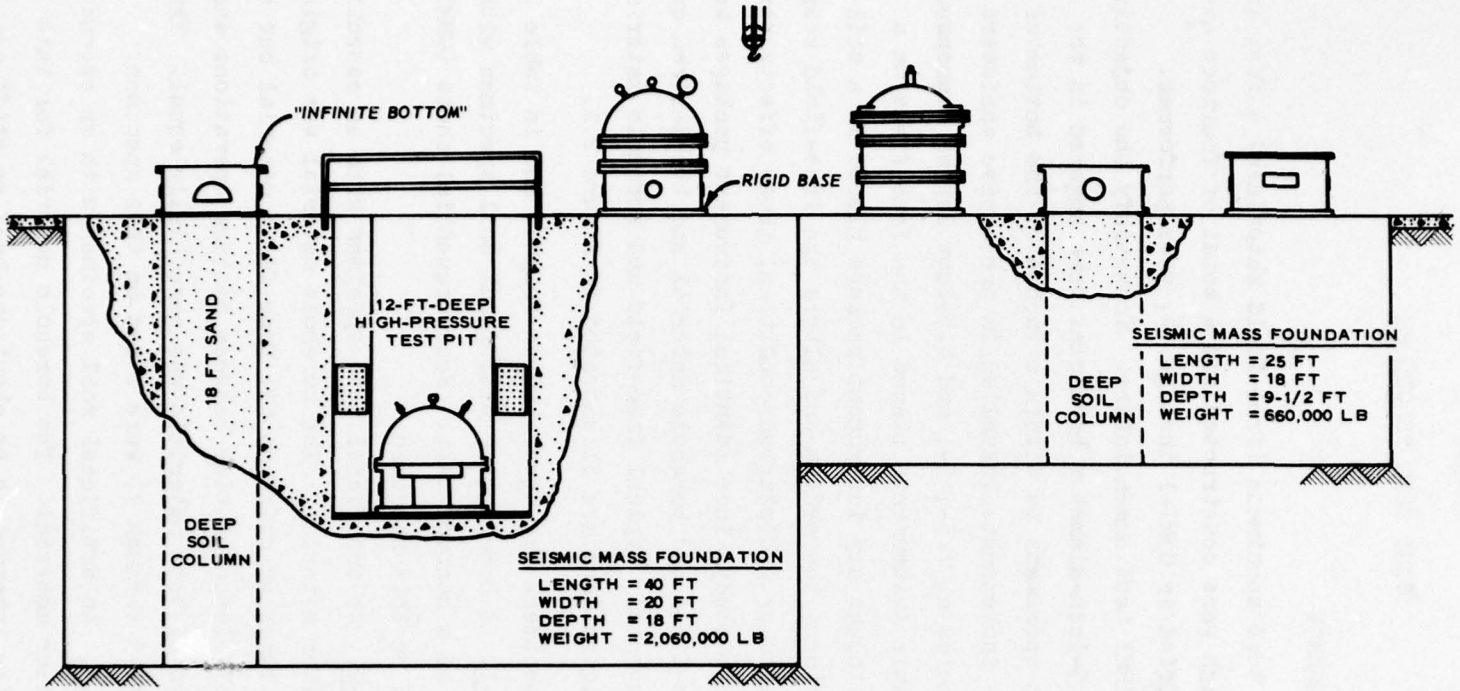

CHARACTERISTICS

1. PEAK DYNAMIC PRESSURE: VARIABLE FROM 10 TO 250 PSI
2. MAXIMUM STATIC PRESSURE: 2000 PSI
3. PRESSURE RISE TIME: 2 TO 5 MSEC
4. DURATION OF PRESSURE: ≈1 SEC
5. INSIDE DIAMETER OF CHAMBER: 46-3/4 IN
6. DEPTH OF SAMPLE: 2 IN TO 38 FT

Figure 1.2 SBLG Test Facility.

CHAPTER 2

CBMI TEST PROCEDURE

2.1 EXPERIMENTAL SEQUENCE

Five individual test specimens (free-field materials) 4 feet in diameter by 6 feet high were constructed and a total of fourteen explosive tests, identified as CBMI-1 through 14, were performed. Table 2.1 lists the CBMI test nomenclature. To satisfy the objectives of the CBMI program, 5-inch-diameter boreholes were augered in the center of the various specimens to within 6 inches of the bottom of the specimen. Motion instruments installed in protective canisters were placed in these boreholes at 1.5-, 3-, and 4.5-foot depths commensurate with those of comparable instruments placed in the free field on a radius of 1 foot. Although any instrument package placed in a soil or soillike material perturbs the medium and alters the free-field response from that of the in situ or undisturbed condition, these effects were not considered for this study since identical instrument packages were used in both the free-field and borehole material and the desired quantity was relative response. Typical free-field and borehole material instrumentation configurations are illustrated in Figure 2.1.

The five test specimens are described as follows and in Table 2.1:

1. Specimen P2-1. A homogeneous artificial soil specimen without a borehole, intended as a control test. Four sequential shots (CBMI-1 through 4) were fired on this specimen.

2. Specimen P2-2. An artificial soil specimen with an essentially matching borehole filler material. The borehole material was originally intended to be about twice as stiff as the free-field material but because of a considerable lapse of time between casting operations and testing, the stiffness of both materials was essentially equal. Three sequential shots (CBMI-5 through 7) were fired on this specimen.

3. Specimen P2-3. An artificial soil specimen with an essentially matching borehole filler material. The borehole material for this specimen was originally intended to be about one-half as stiff as the

free-field material, but turned out to be approximately equal in stiffness. Two sequential shots (CBMI-8 through 9) were fired on this specimen.

4. Specimen P2-4. A uniform specimen without a borehole intended as a repeat of the control test on Specimen P2-1, deemed necessary because of internal inconsistencies in the P2-1 data (CBMI-1 through 4). Two sequential shots (CBMI-10 and 11) were fired on this specimen.

5. Specimen P2-5. The materials used for this specimen were similar to those used for Specimen P2-4. Three different borehole material configurations were evaluated using this specimen. The borehole filler materials were removed after each test and replaced with the next filler material configuration (CBMI-12 through 14). In CBMI-12, a soft uniform borehole filler material was used to simulate a borehole/free-field stiffness ratio of 0.05. The configuration of CBMI-13 was the same as CBMI-12 except that a small amount of hard, expansive grout (designated "canister-locking" grout) was used to fill the annulus immediately surrounding each borehole instrument canister. In CBMI-14, a stiff uniform borehole filler material was used to simulate a borehole/free-field stiffness ratio of about 2.

All test specimens were surface-loaded through a neoprene membrane by detonating Primacord in the firing chamber above the artificial soil. Input airblast pressures were nominally 250 psi with rise times on the order of 2 ms.

All specimens except specimens P2-2 and P2-3 were prepared over the rigid concrete base. Specimens P2-2 and P2-3 were placed over the "infinite" or deep sand column base. Internal inconsistencies were observed in the instrument data from Shots 2 through 4 (specimen P2-1), which were initially attributed to early reflection phenomena from the rigid base. Consequently, the second and third specimens (P2-2 and P2-3) were constructed over an 18-foot-deep sand column in hopes of providing a longer delay between the incident and assumed reflected loading pulses. Subsequent analysis of the data from the earlier tests revealed improper instrument installation and signal cable effects rather than wave

reflection from the rigid base to have caused the basic problems in the tests in question (Shots 2 through 4).

No real advantages were observed by using the sand column base. However, a number of offsetting disadvantages became apparent. To assure a repeatable environment, the sand had to be excavated and replaced for each shot. Slight moisture entrainment in the sand caused by moisture bleeding from surrounding concrete and the overlying uncured grout created a reflection interface just below the contact of the grout and sand. Thus, the reflection phenomenon was not significantly retarded compared with that resulting from the rigid concrete base. Moisture entrainment, therefore, must be minimized by lining the entire length of the chamber with a moisture barrier, which must be inspected after every test. Sidewall friction relief, which must be provided, at the same time allowed the long column of relatively compressible material to displace vertically, resulting in excessive surface displacements. Since the specimen was end-loaded through a membrane, the large surface void had to be refilled with new grout for subsequent shots on the same specimen, creating an additional interface near the surface. (The material stiffnesses were different because of the relative cure time of the grout and variances between grout batches.) On analysis of the cost/benefit trade-offs, it was decided to complete the test series using the rigid concrete base.

2.2 INSTRUMENTATION

In addition to the velocity gages, the primary sensors used in this study, accelerometers were installed in the boreholes on Shots CBMI-5, -12, -13, and -14. A limited number of stress gages were placed in the free field to measure the transmitted load distribution with depth. Stresses were not measured in the various CBMI boreholes. All displacement data were derived by digital integration of the velocity signals. Additional discussion of instrumentation is presented in Appendix C.

TABLE 2.1 CBMI TEST PROGRAM

Note: All CBMI tests involved dynamic step-type loads to approximately 250 psi. H = height of test specimen, feet.

Specimen	CBMI Shot No.	Free-Field/ Borehole Materials	$\frac{B_{bh}}{B_{ff}}$[a]		$\frac{\rho_{bh}}{\rho_{ff}}$[b]		Type of Bond Between Borehole and Free Field	Comments
			Intended	Actual	Intended	Actual		
P2-1	1[c]	Homogeneous grout	1	1	1	1	Strong	Control Test 1 conducted in SBLG (H = 6 ft) with rigid base
	2							
	3							
	4							
P2-2	5[c]	Grout/matching grout	2	1	1	1	Strong	Conducted in SBLG (H = 6 ft) with deep sand column base
	6							
	7							
P2-3	8	Grout/matching grout	0.5	1	1	1	Moderate	Conducted in SBLG (H = 6 ft) with deep sand column base
	9							
P2-4	10[c]	Homogeneous grout	1	1	1	1	Strong	Repeat of Control Test 1, Specimen P2-1, different grout
	11							
P2-5	12[c]	Grout/soft grout	0.5	0.05	1	0.5	Weak	Conducted in SBLG with rigid base (H = 6 ft)

(Continued)

[a] Stiffness ratio, borehole (bh) to free field (ff). B = constrained secant modulus to 300 psi.
[b] Density ratio, borehole (bh) to free field (ff).
[c] One-dimensional calculations were performed by AA on these designated tests.

TABLE 2.1 (CONCLUDED)

Specimen	CBMI Shot No.	Free-Field/ Borehole Materials	$\frac{B_{bh}}{B_{ff}}$ Intended	$\frac{B_{bh}}{B_{ff}}$ Actual	$\frac{\rho_{bh}}{\rho_{ff}}$ Intended	$\frac{\rho_{bh}}{\rho_{ff}}$ Actual	Type of Bond Between Borehole and Free Field	Comments
P2-5 (Cont'd)	13[c]	Grout/soft grout	0.5	0.05	1	0.5	Strong	Conducted in SBLG (H = 6 ft) with rigid base, same free field as CBMI-12 but borehole material replaced with same type filler as CBMI-12 and canisters locked to free field with very stiff expansive grout
	14[c]	Grout/stiff grout	2	2	1	1	Strong	Conducted in SBLG (H = 6 ft) with rigid base, same free field as CBMI-12 and -13, but borehole materials replaced with uniform stiff expansive grout

[c] One-dimensional calculations were performed by AA on these designated tests.

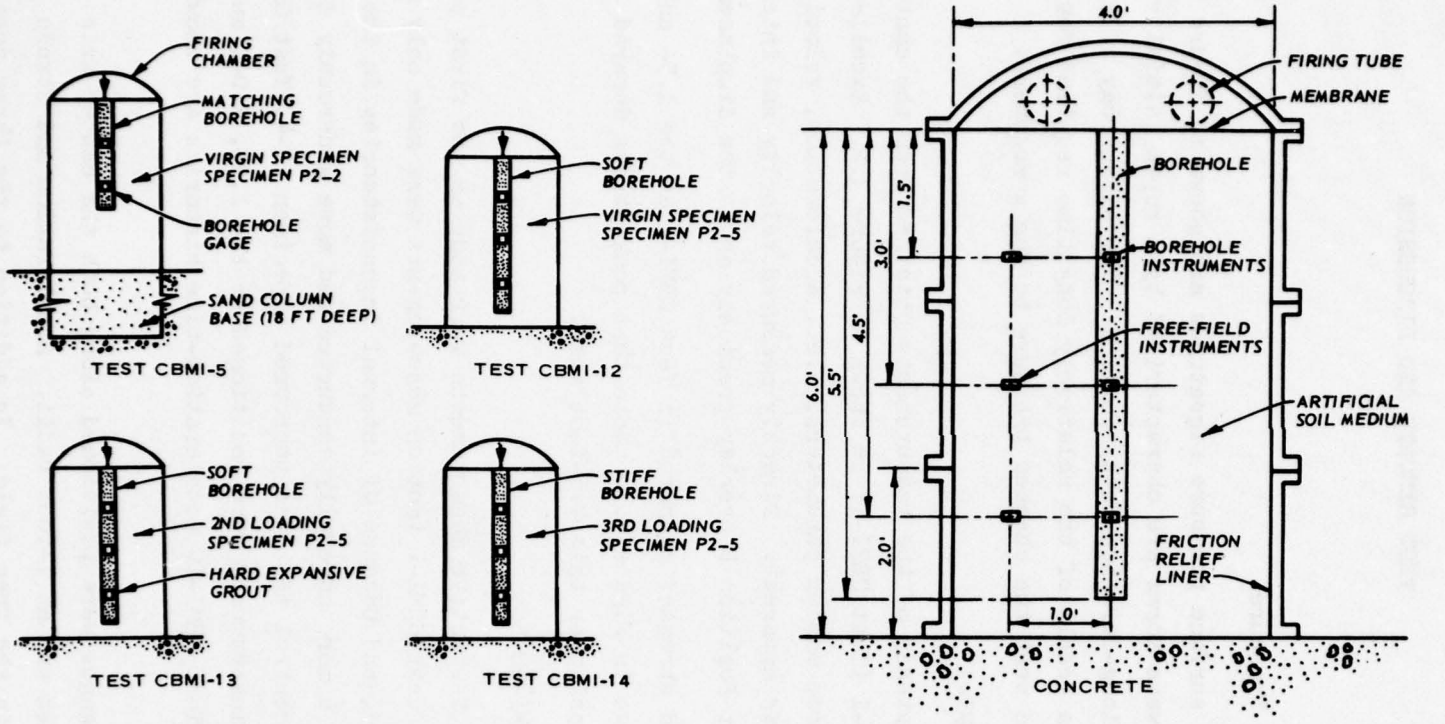

a. BOREHOLE TEST CONDITIONS

b. DYNAMIC TEST CHAMBER WITH TYPICAL SPECIMEN IN PLACE

Figure 2.1 Typical CBMI test conditions and typical test specimen section.

CHAPTER 3

TEST RESULTS AND DISCUSSION

3.1 RESULTS

3.1.1 Surface Pressure

Composite surface pressure signatures are shown in Figure 3.1. Surface input wave forms are characterized by a rapid initial rise time followed by a long-duration decay portion. The slow decay of the pressure pulse is a result of the relatively long time required for the blast valves to vent the chamber pressure to the atmosphere.

3.1.2 Test CBMI-1

The consistency of the measurements obtained from the control test on Specimen P2-1 (Test CBMI-1) is shown in Figure 3.2. Excellent agreement in all three motion parameters, i.e., acceleration, velocity, and displacement, is apparent. Directly measured velocity and integrated acceleration at Position B overlay precisely as do the displacements.

Free-field stresses measured in Test CBMI-1 at the 1.5- and 6-foot depths are shown in Figure 3.3. Note that peak stress decayed from 308 psi to 96 psi over this 4.5-foot span.

3.1.3 Test CBMI-10

Since too few active measurements were made on the first control test specimen, Test CBMI-1 (motion measurements were made only at the 1.5-foot depth), and because of internal inconsistencies in the data (Reference 3), a more carefully conducted and more generously instrumented repeat control test was performed (Specimen P2-4, Test CBMI-10). In this test, instruments were positioned at the 1.5-, 3.0-, and 4.5-foot depths. Test CBMI-10 acceleration-time histories are shown in Figure 3.4.

Velocity gages were positioned along both the center axis of the uniform specimen and at 1-foot radii. Acceleration and stress were measured only in the free field. In addition to the three depths

instrumented, stress gages were positioned at the top and bottom surfaces of the test specimen.

Comparison of measured velocities between gages placed along the center axis of the specimen and those positioned at 1-foot radii show an amplitude spread on the order of 20 percent (Figure 3.5). Higher amplitudes were recorded in the center of the specimen at the 3- and 4.5-foot depths; but at the 1.5-foot depth, the highest amplitude was measured at the 1-foot radius (free field). The apparent random order of these amplitude variations suggests a possible variance in uniformity of the specimen and perhaps nonideal gage placement.

CBMI-10 displacements (Figure 3.6) show the same trend as noted in the measured velocities.

Free-field stresses (Figure 3.7) show a relatively constant stress response at all depths. A steep wave front is observed at the 1.5-foot depth that gradually flattens with increasing depth. At the 6-foot depth, stress reflection off the rigid base of the test facility is apparent in the sharp front on the stress wave form.

3.1.4 Test CBMI-5

Measurements were taken only at two depths in Test CBMI-5, at 1.5 and 3.0 feet. This test involved a borehole backfill that essentially matched the surrounding free field. Test results indicate that excellent motion comparisons were noted between the borehole and the free field. Comparative accelerations, shown in Figure 3.8, agreed well in both amplitude and phase. Measured velocities were also identical (Figure 3.9), as were the displacements (Figure 3.10). Measured stress-time histories are displayed in Figure 3.11.

3.1.5 Test CBMI-12

The soft borehole filler material used in this test was extremely compressible ($\approx$ 50 percent air-filled porosity, Appendix B). During the test, the borehole plug compressed about 7 inches while the free-field material compressed only about 2 inches, allowing the loading

diaphragm (top membrane) to perforate and the explosive gases to vent into the borehole. Because of this difference in compressibility, the test results were drastically different from the others in the series; however, it is important that they be included in the discussion of the CBMI results to provide insight into a worst-case placement condition. The extreme compression effects experienced in the upper zone of the borehole are dramatically illustrated in the acceleration, velocity, and displacement wave forms. Borehole accelerations (Figure 3.12) are in relatively good agreement for the initial loading phase; however, some degree of dephasing is apparent between borehole and free-field acceleration wave forms, especially at late time. A characteristic negative (upward) acceleration spike immediately following the initial loading pulse is present in the borehole acceleration wave forms but is not observed in the free-field wave forms. A large secondary downward acceleration was recorded at 10 ms by the shallow (1.5-foot depth) borehole accelerometer; the amplitude of this pulse is some 20 times that in the free field and is the result of the firing chamber gages venting into the borehole.

Measured velocities are shown in Figure 3.13. Although the measured peak borehole velocity at the 1.5-foot depth was some four times greater than that in the free field, the gage faithfully followed the free-field response up to the time of venting ($\approx$ 10 ms), in agreement with the acceleration data. The deeper borehole gages show excellent correlation in spite of the unusual nature of the applied load, i.e. direct venting of the explosion gaseous byproducts only into the borehole causing a significant differential in pore pressure between the borehole and surrounding free-field material.

Displacements and stresses in Test CBMI-12 are shown in Figures 3.14 and 3.15, respectively.

Even though Test CBMI-5 presented an extreme condition, it is clear that significant adverse effects were present only at the shallow (1.5-foot depth) borehole gage position. Motion responses in the borehole and the free field at the 3.0- and 4.5-foot depths were consistent for all

three motion parameters evaluated. These observations imply that at sufficient depth in uniform material, borehole mismatch conditions may be of relatively minor importance to particle velocity measurements.

3.1.6 Test CBMI-13

Test CBMI-13 was a repeat shot on Specimen P2-5. The CBMI-12 borehole material was removed and replaced with fresh soft filler material having the same characteristics as those of the CBMI-12 filler. In a departure from the previous soft uniform borehole condition, however, the CBMI-13 borehole gages were strongly locked to the free-field matrix with a stiff expanding grout placed only in the annulus immediately surrounding each instrument canister. In addition, the 2-inch-wide free space across the top of the specimen, which resulted from Test CBMI-12, was filled with fresh free-field material.

Comparative wave forms are shown in Figures 3.16 through 3.19. Measured borehole acceleration pulse amplitudes and durations (Figure 3.16) were in good agreement with those in the free field at all depths. Borehole acceleration peaks were slightly higher than the free-field peaks at the 3.0- and 4.5-foot depths and slightly lower at the 1.5-foot depth. Measured borehole velocities (Figure 3.17) were in better agreement with the free field than were the accelerations (Figure 3.16). Velocity phasing was in excellent agreement at all placement depths; however, peak amplitudes were slightly lower at the two deepest positions in the borehole. In contrast, the borehole accelerations were slightly higher.

Excellent comparison was also observed for the displacements, as seen in Figure 3.18. No measurable compression was observed across the top of the specimen. Free-field stress wave forms measured in CBMI-13 are shown in Figure 3.19.

3.1.7 Test CBMI-14

Test CBMI-14 was a third loading of Specimen P2-5. The CBMI-13 borehole filler materials were removed and replaced with a material having a stiffness somewhat greater than twice that of the free-field matrix. (Even though Specimen P2-5 had stiffened, i.e. shock hardened,

from the repeated loadings, laboratory tests conducted on the borehole filler showed it to be sufficiently stiff to satisfy the requirement of a factor of 2 or greater of the test.)

Measured borehole accelerations in the stiff filler compared reasonably well with those in the free field (Figure 3.20). The characteristic negative (upward) acceleration spike immediately following the initial downward acceleration pulse observed in both CBMI-12 and CBMI-13 was also present in the CBMI-14 data, and was even more pronounced. A slight outrunning is noted in the borehole data.

Velocity wave forms are compared in Figure 3.21. Borehole velocities were in excellent agreement with those of the free field in both phasing and amplitude, but exhibited a slightly faster rise time (as did the accelerations). The shorter rise time in the borehole was expected because of its greater stiffness and consequent faster propagation velocity over that of the free-field material. A pronounced double peak was observed in the borehole velocity wave forms at all depths. This tendency was evident at the shallow free-field gage position but did not develop at the deeper locations. The early peak observed in the borehole appears to be an outrunning type of precursor while the second (trailing) peak appears to be associated with passage of the wave front in the free field.

Displacements are compared in Figure 3.22. Peak displacements were slightly higher at the 1.5- and 4.5-foot depths in the borehole. The free-field peak displacement was slightly higher at the middepth (3-foot) position.

Only the 1.5-foot-depth free-field stress gage remained active for this test. The recorded stress wave form is shown in Figure 3.23.

3.1.8 Motion Response Comparison, Tests CBMI-12, -13, and -14.

Motion responses at the 1.5-foot depth for Tests CBMI-12, -13, and -14 are compared in Figures 3.24 through 3.26. Free-field stresses at this depth are compared in Figure 3.27. Borehole acceleration, velocity,

and displacement faithfully tracked the free-field response in the early portion of the motion history at the shallow depth in Test CBMI-12 before the borehole material punched. Acceleration and velocity in the borehole again replicated the free field after about 34 ms (Figures 3.24 and 3.25).

The effect of the stiff borehole (CBMI-14), a noticeably faster arrival time, is evident in the bottom wave forms of Figures 3.24 through 3.26.

Free-field stresses at the shallow depth are quite similar for all three tests (CBMI-12, -13, and -14, Figure 3.27).

3.1.9 Peak Data

Peak accelerations from the sequential Tests CBMI-12, -13, and -14 are plotted versus depth in Figure 3.28. Data from all three tests show a consistent trend at the two deepest gage positions in both the free field and the borehole. A considerable spread in values is noted at the shallow depth where material properties effects are probably more influential on acceleration response. The initial peak acceleration in Test CBMI-12 compares favorably; however, the acceleration spike associated with the venting (punching) problem experienced in this test is at least 20 times higher than that of the associated free field.

A more meaningful way of displaying the relation between borehole and free field is to normalize measured borehole values to those of the free field for a given depth. Accelerations thus normalized are shown in Figure 3.28b. The ideal response is indicated by the vertical line at a ratio equal to one. Initial acceleration response at 1.5 feet for both soft boreholes falls below unity. The venting spike in Test CBMI-12 is 2.4 times the ideal response. Borehole responses were higher for all cases at the deeper gage position, averaging 23 percent greater than ideal.

Peak velocity and peak displacement are plotted versus depth in Figure 3.29. The effect of repetitive loading on virgin Specimen P2-5 is manifested as a progressive decrease in both peak particle velocity

and displacement along with a reduction in their attenuation rates with depth with each successive loading. In general, for a given input, the higher the material stiffness, the higher the pulse frequencies and the lower the associated particle velocity and displacement.

Borehole and free-field attenuation rates were similar for a given test condition. Test CBMI-12, with a soft borehole filler and gages not locked to the free field, displayed the worst displacement for the conditions evaluated. Figure 3.30 normalizes borehole velocities and displacements to the comparable free-field values. It is seen that for all borehole placement conditions studied, the data fall within a bound of $\pm$20 percent with the exception of the 1.5-foot borehole position of Test CBMI-12, which was influenced by the explosive gases that penetrated into the borehole. This scatter is the same as that observed for the uniform placement condition, i.e. Test CBMI-10.

3.2 DISCUSSION

3.2.1 Particle Motion

A strong interface bond between the borehole filler material and the free-field material assures particle velocity response that is essentially insensitive to large impedance mismatches between the two materials (Figures 3.17, 3.21, 3.25, and 3.29a), i.e., when a strong bond is present, a vertical velocity gage will accurately measure a vertically induced free-field motion. Since displacements are derived from acceleration and velocity data, it follows (and has been demonstrated by this investigation) that displacement wave forms that accurately depict the free-field response are also obtained (Figures 3.18, 3.22, 3.26, and 3.29b). Even when weak borehole filler materials are used, good velocity measurements can be obtained if the canisters are firmly coupled to the free field (Figure 3.18).

Acceleration measurements are somewhat more sensitive to placement effect than are particle velocity measurements. In the superseismic regime, a short-duration, fast-rise-time acceleration signal will outrun its free-field counterpart down a borehole when the borehole backfill

material is stiffer (higher wave speed) than the free field (Figure 3.20). This results in a wave guide situation (in contrast to a plane wave situation) that will affect the acceleration signature to an extent dependent on the delay time between the borehole and free-field wave fronts and the stress-strain characteristics of the relevant materials. This phenomenon has a smaller effect on particle velocity, since the impedance mismatch responsible for the outrunning situation simultaneously provides for an enhanced peak stress and a compensatory reduction in the peak particle velocity amplitude.

3.2.2 Stress

The background study (Section 1.5, Appendix A, Reference 1) indicated that for reliable measurements, stress gage placement required much more careful placement than did velocity sensors; in particular, a much closer match of the borehole filler mechanical properties to those of the surrounding free field is required than for motion measurements. This match is required because significant stress transfers will occur between the borehole and free field, whereas particle velocity will tend to self-compensate for those transfers. Intimate contact must be maintained between the sensing surfaces of a stress gage and its embedment medium for meaningful stress measurements.

3.2.3 Artificial Soils (Grouts)

Artificial soils (grouts), Appendix B, must be mixed and used with careful attention to quality control. Relatively little is known about the material properties of these materials and factors affecting these properties. Preparation and placement of various grouts to achieve consistent stress-strain properties for all batches necessitate much more care than preparing and placing grouts for general use. It cannot be assumed that small changes in constituents, preparation methods, and placement methods will not affect the properties of the grout.

3.2.4 Placement Techniques

Some placement techniques that have been used in the past are reviewed briefly as follows:

1. Large Cavity Method. One method of gage placement that has been used from time to time is that of sinking a vertical shaft large enough for a technician to enter. The technician then excavates a small cavity in the sidewall, inserts and positions the gage package, and hand-tamps in situ material around the package. After the technician leaves, the large vertical access hole is then backfilled and tamped with the previously excavated material. This method is considered to be undesirable for several reasons. First, there is an inordinate cost in excavating a large-diameter cavity to any great depth. Secondly, a relatively large disturbance has been made in the in situ material, and its effects on adjacent instrument response cannot be known. The uniformity of the backfill, because of its great volume, is highly questionable. Safety may also be a problem in unstable soils unless the hole is cased. This technique is not recommended.

2. Small Borehole Method. The simplest method for gage emplacement is insertion of the instrument packages in small boreholes. Cables are protected by bringing them to the surface through a slant hole that intersects the vertical instrument hole below the deepest instrument position. This approach is the one most widely used. A problem arises, not with this concept, but with the methods of coupling the instrument package to the in situ material and properly backfilling the hole. Early attempts relied on either hand tamping in situ material around the canisters and filling the hole with the same material or on raining dry sand around the packages and subsequently filling the borehole with sand. It is difficult to pack dry soil in boreholes deeper than 5 or 6 feet. The material tends to bulk and large variances in density occur. It is also difficult to maintain proper orientation of the canister while tamping. This is critical when using tilt-sensitive instruments such as the DX pendulum-type velocity gages. Moist cohesive materials such as clays tend to become doughy upon repeated tamping, and density control becomes almost impossible to maintain. Placing dry sand in boreholes has several disadvantages: (1) it requires raining and vibrating to compensate for bridging effects and gross density variations; (2) the sand will be considerably denser than most in situ

materials; (3) it is prone to absorb moisture from the in situ materials; and (4) it is subject to saturation if it contacts a water table or if the test site is subjected to rain. Because of the relatively large air void ratio in dry sand, pore pressure from surface airblast loading can present problems. Sand backfill has been used successfully in sandy or silty geologies. Most geologies, however, do not lend themselves to this method. Use of tamped backfill materials are not recommended for depths greater than 5 or 6 feet.

In recent years, grouts have been used as backfill materials in soils for placements deeper than 5 feet or so. WES has used this approach almost exclusively since 1968 with highly satisfactory results. It was felt that the most critical aspect of motion instrument placement was ensuring firm coupling of the instrument canister to the ground. This is accomplished by using a relatively stiff, expanding grout in the immediate area of the canister. A grout mixture roughly matching the density and stiffness of the in situ materials is used to backfill the remainder of the borehole. This method has been verified by the CBMI study and is the recommended placement technique.

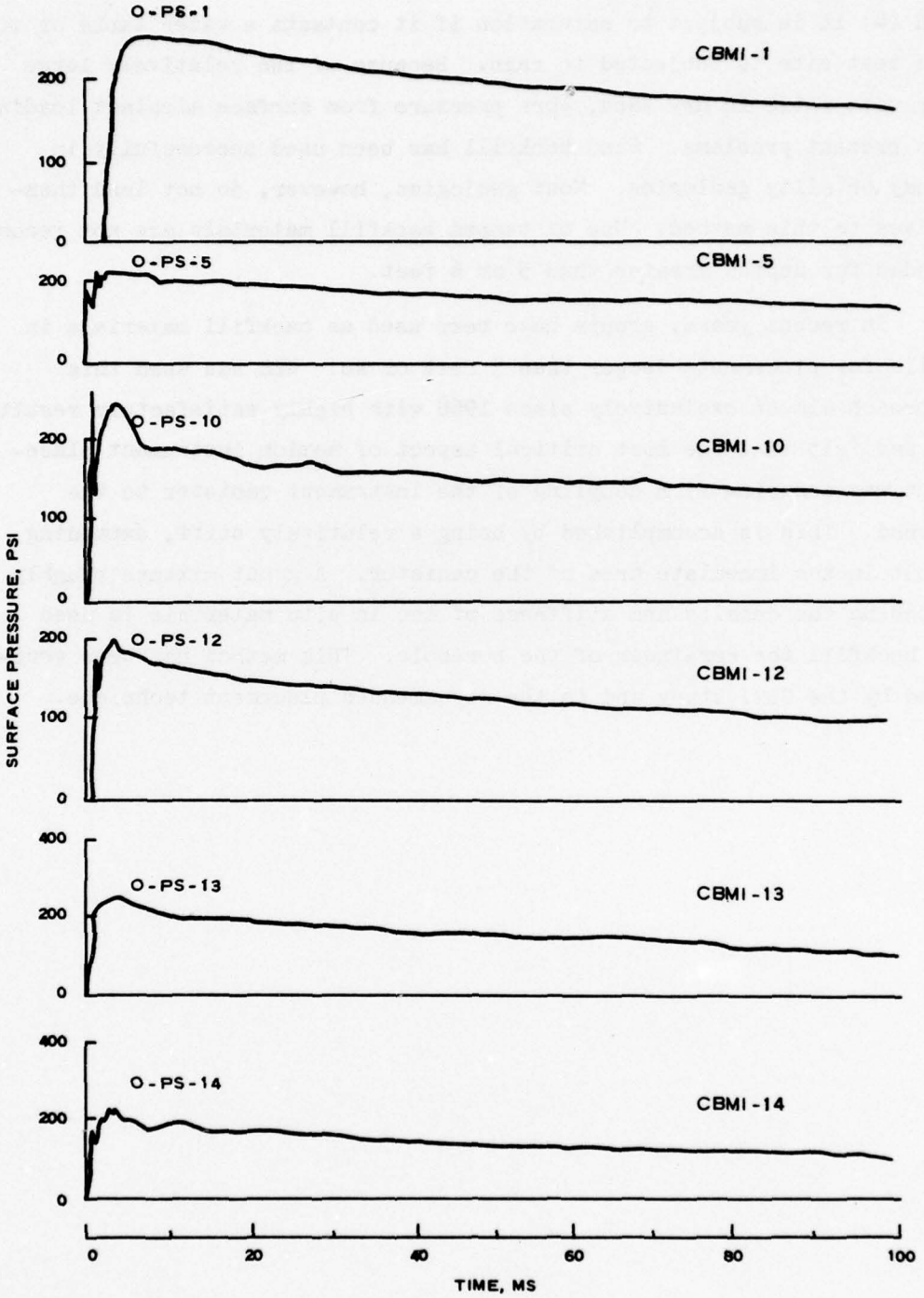

Figure 3.1 Composite surface pressures measured in CBMI test series.

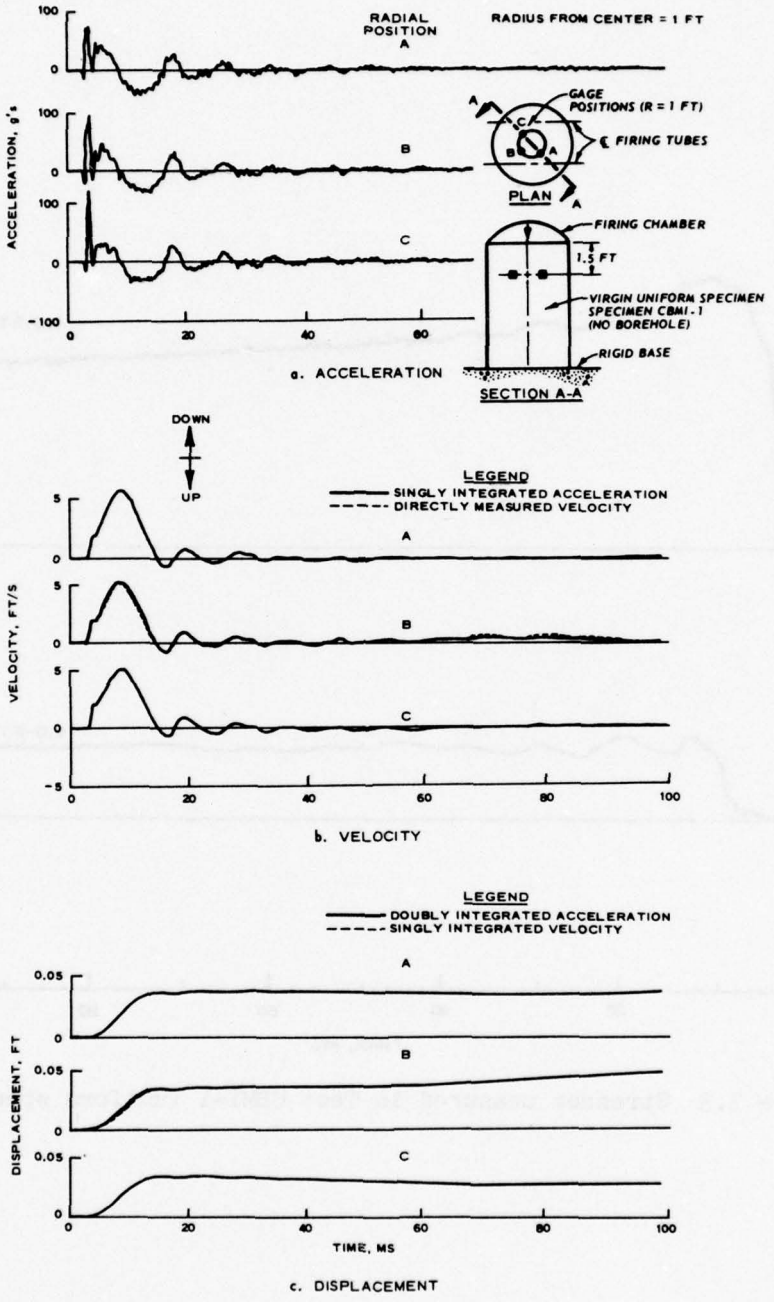

Figure 3.2 Uniformity of measured motions at the 1.5-foot depth for three radial positions, Test CBMI-1 (uniform specimen).

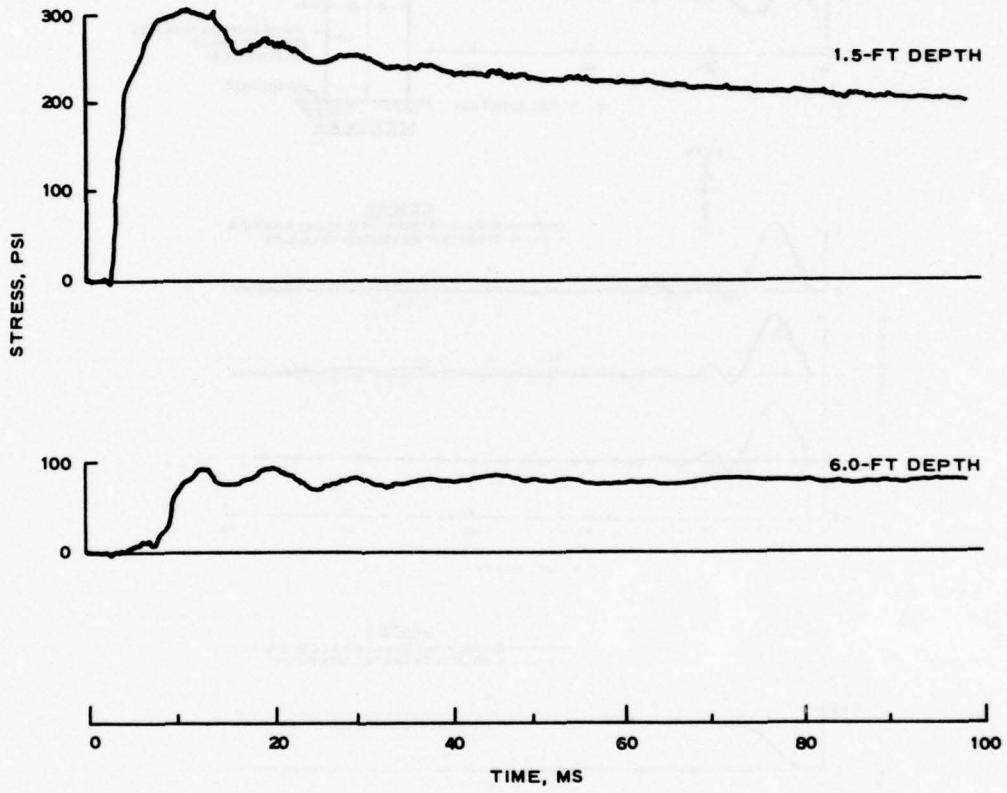

Figure 3.3 Stresses measured in Test CBMI-1 (uniform specimen).

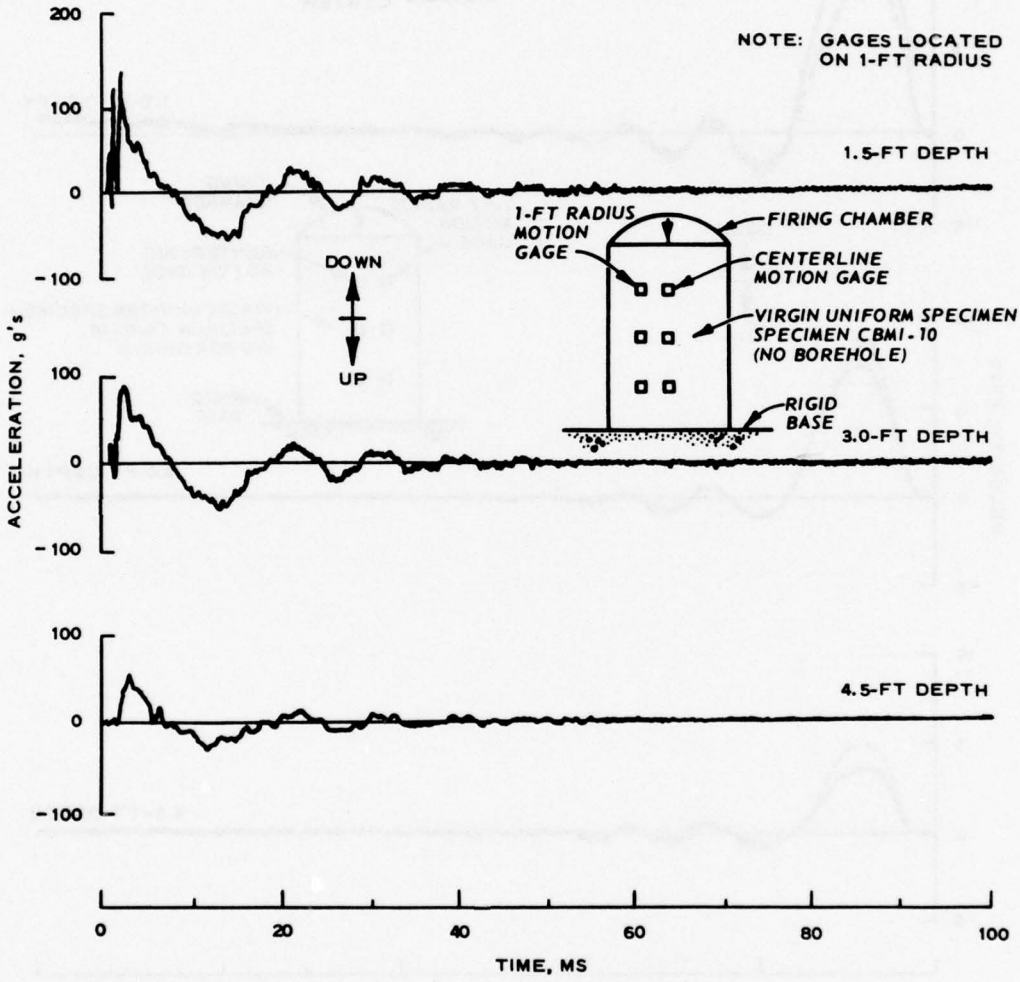

Figure 3.4 Comparative accelerations measured in Test CBMI-10 (uniform specimen).

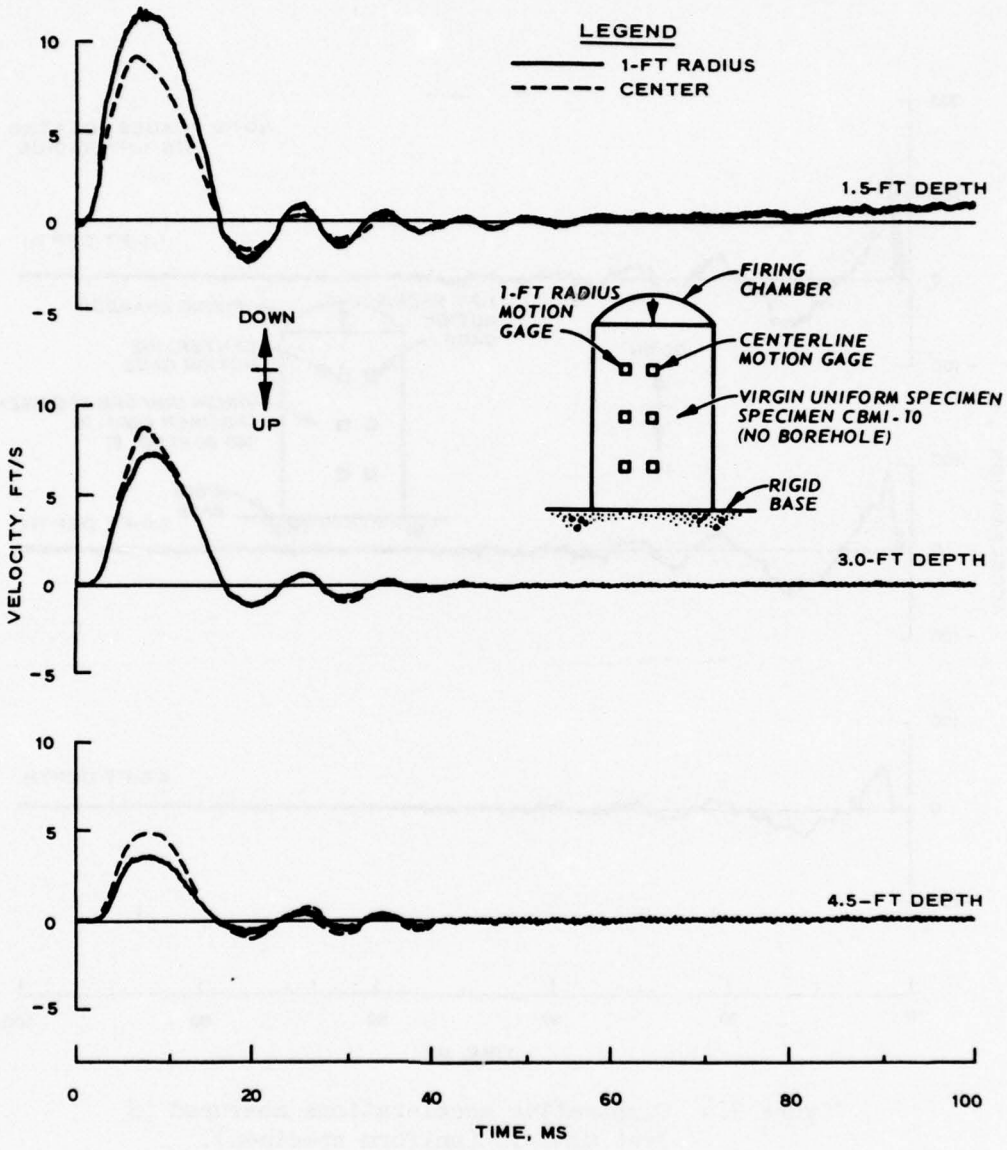

Figure 3.5 Comparative particle velocities measured in Test CBMI-10 (uniform specimen).

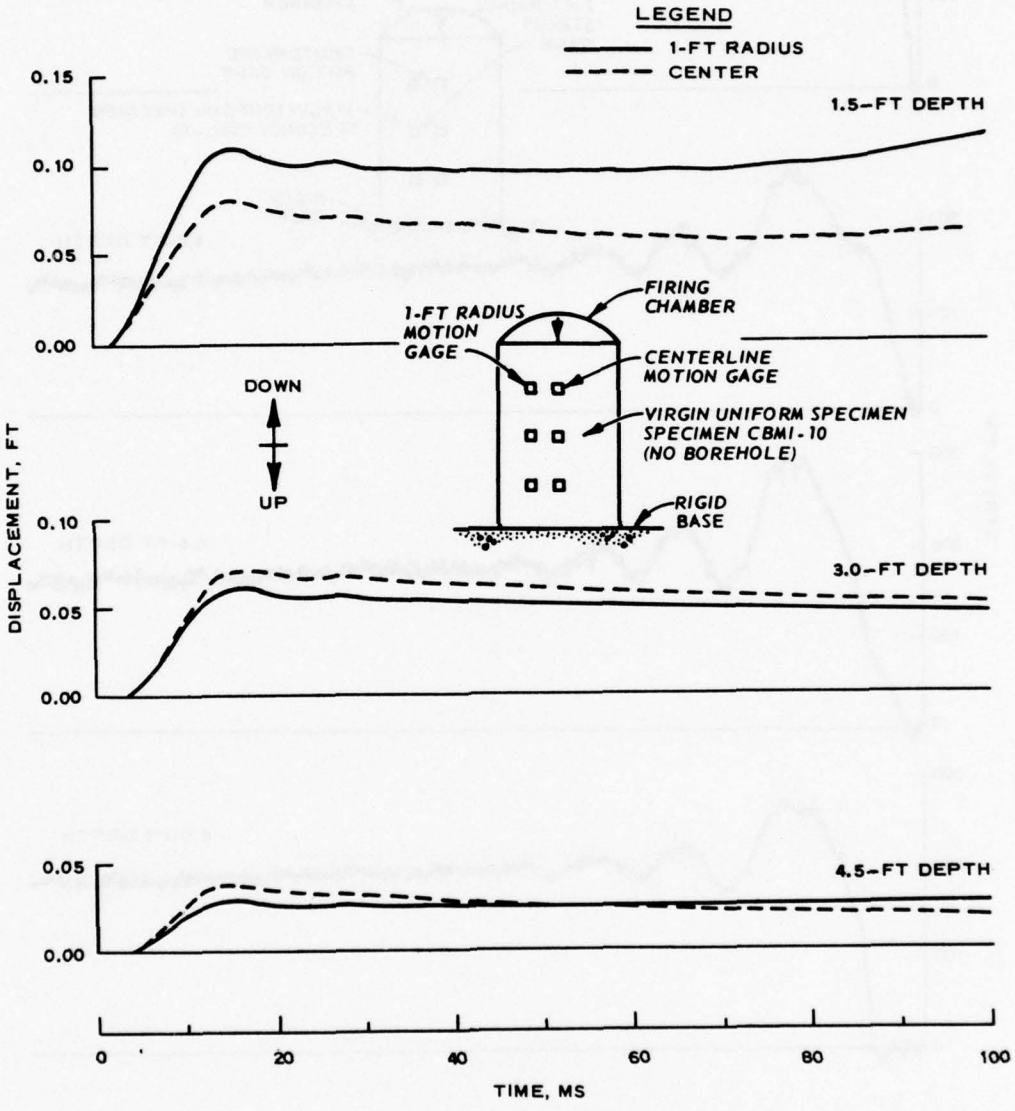

Figure 3.6 Comparative displacements from Test CBMI-10 (uniform specimen).

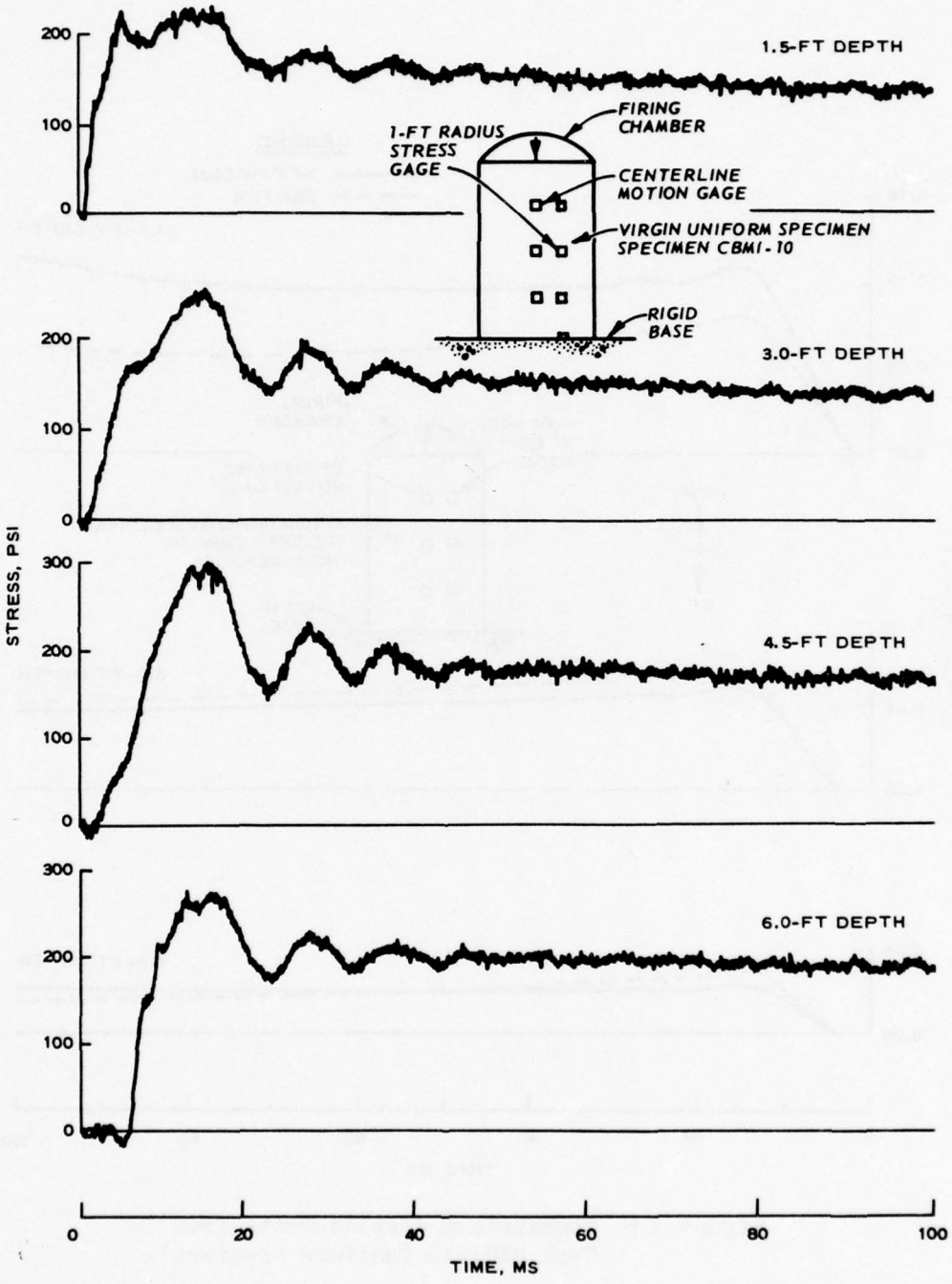

Figure 3.7 Comparative free-field stresses measured in Test CBMI-10 (uniform specimen).

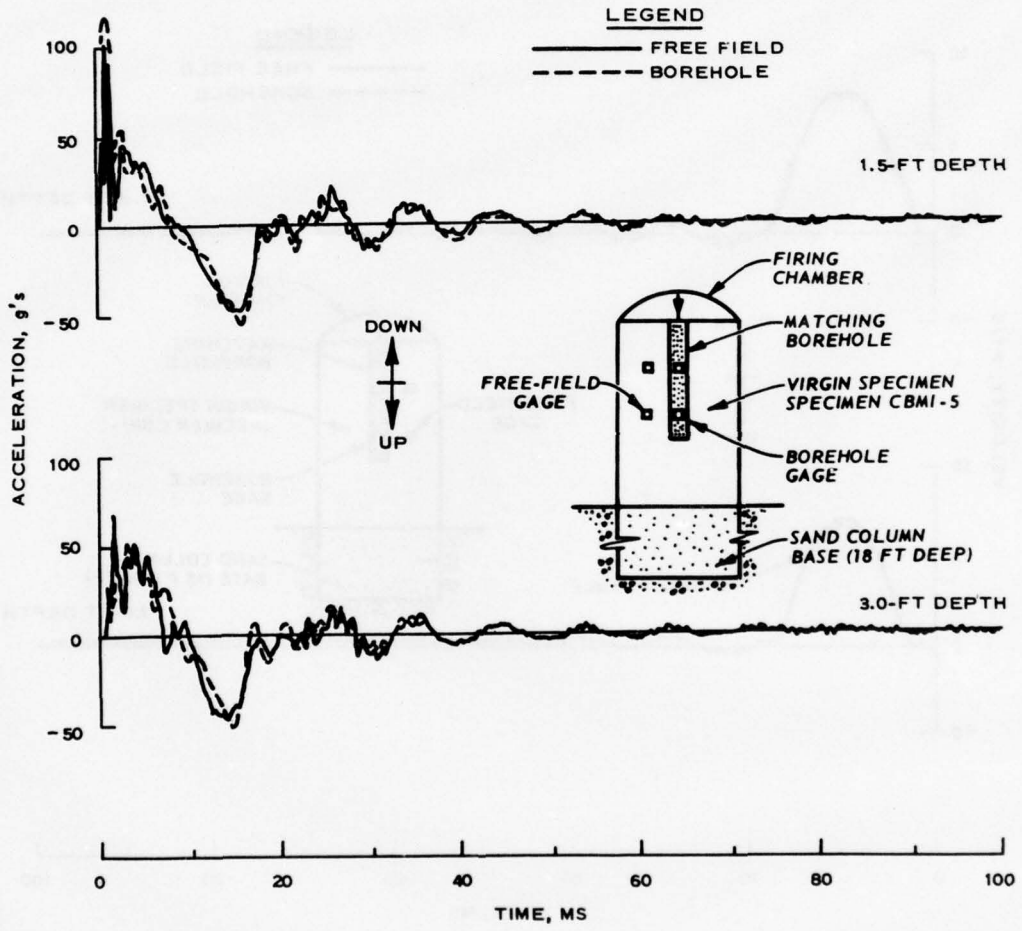

Figure 3.8 Comparative accelerations measured in Test CBMI-5.

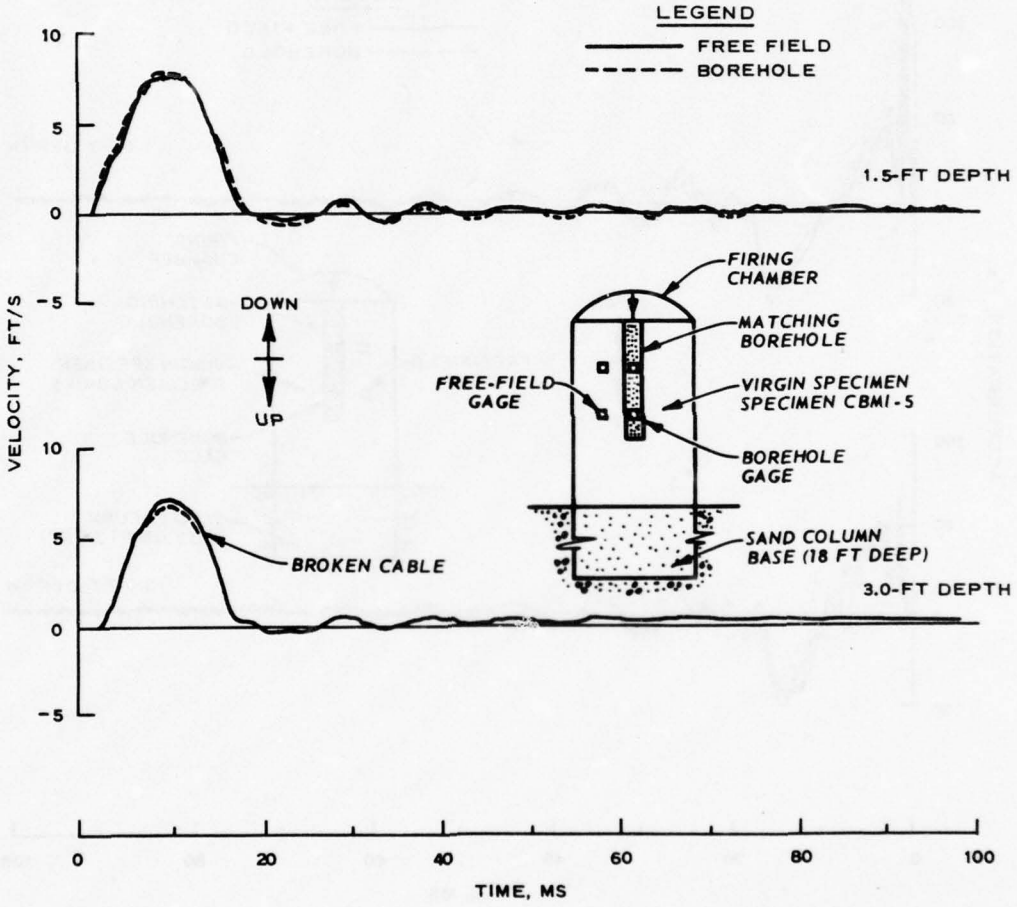

Figure 3.9 Comparative particle velocities measured in Test CBMI-5.

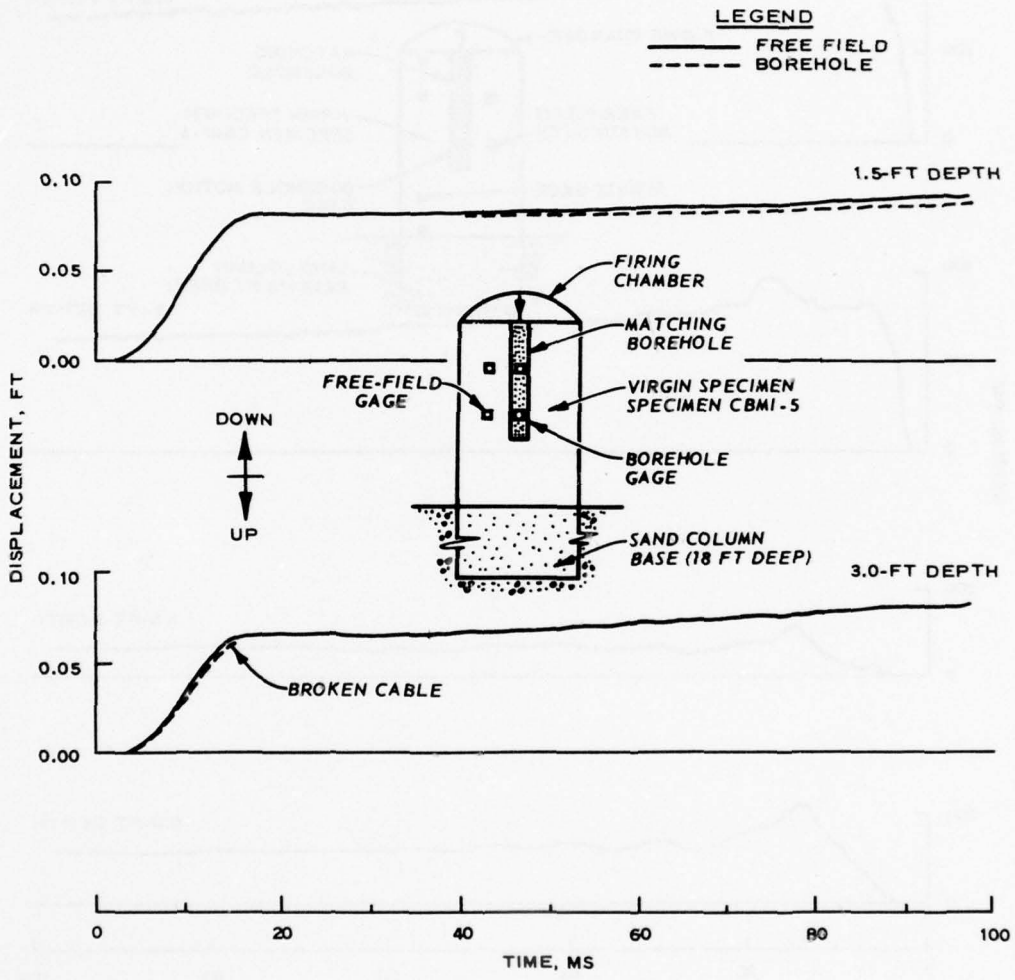

Figure 3.10 Comparative displacements measured in Test CBMI-5.

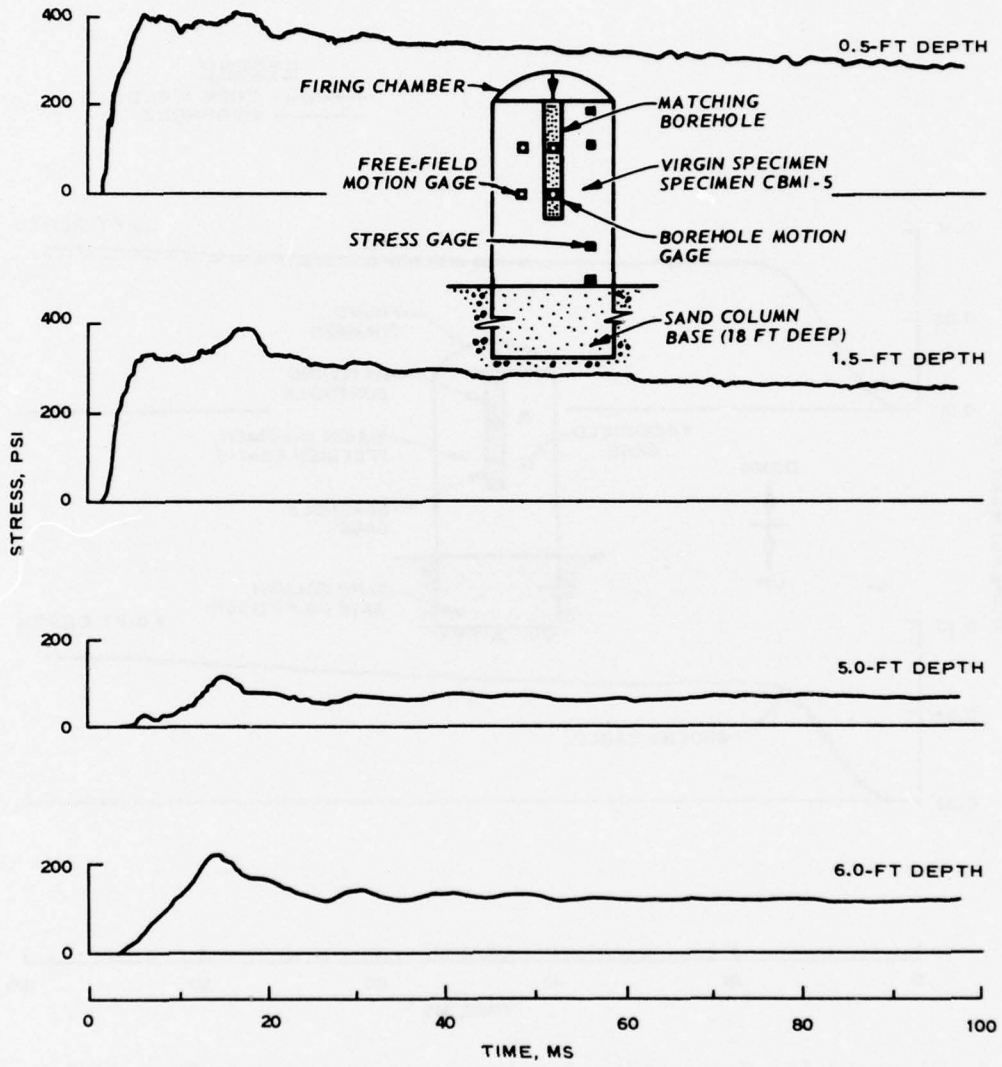

Figure 3.11 Comparative free-field stresses measured in Test CBMI-5.

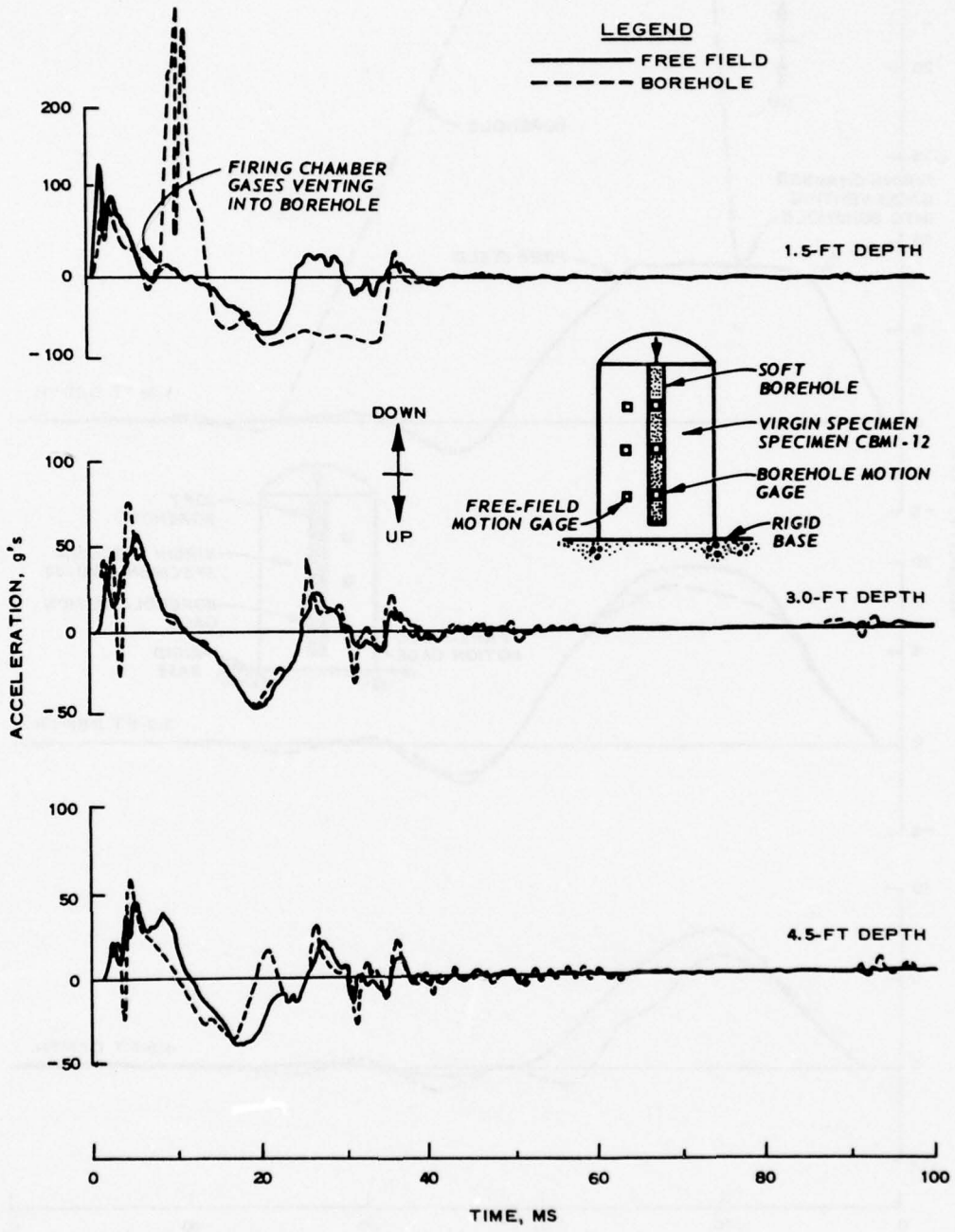

Figure 3.12 Comparative accelerations measured in Test CBMI-12 (uniform soft borehole filler, canisters not locked in).

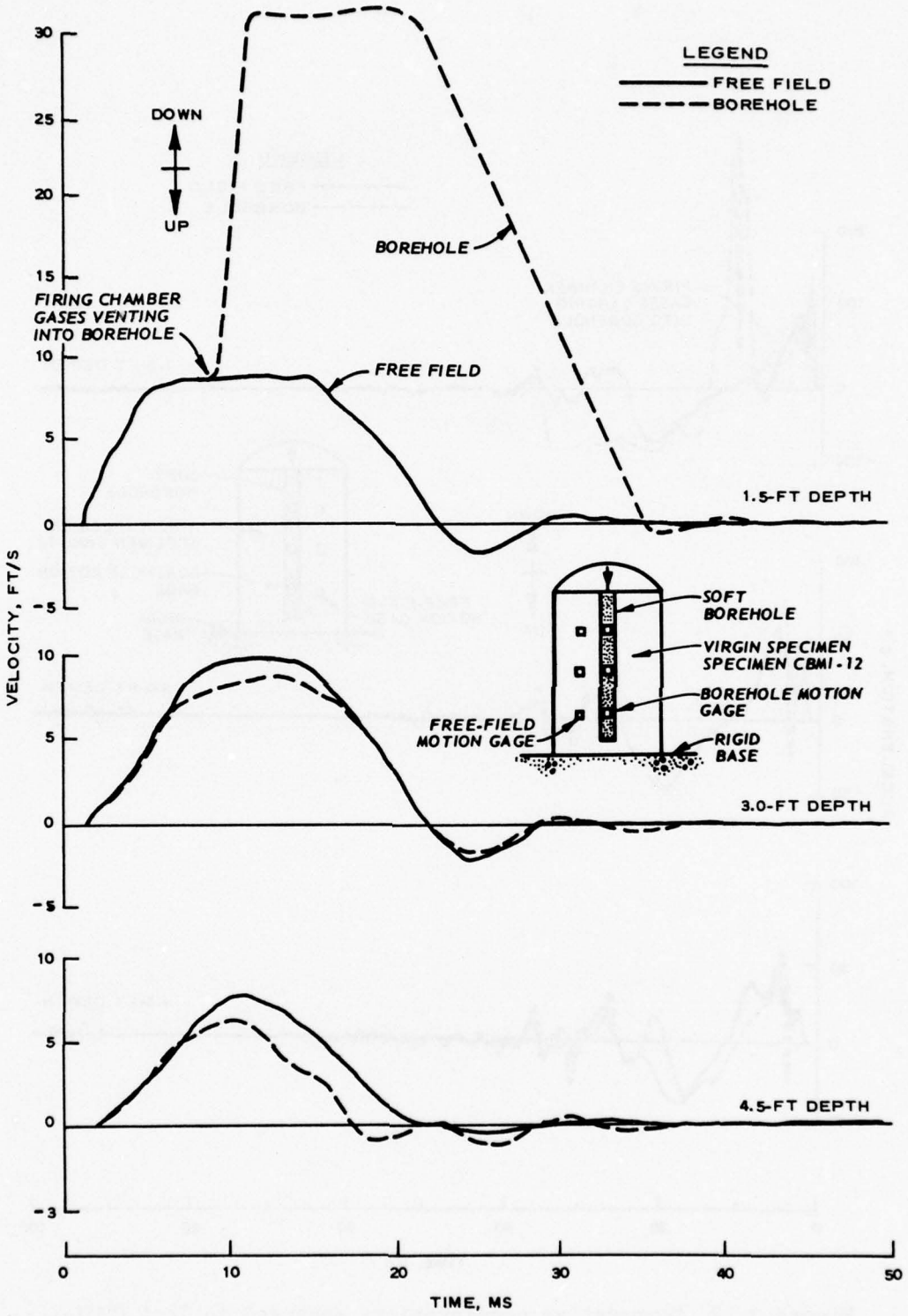

Figure 3.13 Comparative particle velocities measured in Test CBMI-12 (uniform soft borehole filler, canisters not locked in).

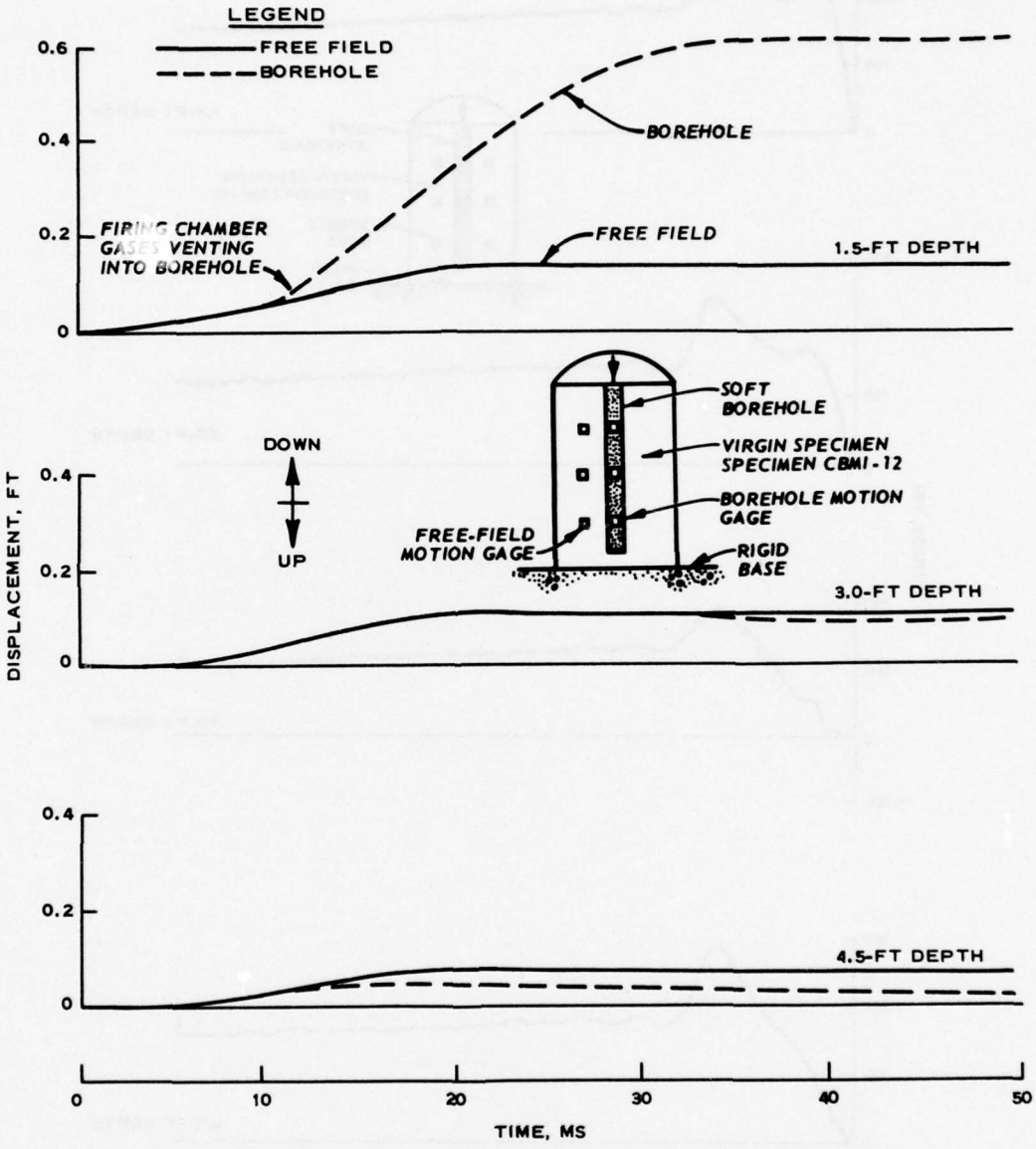

Figure 3.14 Comparative displacements in Test CBMI-12 (uniform soft borehole filler, canisters not locked in).

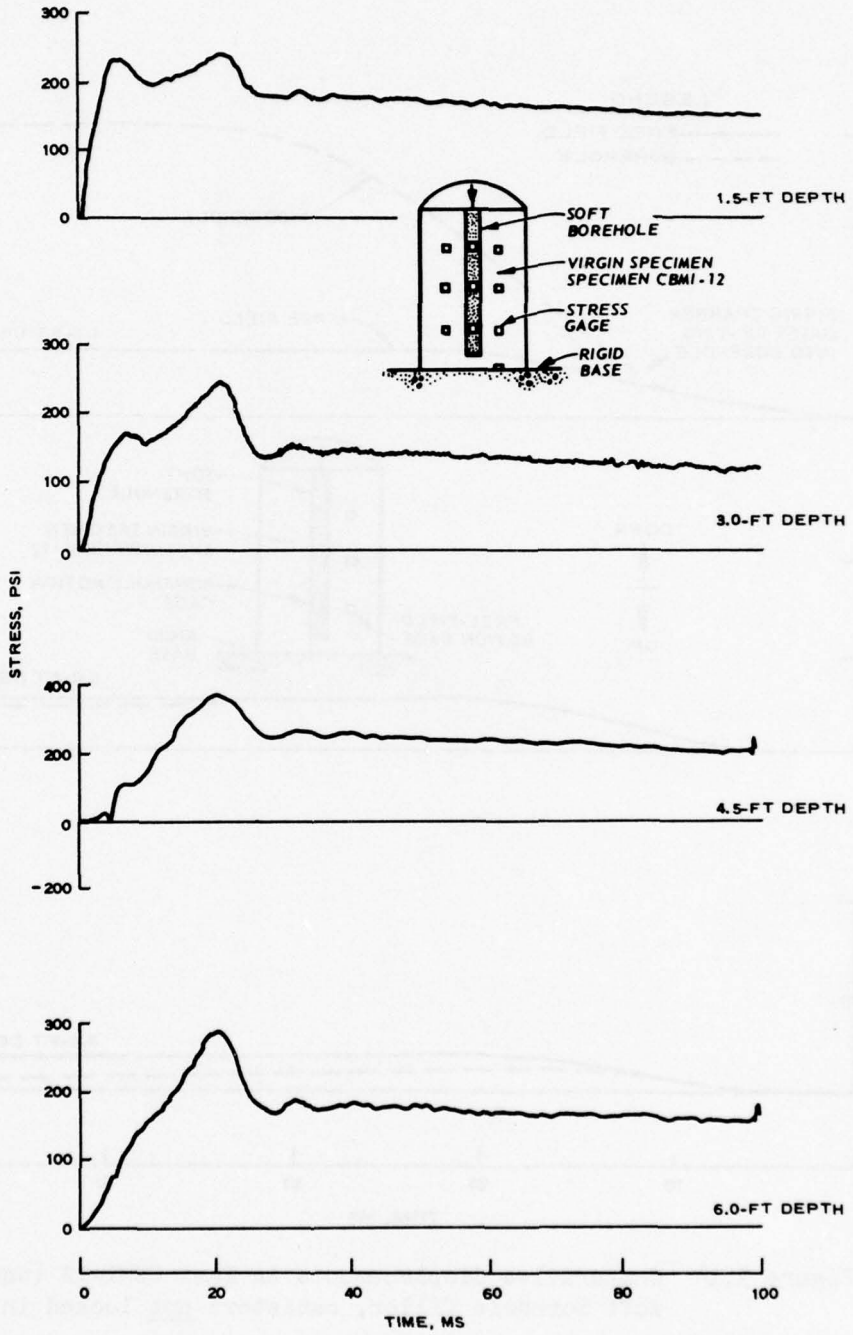

Figure 3.15 Comparative free-field stresses measured in Test CBMI-12 (uniform borehole filler).

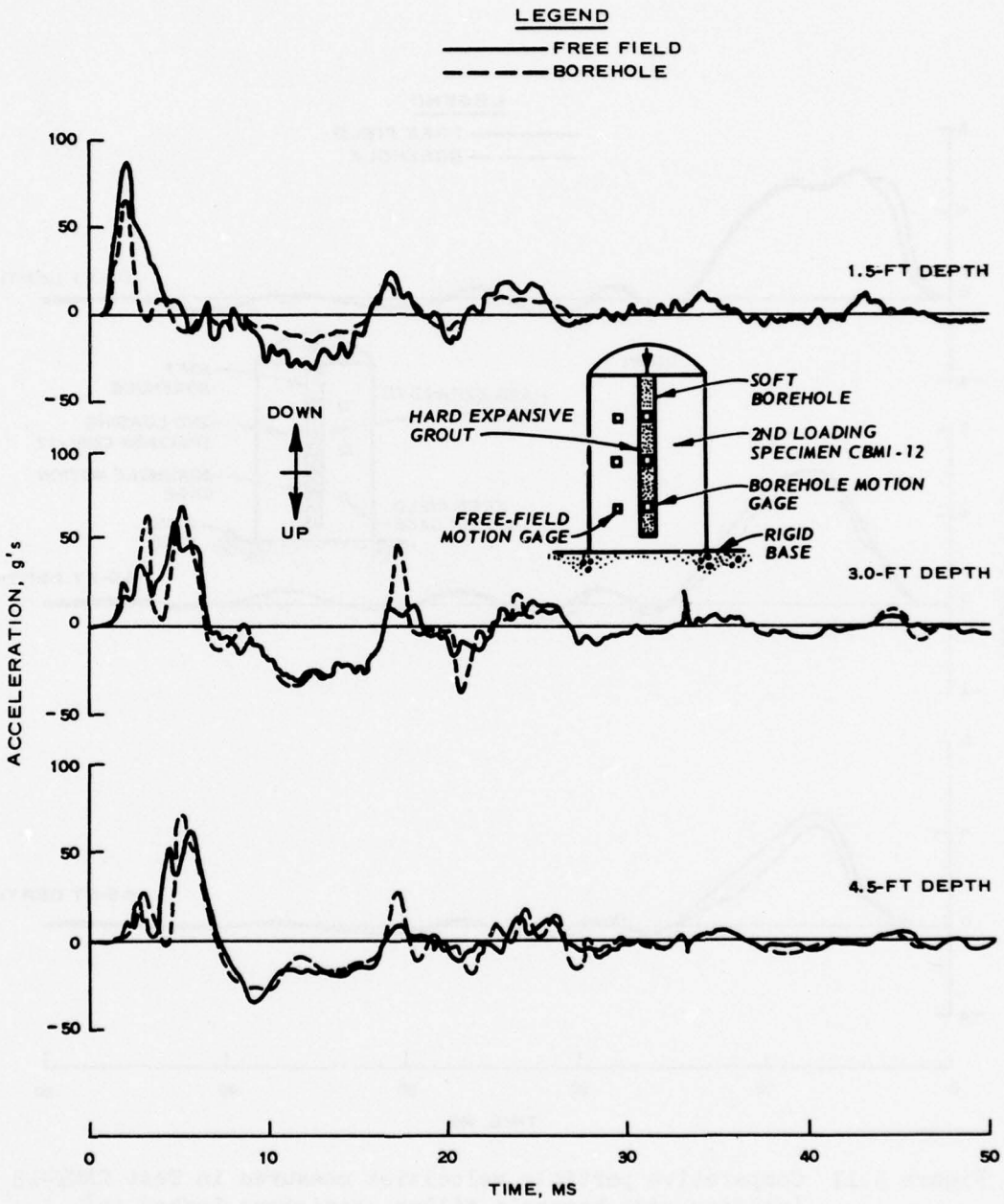

Figure 3.16 Comparative accelerations measured in Test CBMI-13 (uniform soft borehole filler, canisters locked in).

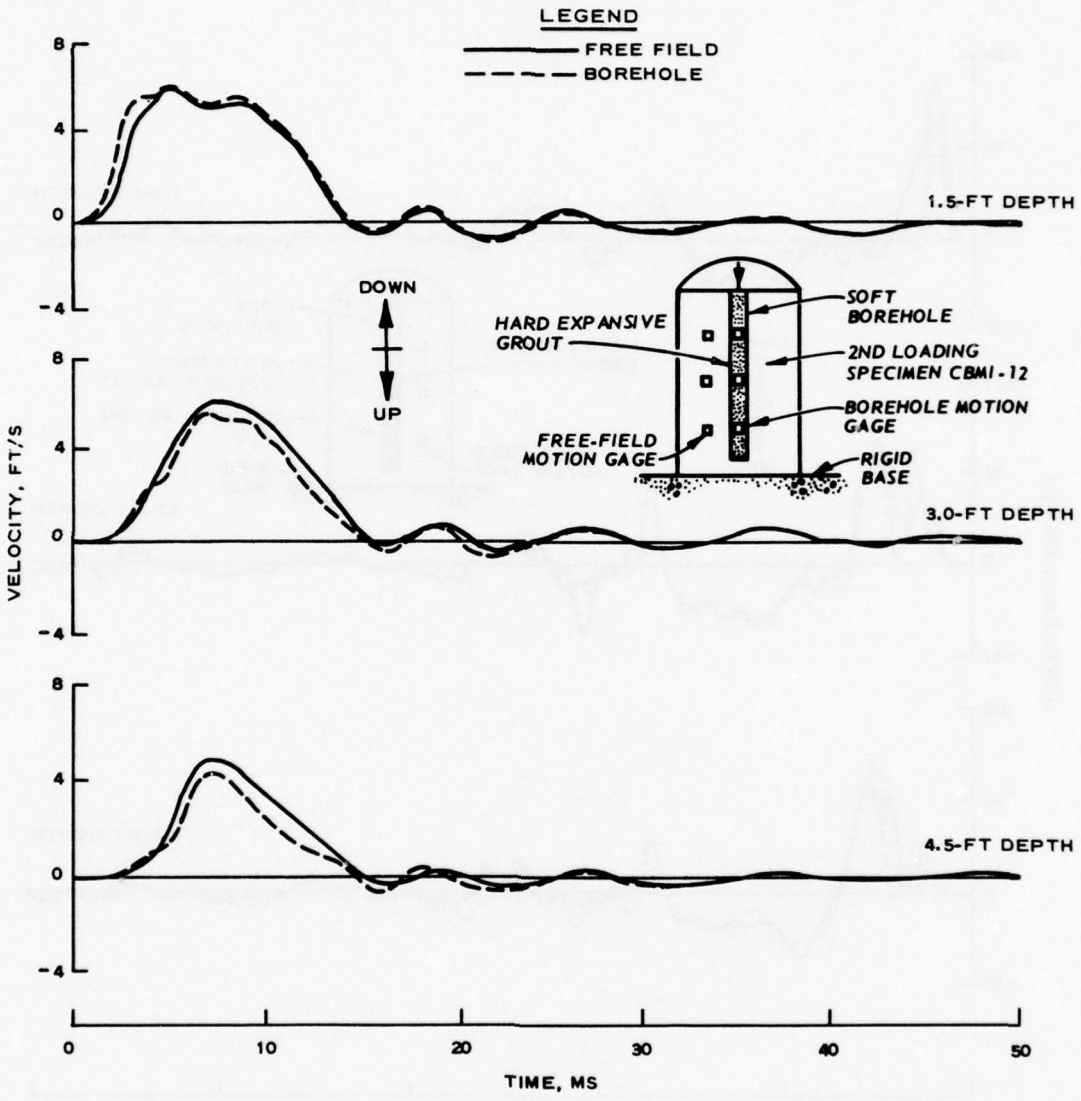

Figure 3.17 Comparative particle velocities measured in Test CBMI-13 (uniform soft borehole filler, canisters locked in).

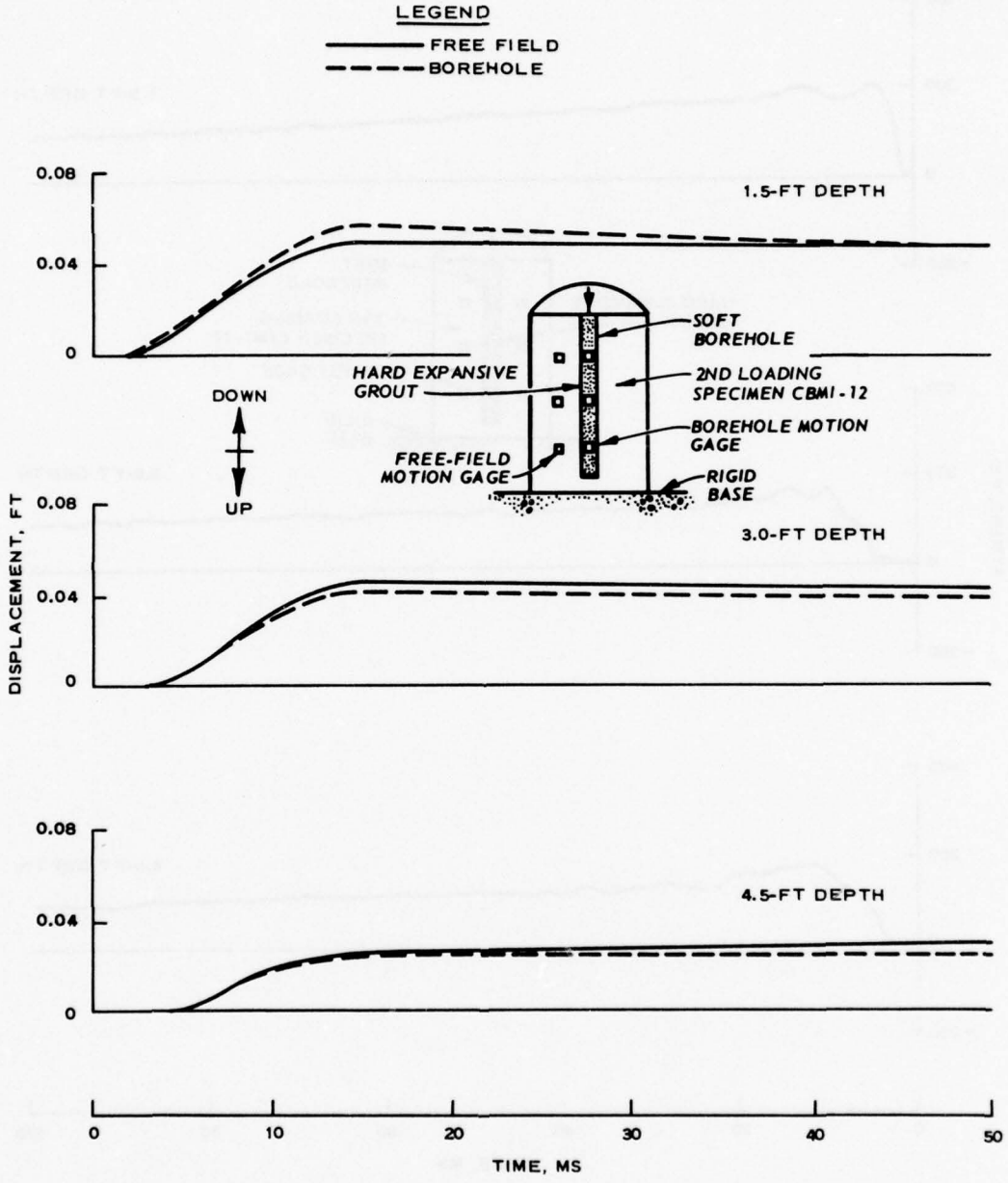

Figure 3.18 Comparative displacements in Test CBMI-13 (uniform soft borehole filler, canisters locked in).

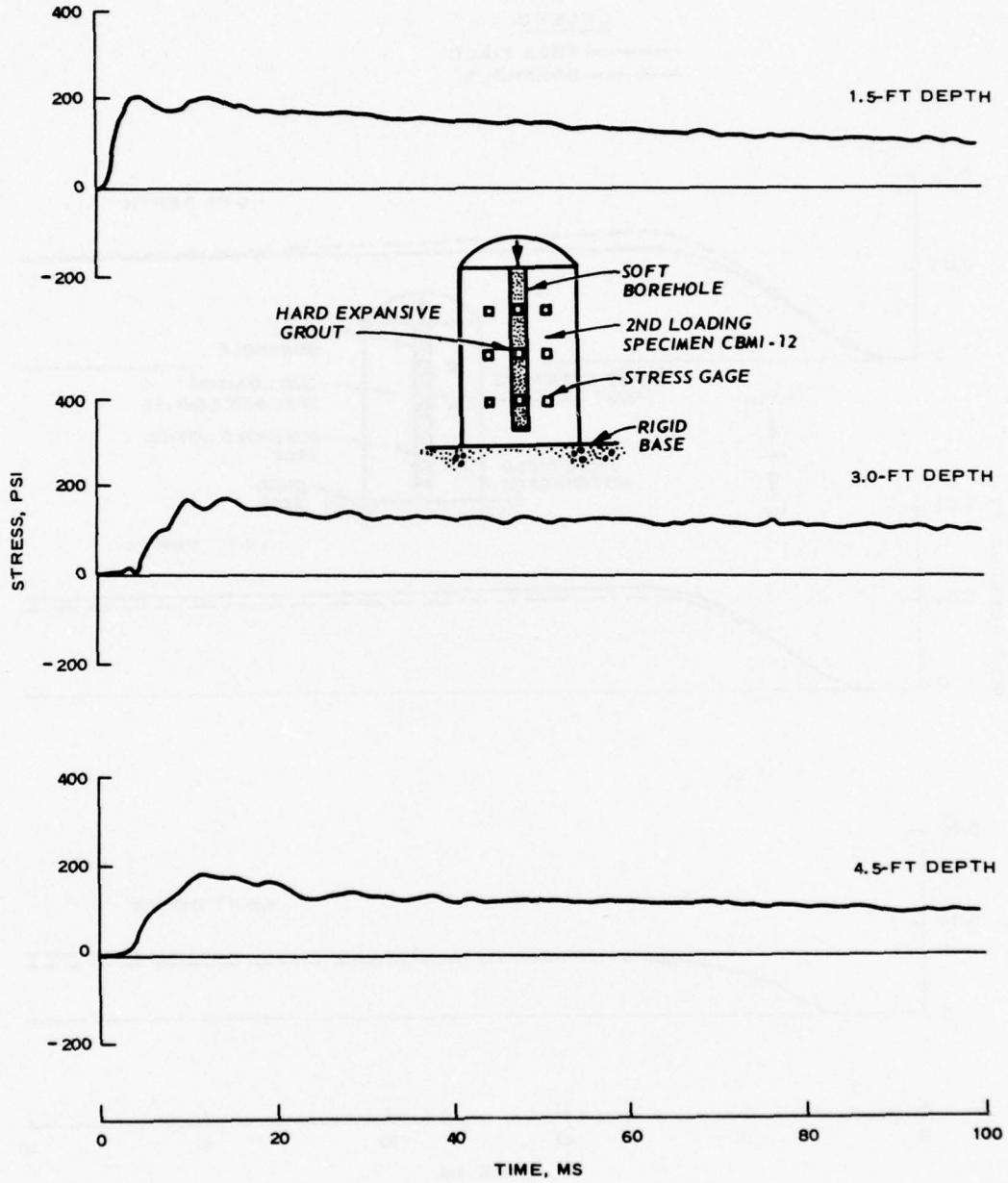

Figure 3.19 Comparative free-field stresses measured in Test CBMI-13 (soft borehole).

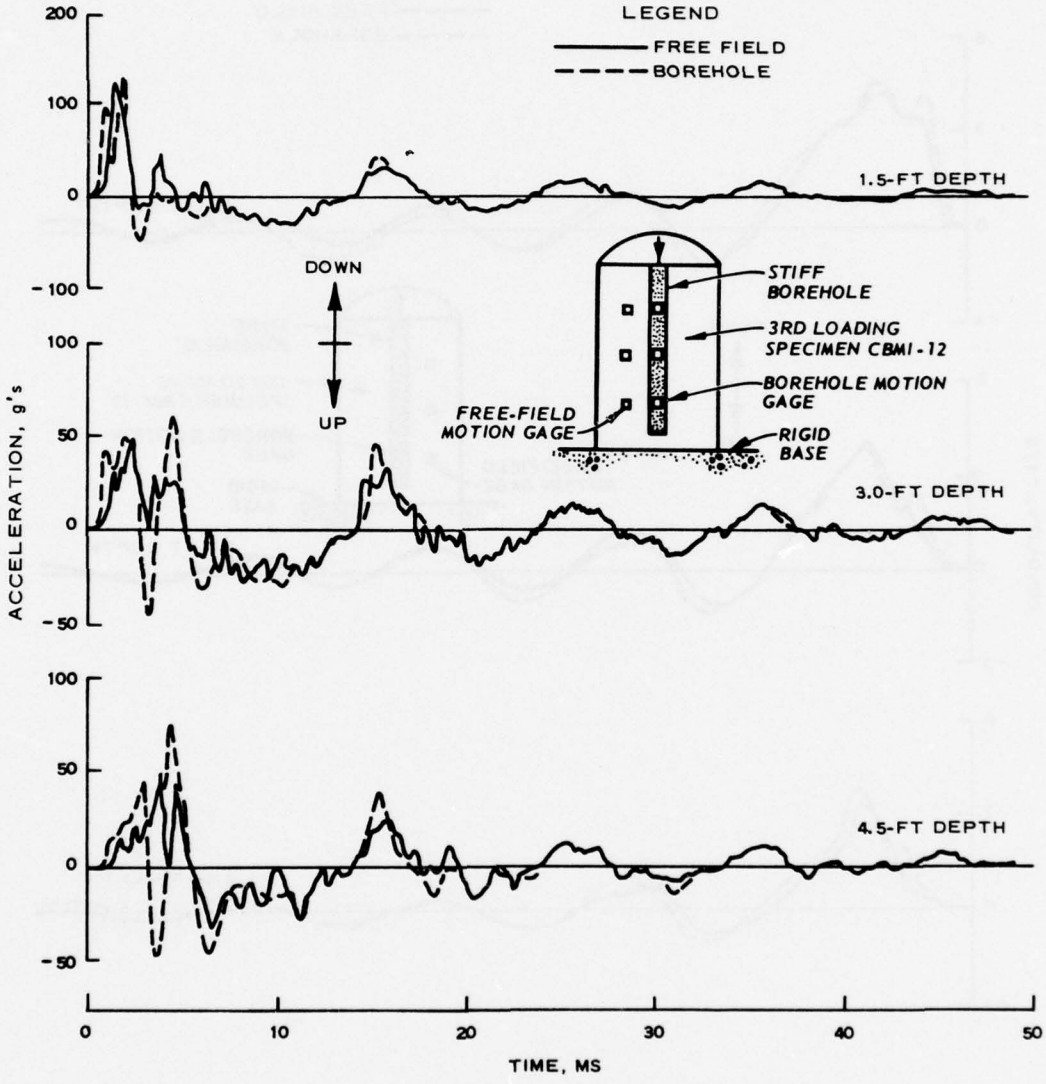

Figure 3.20 Comparative accelerations measured in Test CBMI-14 (stiff borehole).

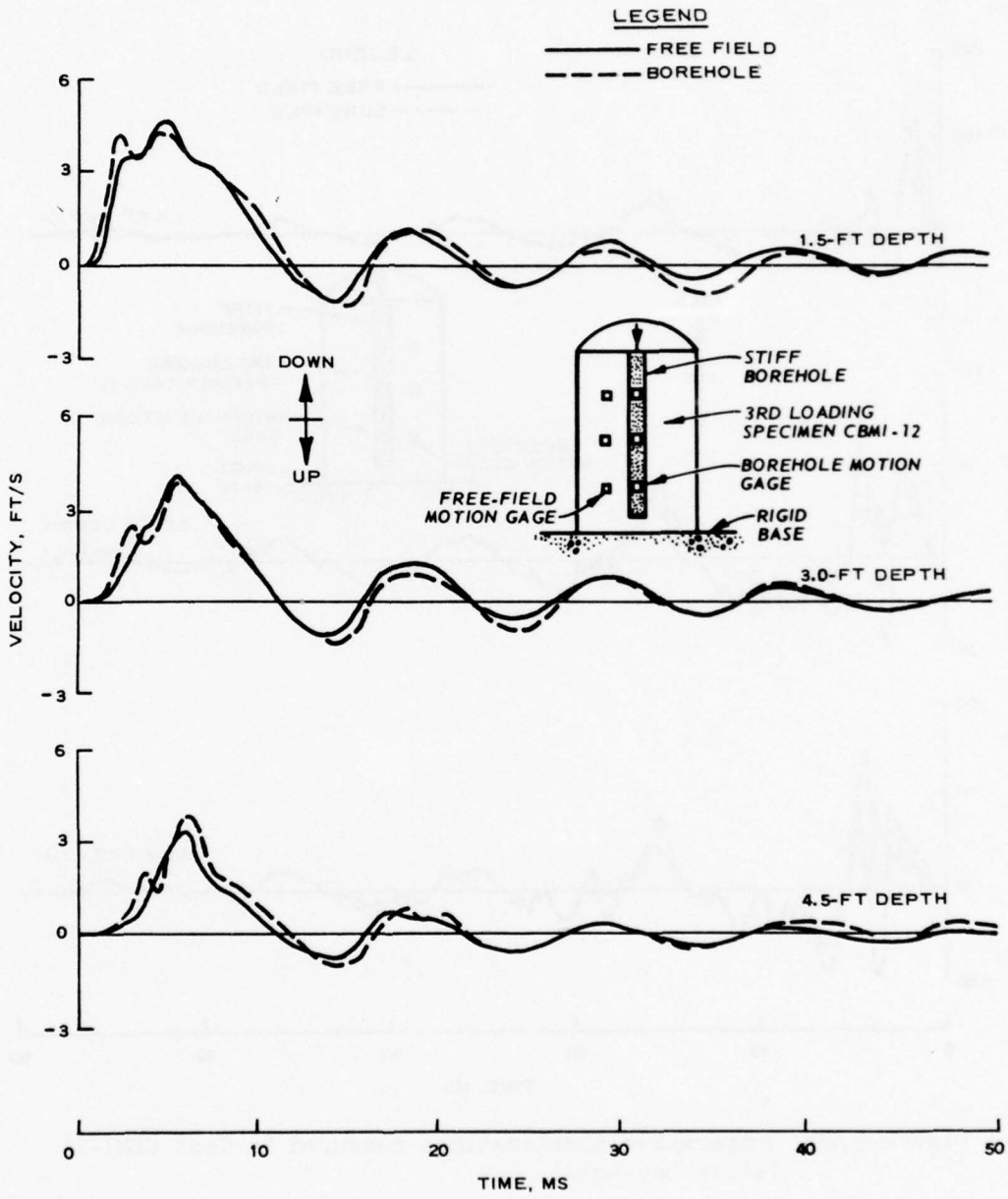

Figure 3.21 Comparative particle velocities measured in Test CBMI-14 (stiff borehole).

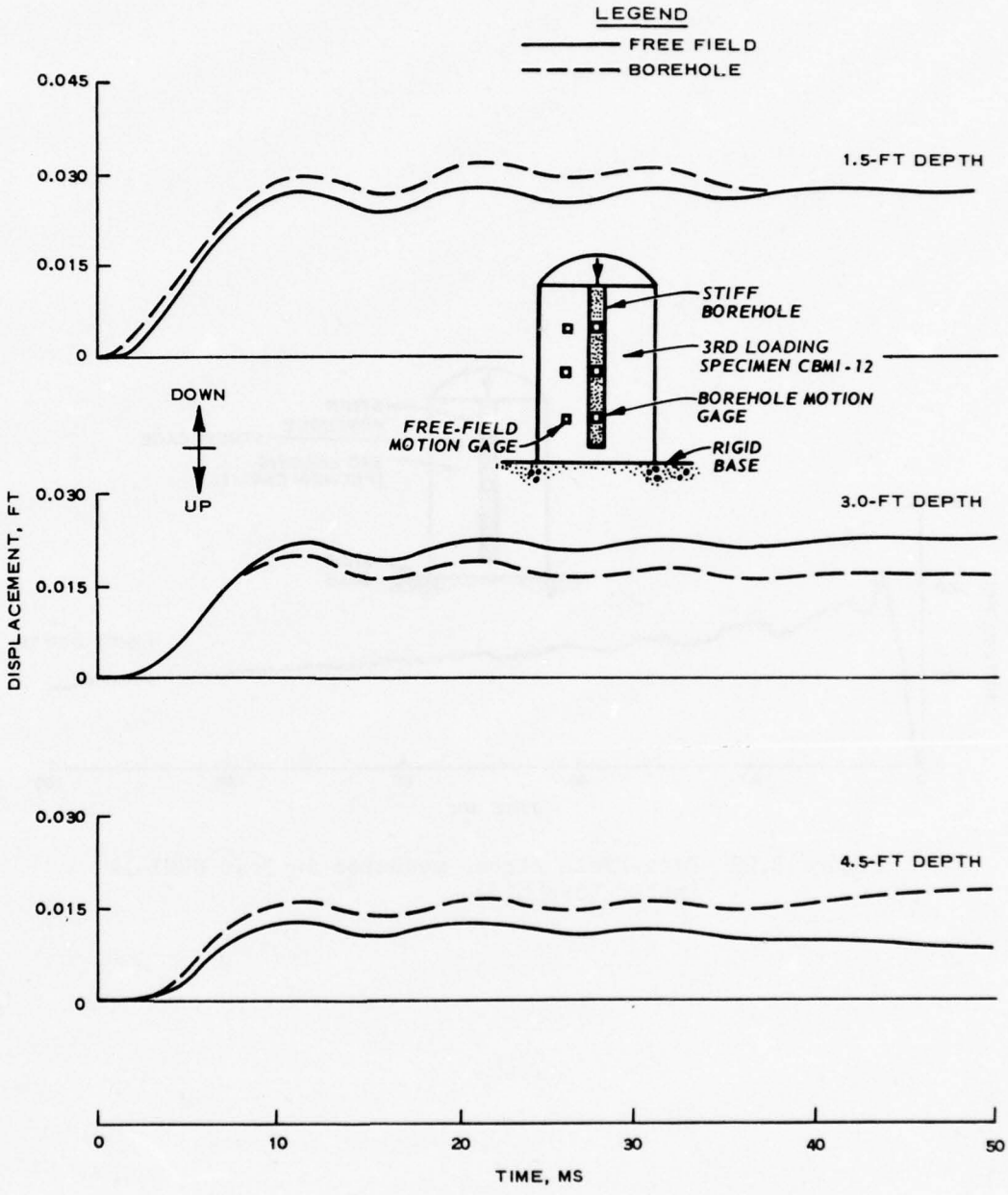

Figure 3.22 Comparative displacements in Test CBMI-14 (stiff borehole).

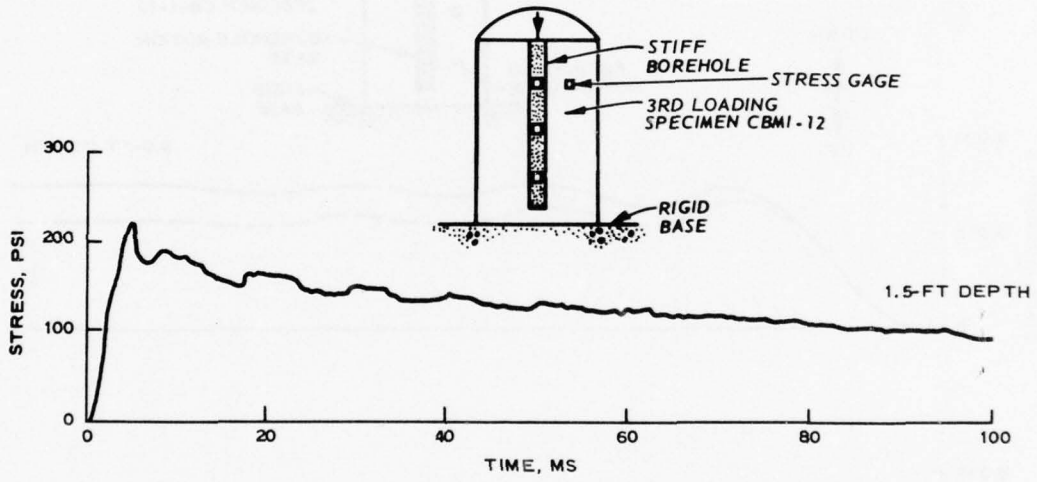

Figure 3.23 Free-field stress measured in Test CBMI-14 (stiff borehole).

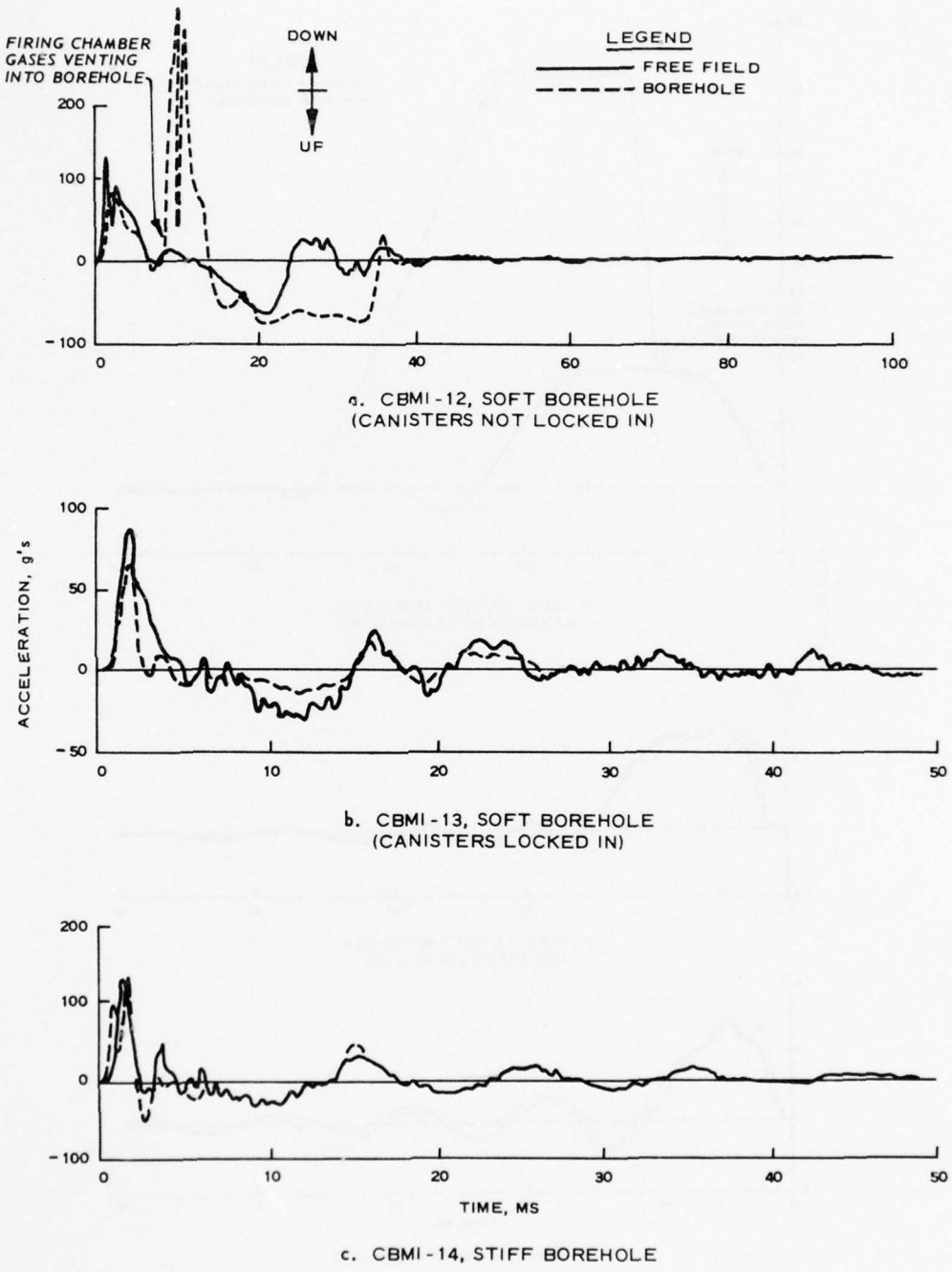

Figure 3.24 Comparison of acceleration wave forms at the 1.5-foot depth, Tests CBMI-12, -13, and -14.

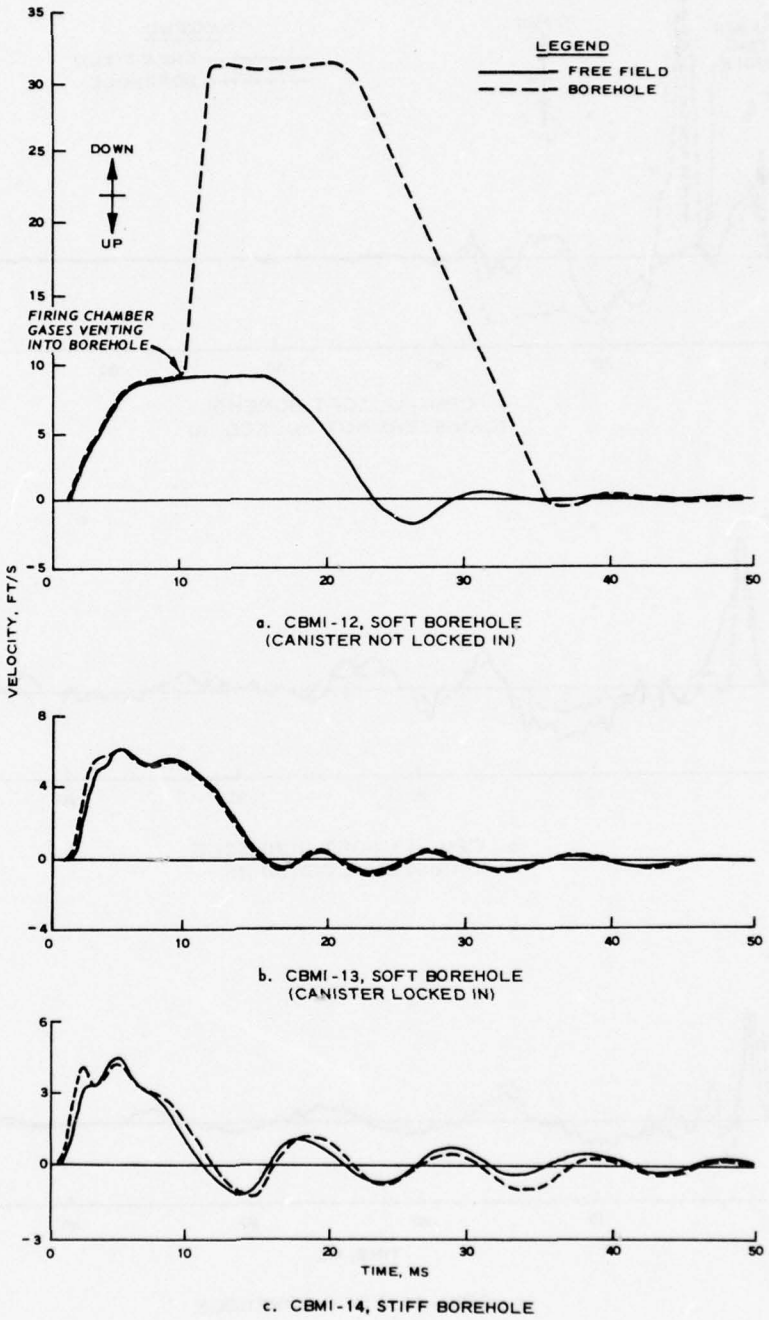

Figure 3.25 Comparison of particle velocity wave forms at the 1.5-foot depth, Tests CBMI-12, -13, and -14.

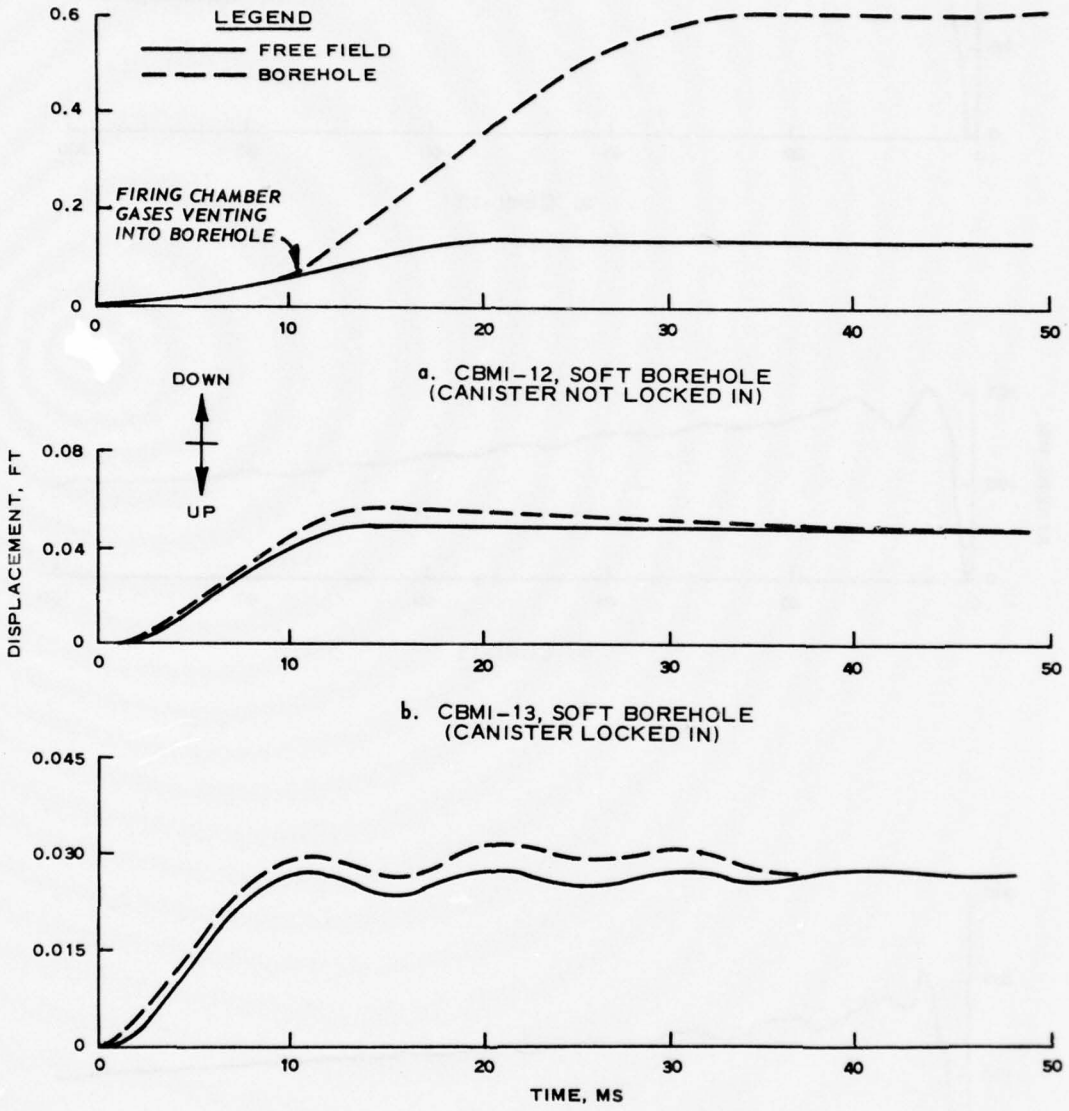

Figure 3.26 Comparison of displacement wave forms at the 1.5-foot depth, Tests CBMI-12, -13, and -14.

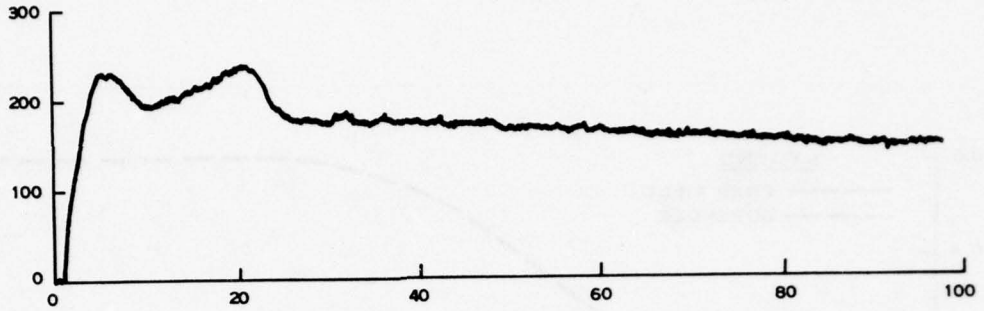

a. CBMI-12

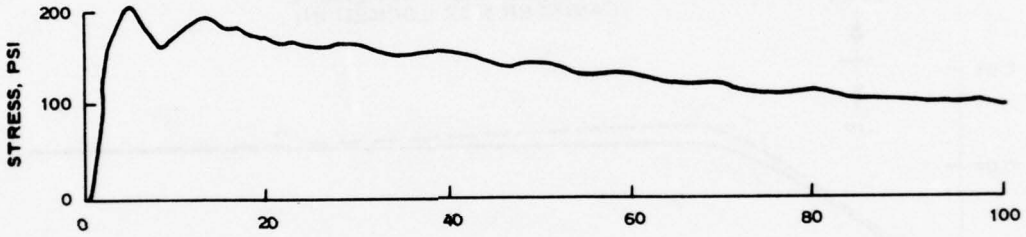

b. CBMI-13

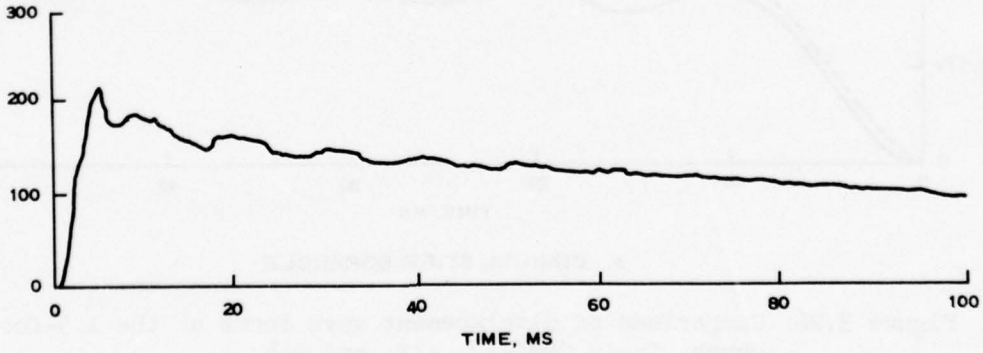

c. CBMI-14

Figure 3.27 Comparison of free-field stress wave forms at the 1.5-foot depth, Tests CBMI-12, -13, and -14.

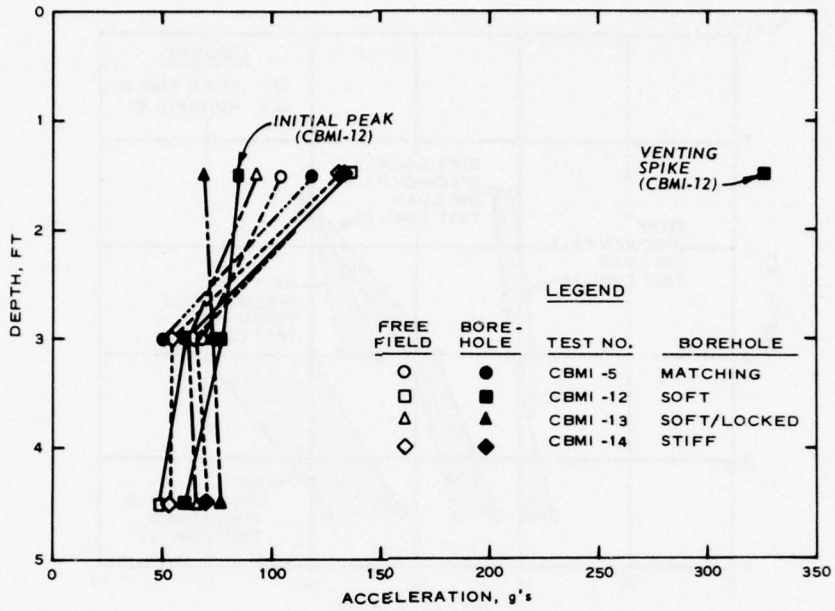

a. PEAK ACCELERATION VERSUS DEPTH

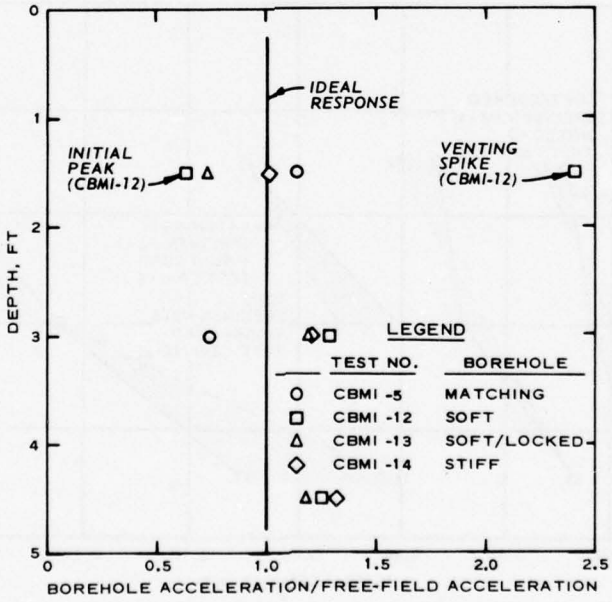

b. NORMALIZED PEAK ACCELERATION VERSUS DEPTH

Figure 3.28 Acceleration response as a function of depth and placement condition, CBMI tests.

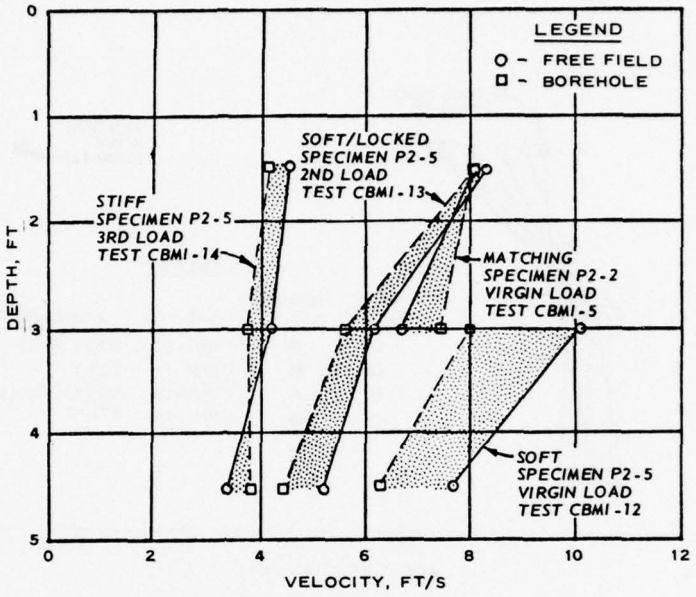

a. PEAK VELOCITY VERSUS DEPTH

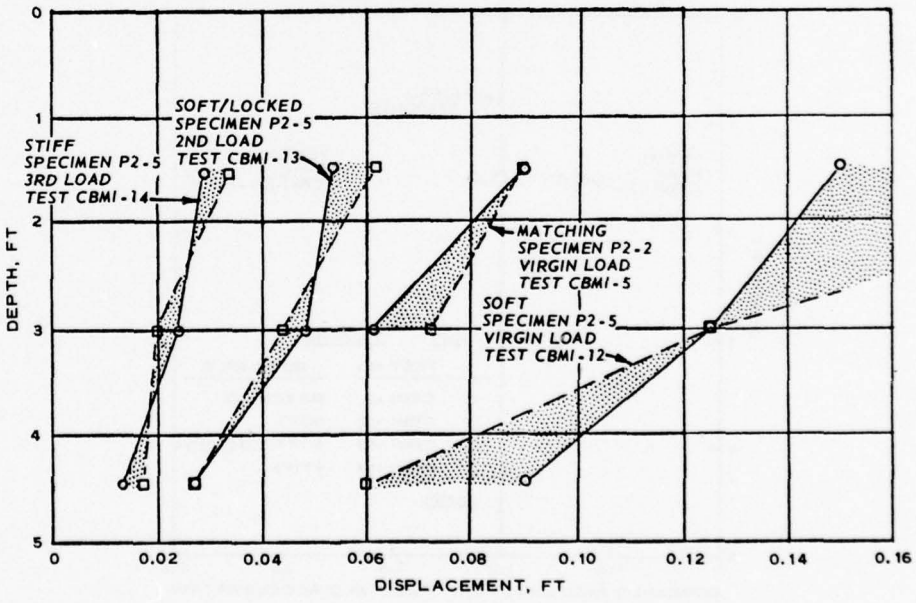

b. PEAK DISPLACEMENT VERSUS DEPTH

Figure 3.29 Peak particle velocity and displacements as functions of depth and placement condition, CBMI tests.

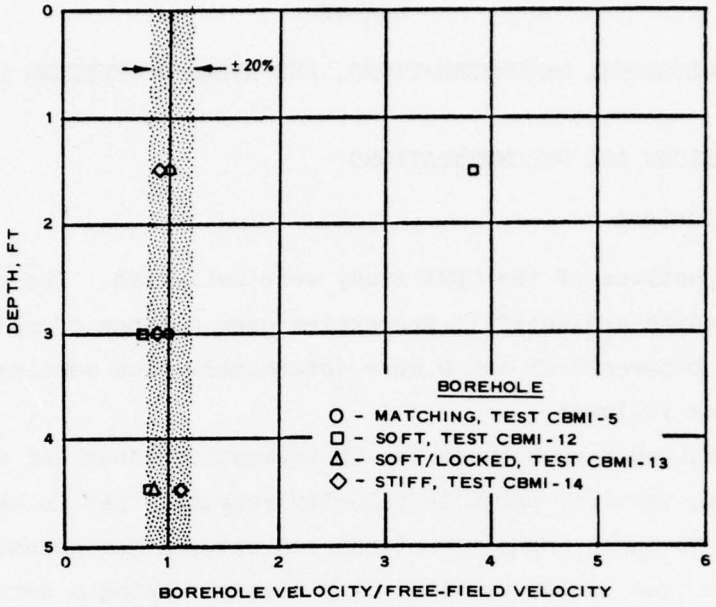

a. NORMALIZED VELOCITY VERSUS DEPTH

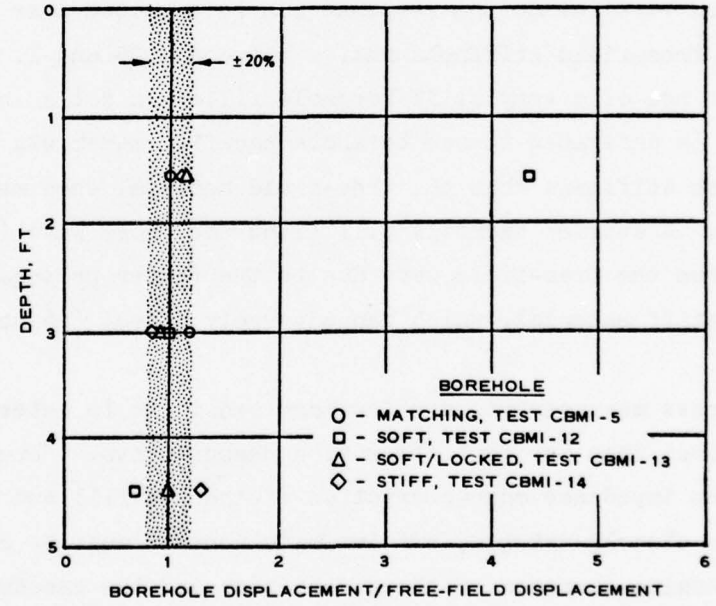

b. NORMALIZED DISPLACEMENT VERSUS DEPTH

Figure 3.30 Normalized velocities and displacements as functions of depth and placement condition, CBMI tests.

CHAPTER 4

CONCLUSIONS, RECOMMENDATIONS, AND AREAS OF FURTHER STUDY

4.1 CONCLUSIONS AND RECOMMENDATIONS

4.1.1 Conclusions

The objectives of the CBMI study were satisfied. The relative effects of earth and backfill properties over a range of material stiffness ratios between 0.05 and 2 were determined. The conclusions are summarized as follows:

1. A strong bond between the instrument canister and the free field assures vertical particle velocity response that is essentially insensitive to large impedance mismatches between the borehole filler soil and the free field; vertical displacement, being a derived quantity, will also be within reasonable bounds.

2. Good vertical motion response can be expected over a range of borehole to free-field stiffness ratios between 0.05 and 1.

3. The use of a very stiff borehole filler in soils is not recommended. It is desirable to use borehole backfill materials of equal or slightly less stiffness than the free-field material when measuring accelerations. A stiffer backfill will allow the shock wave in the borehole to outrun the free-field wave due to the faster propagation velocity of the stiff material, which can adversely affect the acceleration response.

4. Stress measurements are far more sensitive to material property mismatches than are particle motion measurements. Hence, not only must the impedance characteristics of the backfill and free-field materials be closely matched, but intimate contact must be assured between the sensing surfaces of the stress gage and the embedment material.

Conclusions pertinent to define accurately the calculational properties of the artificial soils used for the CBMI study are presented in Appendix D.

4.1.2 Recommendations

The following procedures are recommended for field placement of transient motion and stress sensors.

4.1.2.1 MOTION INSTRUMENTS.

1. Assure a firm bond between motion canister and free field either by using a relatively stiff expansive grout to surround the instrument canister or by overreaming at the instrument position, forming a ledge to seat nonexpanding grout. Use of expansive grout around the instrument package is recommended.

2. Restrict the stiffness of borehole filler material to a range of 1 to 0.05 times that of the free field. The stiffness indicator suggested for use in designing a backfill material is the secant modulus.

4.1.2.2 STRESS GAGES.

1. Assure intimate contact between sensing surfaces of gage and embedment material. This can be achieved by two methods: (1) the stress gage can be mounted in a tapered paddle and forced into a preformed slot slightly smaller than the gage paddle and the remaining hole backfilled with a properties matching grout (this method is usually practical only for horizontal sensing gages and limits the installation to only one gage at the bottom of each borehole); or (2) the stress gages may be cast in cylindrical plugs of slightly expansive matching grout and installed like motion instrument canisters.

2. Strive to match impedance and strength characteristics of backfill material to those of the local free field. This can be achieved only by carefully determining the in situ properties and by developing a chemical grout that adequately simulates the sonic velocity, density, and secant modules of the in situ material.

4.2 FURTHER STUDY

The laboratory investigation has provided needed insight into the gage placement problem; however, it falls short in that it does not provide information on gage response from ground shock loading angles

other than in the axial plane, i.e. the real-world situation. Nor does it provide information from combined airblast- and direct-induced loading conditions. In order to resolve these important information gaps, the following evaluation studies are recommended.

A series of small-scale field high-explosive tests at a relatively homogeneous free-field site (i.e. a simulated half-space is needed) should be conducted. This approach is recommended because it avoids the SBLG's problems; however, it simultaneously introduces problems associated with accurate definition of the native soil properties.

"Standardized" motion canisters should be used throughout such a field test series. A relative free-field baseline should be established by instruments hand-emplaced in the native site material. At least two borehole placement conditions should then be addressed:

1. Instrument canisters placed in a borehole backfilled with a property-matching grout (artificial soil).

2. Canisters placed in a borehole with each canister firmly grouted to the local free-field wall and the remaining volume of the borehole backfilled with some relatively weak, readily available, inexpensive filler material.

Several identical holes should be placed on equivalent radii for each test condition to provide a basis for statistical comparison. Explosion charges should be detonated to test the gage placement procedures under airburst, contact burst, and buried burst conditions. Instruments should be placed such that at least three pressure levels are evaluated: tentatively, 2000, 1000, and 250 psi, with the lowest pressure range providing a direct link to the laboratory CBMI test results. Boreholes should be installed such that at least three blast wave loading angles can be studied; 0 degrees (borehole end-loading), 45 degrees, and 90 degrees (side-on to the borehole). A minimum of four to five shots should be fired for each test condition (a total of about 45 shots).

After the small-scale field study, a series of relatively large-scale (20- to 50-ton) high-explosive tests should be conducted at a test

site where material properties and shock response are well documented. These tests would serve to verify the consistency of the recommended placement techniques and procedures resulting from this study as well as to establish limits of data variation that could be expected as a result of gage placement methods. The test program should be comprehensive enough to include a critical study of free-field stress measurement techniques and to provide a realistic environment for evaluating prototype transducers and recording systems developed as part of other Test Instrumentation Development projects or related efforts.

REFERENCES

1. J. K. Ingram; "Placement Effects on Ground Shock Instrumentation"; Miscellaneous Paper N-70-7, July 1970; U. S. Army Engineer Waterways Experiment Station, CE, Vicksburg, Miss.

2. M. B. Balachandra and J. A. Malthan; "Interim Report, Influence of Grout/Soil Interaction on Velocity Gage Response"; Draft Contract Report No. R-7364-7-4100, February 1976; Agbabian Associates, El Segundo, Calif.

3. D. E. Van Dillen and D. P. Reddy; "Analysis of Control Test 1 of Experimental Canister/Grout/Soil Interaction Study"; Interim Report R-7364-1-3663, Revision 1, May 1975; Agbabian Associates, El Segundo, Calif.

4. G. E. Albritton; "Description, Proof Test, and Evaluation of Blast Load Generator Facility"; Technical Report No. 1-707, December 1965; U. S. Army Engineer Waterways Experiment Station, CE, Vicksburg, Miss.

5. P. F. Hadala; "Sidewall Friction Reduction in Static and Dynamic Small Blast Load Generator Tests"; Technical Report S-68-4, August 1968; U. S. Army Engineer Waterways Experiment Station, CE, Vicksburg, Miss.

6. F. M. Sauer, G. B. Clark, and D. C. Anderson; "Nuclear Geoplosics, A Sourcebook of Underground Phenomena and Effects of Nuclear Explosions; Empirical Analysis of Ground Motion and Cratering"; DASA-1285 (IV), Part IV, May 1964; Defense Atomic Support Agency (Defense Nuclear Agency), Washington, D. C.

7. J. K. Ingram; "Development of a Free-Field Soil Stress Gage for Static and Dynamic Measurements"; Technical Report No. 1-814, February 1968; U. S. Army Engineer Waterways Experiment Station, CE, Vicksburg, Miss.

8. P. F. Hadala; "Effect of Placement Method on Response of Soil Stress Gage"; Technical Report No. 3-803, November 1967; U. S. Army Engineer Waterways Experiment Station, CE, Vicksburg, Miss.

9. D. E. Van Dillen and D. P. Reddy; "Analysis of Test CBMI-5 of the Canister/Grout/Soil Interaction Study"; Interim Report R-7364-1-3836, April 1975; Agbabian Associates, El Segundo, Calif.

10. "Norwood Model 211 Airblast Gage Specification Bulletin"; January 1963; American-Standard Corporation, Advanced Technology Laboratories Division, Monrovia Instrument Division, Monrovia, Calif.

11. J. K. Ingram; "Procedure for Assembling SE-Type Soil Stress Gages"; Instruction Report No. 8, March 1967; U. S. Army Engineer Waterways Experiment Station, CE, Vicksburg, Miss.

12. "Endevco Instruction Manual, Model 2264 Piezoresistive Accelerometer Instruction Guide"; 1973; Endevco Corporation, Pasadena, Calif.

13. "Bell and Howell/CEC Model 4-155-0111 Velocity Gage Technical Information Bulletin"; 1973; Instruments Division, Bell and Howell Corporation, Pasadena, Calif.

APPENDIX A

BACKGROUND STUDY

A.1 INTRODUCTION

In 1969, an SBLG study was conducted to investigate the effects of placement technique on soil stress gage response to transient loadings (Reference 1[1]). A secondary objective of this study was to investigate the feasibility of developing an artificial soil material for possible use as a standard instrumentation borehole backfill material in typical clayey soils.[2]

A.2 EXPERIMENTS

Five test specimens were constructed in the SBLG for the background study (Table A.1) and six shots were fired (two on the last specimen). The first four specimens were 4 feet in diameter by 6 feet high. The fifth specimen was 4 feet in diameter by 10 ft high. All boreholes were 9 inches in diameter and were placed in the center of each test specimen. The boreholes were 4.5 feet deep in the short specimens and 9.5 feet deep in the tall specimen.

A.3 GAGE PLACEMENT

The stress gages located in the free-field portion of each specimen were placed as the specimens were constructed. For other than the sand borehole (Test GPS-4), the borehole stress gages were packaged in 6-inch-high by 6-inch-diameter plugs of the borehole backfill material to facilitate down-hole installation and to simulate actual field procedures. For the sand borehole (Test GPS-4), the stress gages were lowered into position with a special placement tool and dry sand was rained to fill the borehole to the next instrument level (this placement technique is described in References 7 and 8).

A.4 LABORATORY MATERIAL PROPERTIES

A series of laboratory uniaxial strain and triaxial compression

---

[1] References mentioned in this appendix are listed in the References at the end of the main text.

[2] J. S. Zelasko and E. B. Perry, unpublished data.

tests was conducted on the four materials used for this study to provide a basis for quantifying material differences and similarities and for use in possible future wave propagation analysis of the six experiments.

The dynamic uniaxial strain response characteristics of the three materials used in the first four experiments, i.e., buckshot clay, Cook's Bayou sand, and a soft artificial soil (a mixture of bentonite clay, gypsum cement, water, and Type III high-early strength portland cement), are depicted in Figure A.1. The stress-strain response of the sand is considerably different from that of the buckshot clay and the artificial soil, whereas the clay and the soil exhibit a reasonable similarity. The formula for the artificial soil is given in Appendix D.

The corresponding dynamic shear strength characteristics of the clay, the artificial soil, and the sand are compared in Figure A.2. As in the case of stress-strain response, the shear strength of the sand shows a large disparity from that of the clay and the artificial soil, which are quite similar.

The material properties of the clay-backfilled borehole (Test GPS-2) were intentionally the same as those of the clay matrix. Likewise, the artificial soil used for Test GPS-3 was designed to match closely the clay matrix properties. Thus, gages embedded in these boreholes would be expected to respond like the free-field gages. On the other hand, the relatively large stiffness and strength differences between the sand and the clay (Test GPS-4) suggested that gages in the sand borehole would respond differently.

To augment study of the effects of a stiff borehole (Test GPS-4) in a relatively soft material, a final specimen was prepared in which the borehole material was designed to be much softer than the free-field material. This specimen (P1-5) was constructed with two artificial soils whose constituents are detailed in Appendix D. The matrix artificial soil had a 10 percent cement content to achieve high stiffness and strength. The borehole filler material was the sand/3 percent cement mix as used in Specimen P1-3, but with a longer curing time. The

stress-strain response characteristics of these two materials are compared in Figure A.3. The effect of cyclic loadings in uniaxial strain on the stress-strain response is also shown in the figure. The stiff material appeared to be weakened slightly after first loading, but maintained a roughly similar response envelope. On the other hand, the soft material experienced a loss of its cementation characteristics after only one cycle (the initial reloading response is softer than the initial virgin loading response) as well as a loss of air-filled porosity (i.e., it compacted irreversibly). The shear strength of the free-field material was some seven times greater than that of the borehole material (Figure A.4.)

A.5 TEST RESULTS

In comparing stress measurements in the clay borehole (Test GPS-2) with those in the surrounding free field (Reference 1), excellent comparison was noted in both phasing and amplitude of the wave forms. The same was generally true for the artificial soil borehole (Test GPS-3) and its associated free field, indicating that impedance matching attempts with these borehole materials were successful.

However, striking differences appeared in the vertical stress wave forms for Specimen P1-4, containing the sand-filled borehole (Test GPS-4). Although the wave forms were essentially in phase, the borehole amplitudes exceeded those of the free field by a factor of two at early times, indicating that the higher impedance and shear strength characteristics of the sand dominated the test phenomenology. In earlier studies of the SE stress gage response (References 7 and 8), it was determined that gage overregistration factors of 1.25 could be expected at stress levels in dense sand, while negligible overregistration could be expected for similar conditions in buckshot clay. Thus, because overregistration alone does not account for the observed disparities, it is concluded that clay-sand interaction, i.e. stress redistribution, occurred during this test as a direct consequence of the borehole impedance mismatch.

The stresses measured in the soft artificial soil borehole of Test GPS-5 were significantly lower than those of any of the other borehole/free-field conditions evaluated. This is another example of the stress redistribution phenomenon, but opposite to that observed in the sand (stiff) borehole of Test GPS-4. The applied stress field in Test GPS-5 was altered by the soft inclusion (borehole) such that a portion of the load was transferred to the surrounding stiffer material.

To illustrate the relative effects of the various placement conditions studied, the incident borehole stress peaks were normalized for each test to the corresponding free-field peaks and plotted against depth (Figure A.5). The uniform clay specimen with a borehole (Test GPS-1) gave unity response as expected. Data from both the clay borehole of Test GPS-2 and the artificial soil borehole of Test GPS-3 were consistent, but slightly below the data for the uniform clay (Test GPS-1). The sand borehole (Test GPS-4) gave the opposite response at a factor exceeding two. The artificial soft borehole in Test GPS-5 gave a very low response, averaging only 0.26 times that of the free field. It is obvious from these results that critical attention must be given to borehole-filler/free-field impedance matching if reasonable stress gage response is desired in field experiments.

TABLE A.1 BACKGROUND STUDY TEST PROGRAM

Test Matrix No.	Test No.	Free-Field/Borehole Materials	$\frac{B_{bh}}{B_{ff}}$ [a]	$\frac{\rho_{bh}}{\rho_{ff}}$ [b]	Applied Surface Load psi	Comments
P1-1	GPS-1	Uniform buckshot clay	1	1	200	Control test, uniform specimen conducted in SBLG (H = 6 ft) with rigid base
P1-2	GPS-2	Buckshot clay/ buckshot clay	1	1	200	Conducted in SBLG (H = 6 ft) with rigid base
P1-3	GPS-3	Buckshot clay/ matching artificial soil	1.5	1	200	Conducted in SBLG (H = 6 ft) with rigid base
P1-4	GPS-4	Buckshot clay/Cook's Bayou sand	8	1	200	Conducted in SBLG (H = 6 ft) with rigid base
P1-5	GPS-5	Stiff artificial soil/soft artificial soil	0.14	1	300	Conducted in SBLG (H = 10 ft) with rigid base
	GPS-6	Same as GPS-5	0.14	1	300	Repeat test on Specimen P1-5

[a] Stiffness ratio, borehole (bh) to free field (ff).
[b] Density ratio, borehole (bh) to free field (ff).

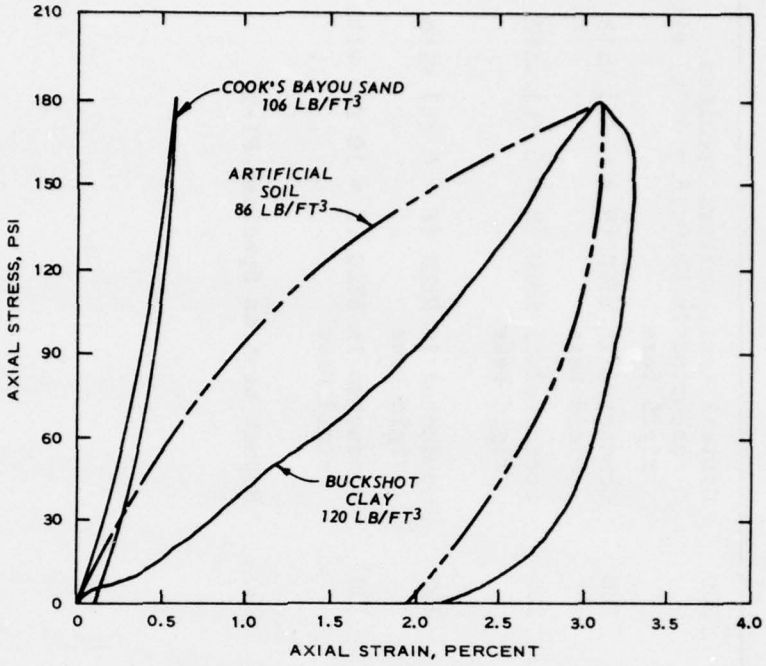

Figure A.1 Comparisons of dynamic stress-strain response in uniaxial strain; comparison between buckshot clay, Cook's Bayou sand, and GPS-3 artificial soil.

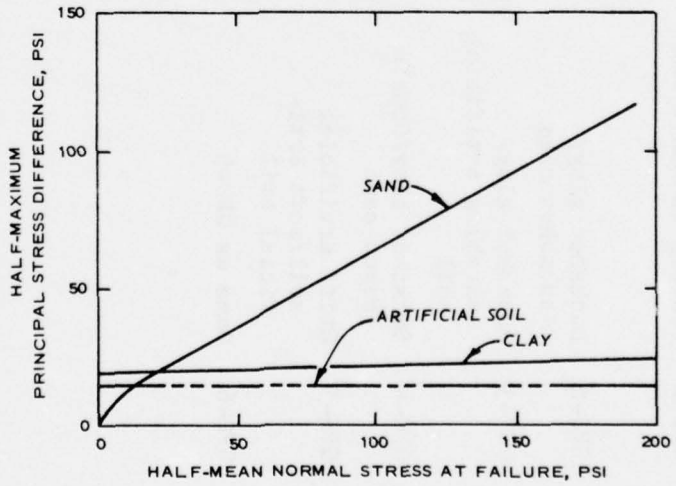

Figure A.2 Comparisons of dynamic shear strength envelopes, buckshot clay, Cook's Bayou sand, and GPS-3 artificial soil.

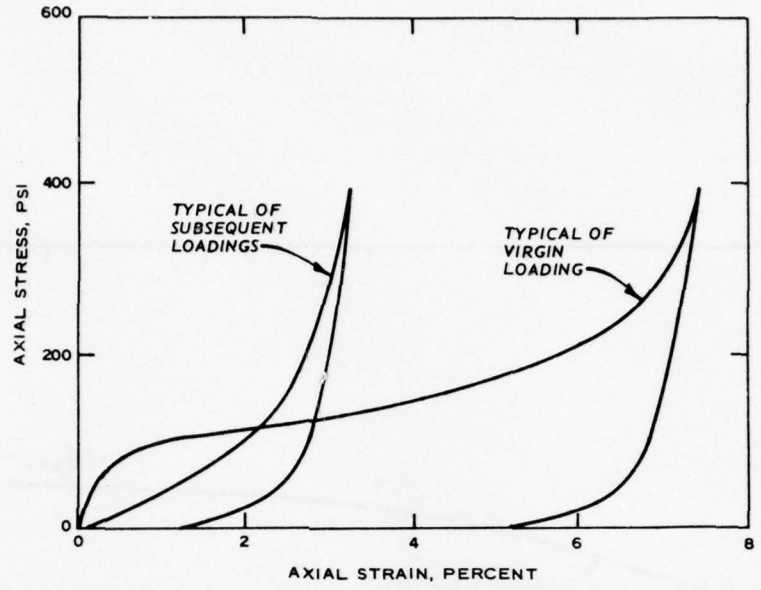

a. GPS-5 SOFT BOREHOLE MATERIAL, 3 PERCENT CEMENT

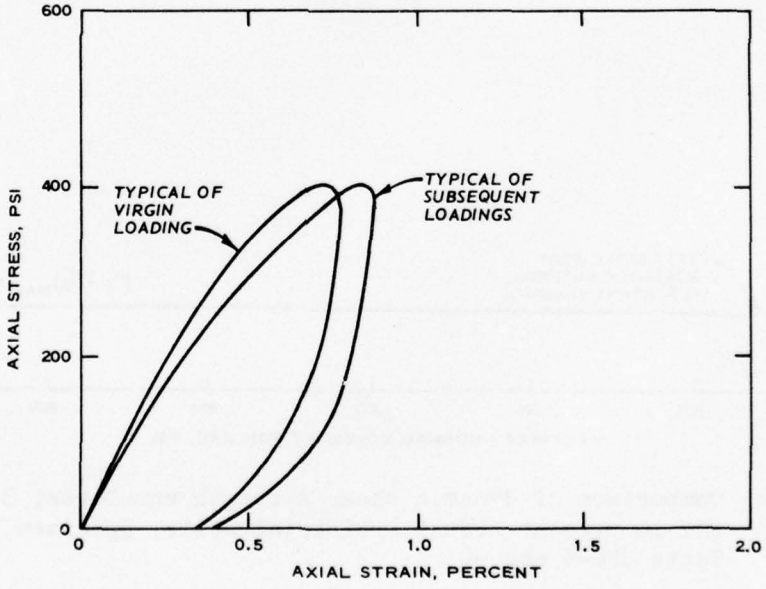

b. GPS-5 STIFF BOREHOLE MATERIAL, 10 PERCENT CEMENT

Figure A.3 Dynamic stress-strain response in uniaxial strain; comparison between 3 percent and 10 percent cement artificial soils for virgin and repeated loadings, Specimen P1-5, Test GPS-5.

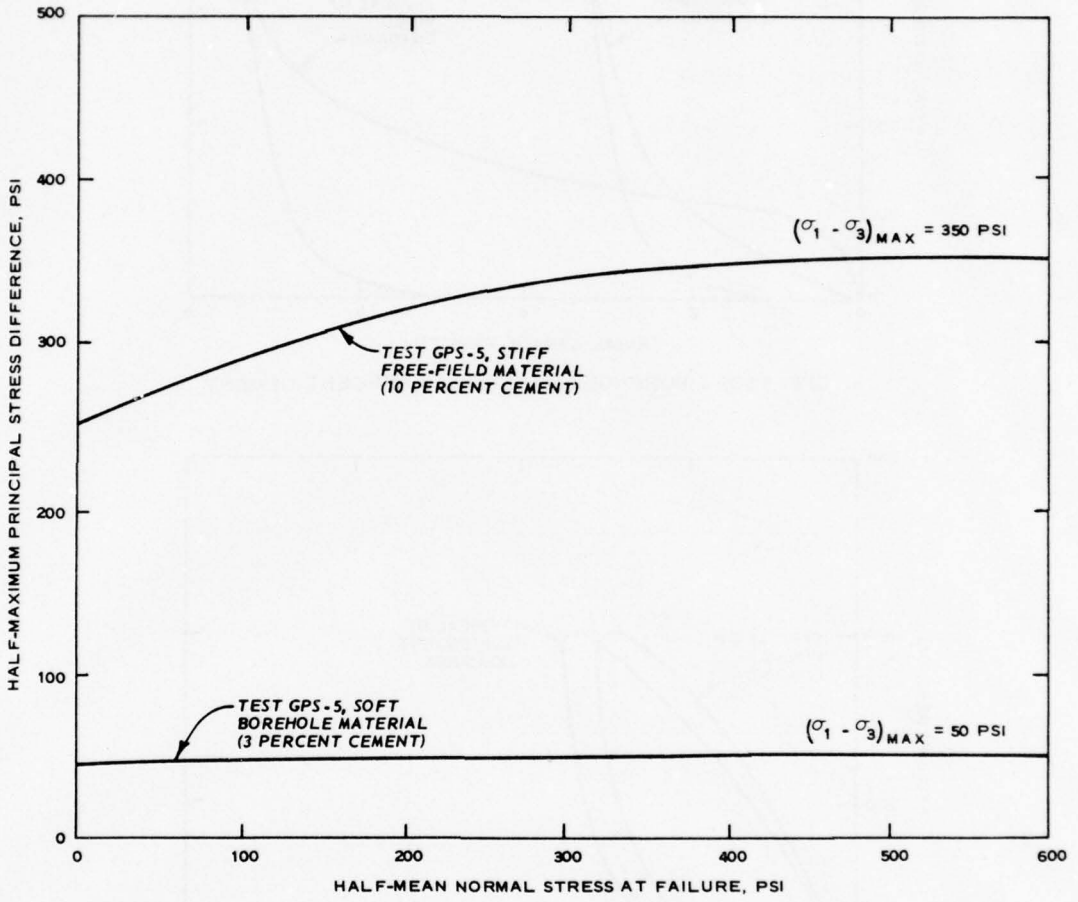

Figure A.4 Comparison of dynamic shear strength envelopes; 3 percent and 10 percent cement artificial soils, Specimen P1-5, Tests GPS-5 and -6.

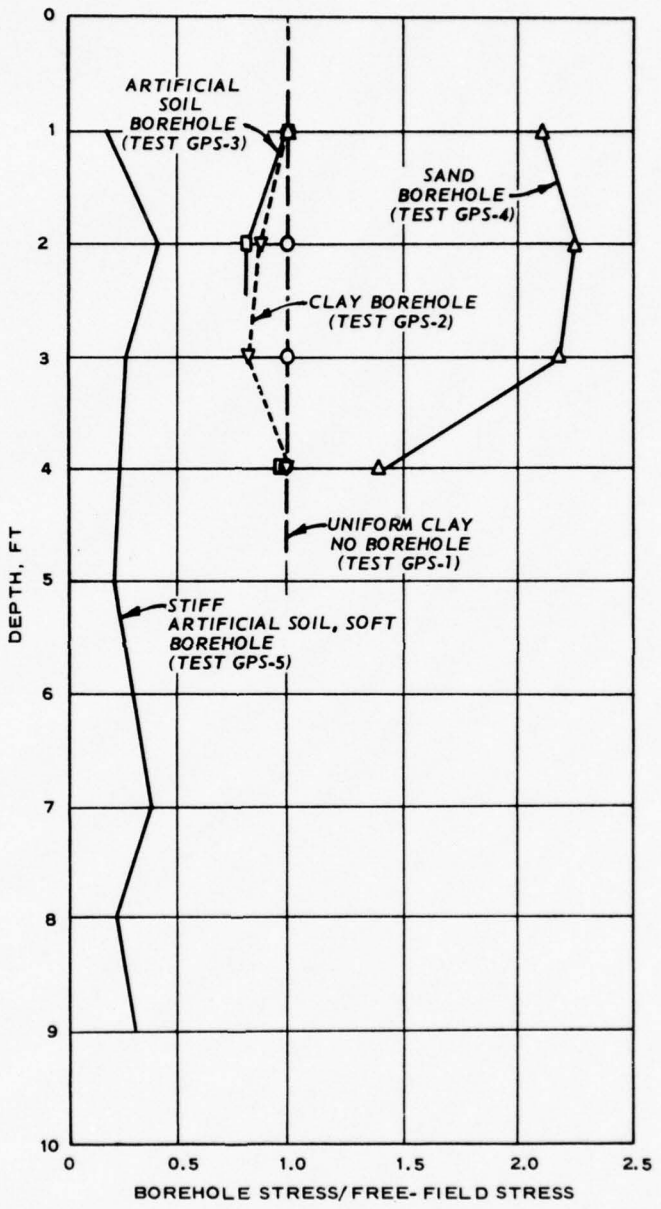

Figure A.5 Normalized peak incident stress as a function of placement condition and depth, Tests GPS-1 through -5.

APPENDIX B

CBMI MATERIAL PROPERTIES SUPPORT

Laboratory material property tests were performed on samples of most of the materials used in constructing the five SBLG specimens involved in the CBMI program. Samples of the first two CBMI specimens (P2-1 and P2-2) were prepared by diverting a portion of the single pour used to cast each 4-foot-diameter by 6-foot-high specimen into 5-inch-diameter steel sample tubes. In addition to these samples, poured 3- and 6-inch-diameter cardboard tube samples and "pushed" 5-inch-diameter steel tube samples were obtained for subsequent CBMI specimens. For Specimen PS-4, a large (4-foot-diameter by 4-foot-high) uninstrumented companion specimen was cast in an auxiliary set of SBLG rings so that block samples and steel tube samples could be extracted after the specimen had cured.

Laboratory material property tests conducted in support of the final three CBMI specimens (P2-1, P2-2, and P2-3) were performed using samples supplied by the CBMI project engineer. The resulting test data were furnished to him via internal memo for his use in selecting calculational properties for early AA calculations (References 3 and 9[1]). For specimens P2-4 and P2-5, however, SDD personnel not only conducted numerous material property tests, but actively participated in the specimen casting and material sampling operations and performed pertinent analysis of the laboratory test data to derive recommended calculational properties of subsequent AA analysis (Reference 2).

Several questions arose during the course of the CBMI study concerning capability to cast truly homogeneous test specimens and obtain truly representative laboratory test samples. The implications of those questions are nested in related questions (References 3 and 9) concerning the ability to characterize the CBMI materials properly

---

[1] References mentioned in this appendix are listed in the References at the end of the main text.

for calculational purposes. These questions will be discussed in the following sections.

B.1 EARLY TESTS, SPECIMENS P2-1 THROUGH P2-3

The applicability of the calculational properties selected for the early CBMI tests, i.e. CBMI-1 through -9, was questionable due to unresolved questions concerning internal inconsistencies in the experimental data (particularly for Specimen P2-1, Reference 3), questions on the representativity of the artificial soil samples and their preparation procedures, and problems in constructing homogeneous specimens (particularly for Specimen P2-3, which required numerous pours to accommodate its more elaborate free-field gage installation plan). Consequently, of the material property information obtained for CBMI-1 through -9, only those test results selected by the CBMI project engineer for CBMI-5 are presented herein. The properties selected for AA's calculations of CBMI-1, however, are documented in Reference 3.

The selected dynamic stress-strain relation and corresponding dynamic failure relation for the CBMI-5 free-field artificial soil are shown in Figure B.1. The selected stress-strain and failure relations for the CBMI-5 borehole filler material are shown in Figure B.2.

B.2 SPECIMEN P2-4, TEST CBMI-10

Analysis of the data obtained from the first three artificial soil specimens indicated that more complete instrumentation and material property test support were necessary to resolve inexplicable conflicts between the SBLG data and the code calculations performed by AA. Specimen P2-4 was therefore constructed as a second uniform free-field matrix without a borehole. During construction, emphasis was placed on mix quality control to ensure a high degree of homogeneity in this specimen. This was evaluated by obtaining numerous 3-inch-diameter cardboard tube samples of the various pours used to construct the specimen, which were subsequently used in conducting laboratory index tests such as water content, density, and static unconfined strength for

the CBMI-10 experiment strength tests.

One-dimensional wave propagation analysis performed at WES for the CBMI-10 experiment using calculational properties recommended by SDD personnel showed poor agreement with the measured vertical motion and stress-time histories; the calculations showed that the laboratory-based properties were too soft. Three important explanations were hypothesized for this discrepancy:

1. Thermal effects. The curing characteristics of the large SBLG specimen differed from those of the poured 5-inch-diameter samples used for uniaxial strain testing, i.e., the temperature of the large mass of artificial soil in the SBLG remained elevated throughout the curing period whereas the temperature of the small tube samples decreased rather quickly after casting. This environmental difference would result in a dryer, stiffer, and stronger material in the SBLG (which was the observed trend).

2. SBLG specimen nonhomogeneity. The samples poured for laboratory testing were prepared from only one of the numerous pours that went into the larger SBLG specimen. Unfortunately this particular pour proved to have an anomalously high water content. The qualitative effect of this anomaly would be a reduction in stiffness and strength (which also helps to explain the analysis-data discrepancy).

3. Sidewall friction effects. Friction between the SBLG specimen and the containment vessel walls (possibly enhanced by the expansive characteristics of the CBMI-10 artificial soil) would have resulted in an apparent stiffening of the material via load transfer to the walls.

A more extensive series of material property tests subsequently performed in support of Test CBMI-12 (Specimen P2-5, which proved to be nonhomogeneous) provided a sufficient data base for adjusting the original CBMI-10 properties to account for the mechanical effects of the water content anomaly (Subparagraph 2) but not for the thermal or sidewall friction effects. Hence, revised calculational properties were recommended for Test CBMI-10. Figure B.3 shows these revised relations.

B.3 SPECIMEN P2-5, TEST CBMI-12

Analysis of the quality control (index) tests conducted for Specimen P2-5 indicated that a three-layered system had been achieved rather than the desired homogeneous specimen. The three-layered system consisted of a layer of relatively stiff material sandwiched between two layers of relatively weaker material. The geometry and composition properties of this specimen are shown in Figure B.4, which also depicts the recommended uniaxial-strain/stress-strain relations for each layer as well as the relation for the borehole-filler material. An average stress-strain relation for the entire specimen is also shown in the figure. Figure B.5 shows the failure envelopes and uniaxial strain-stress path relations corresponding to the stress-strain curves of Figure B.4.

B.4 SPECIMEN P2-5, TESTS CBMI-13 and CBMI-14

The CBMI-13 experiment consisted of a repeat shot on the CBMI-12 free-field specimen, but with fresh borehole filler materials. For this shot the borehole gages were surrounded locally with a very hard canister-locking grout (for which no property tests were conducted) and the gaps between the gages filled with the same soft borehole filler material as used for CBMI-12 (no additional property tests were conducted to verify this specifically).

CBMI-14 was a repeat shot on the CBMI-13 free-field specimen, but with fresh borehole materials; the borehole in this case was uniformly filled with a hard borehole filler grout for which material property tests were conducted.

No samples were taken from the free-field specimen before CBMI-13 was conducted; hence, no direct property determinations were made for the CBMI-13 free-field specimen. However, samples were taken from the free-field specimen after the CBMI-13 shot and prior to the CBMI-14 shot, and laboratory material property tests were conducted. Unfortunately, these samples were disturbed due primarily, it is believed, to the effects of horizontal stress relief, i.e., it is highly

probable that large horizontal stresses existed in the CBMI-12, -13, and -14 free-field specimens as a result of (1) the expansive cement used in the material mix, and (2) the specimen's loading history. Factor (2) is pertinent only to shots 13 and 14. The magnitudes of these horizontal stresses are unknown; therefore, the property tests were conducted under questionable initial conditions and the results cannot be considered representative of the in-place specimen.

Consequently, because of the lack of appropriate free-field matrix property data and because of uncertainties surrounding their previous loading histories, the problems of recommending free-field properties for CBMI-13 and -14 were approached from a bounds point of view, i.e., probable upper- and lower-bound properties were recommended for assumed homogeneous specimens. These bounds can be used by calculators as a basis for choosing the probable free-field properties for each experiment. Recommended uniaxial-strain/stress-strain bounds for the CBMI-13 and -14 specimens are shown in Figure B.6. One failure envelope was recommended for modeling the CBMI-13 and -14 free-field specimens, i.e., that of the pseudo-homogeneous material of CBMI-12 with bounds of $\pm$15 percent (in shear) to accommodate the various uncertainties concerning specimen inhomogeneity (due to casting and/or loading history) as well as the extra cure times sustained between the individual experiments.

The uniaxial strain-stress path corresponding to the lower-bound stress-strain relation is the one recommended for the CBMI-12 pseudo-homogeneous material (Figure B.5). A constant value of Poisson's ratio $\nu = 0.45$ was recommended for the upper-bound relation.

For the soft borehole filler used in CBMI-13, calculational properties for the CBMI-12 filler in Figures B.4 and B.5 were recommended. For the very hard canister-locking grout, properties shown in Figure B.7, which are based on a few laboratory tests conducted earlier in support of CBMI-8, were recommended.

For the hard borehole filler grout used in CBMI-14, calculational properties shown in Figure B.8 were recommended.

B.5 ASSESSMENT OF SAMPLE PREPARATION, SAMPLING, AND TESTING

The following assessment is made of the preparation of artificial soil free-field specimens, placement of borehole filler and canister-locking grouts, sampling of these materials, and testing them in the laboratory.

B.5.1 Sample Uniformity

From the results of quality control tests conducted on samples taken from two 4-foot-diameter by 6-foot-high specimens and one 4-foot-diameter by 4-foot-high specimen, it is concluded that a uniform sample cannot be constructed using the methods and materials of this investigation. The following are possible ways to improve specimen construction: (1) mass-blend dry constituents, (2) mix and place larger batches of material (32 pours were required to fill the SBLG), (3) completely clean and dry mixer prior to preparing each batch, and (4) find a material to replace the bentonite clay. (Bentonite can absorb as high as 400 to 600 percent by weight of water. Small differences in temperature, hydroscopic moisture, and mixing time can make large differences in the amount of water taken on by the bentonite and thus in the material properties of the mix.)

B.5.2 Jacked Samples

Samples of the grout taken by jacking a steel tube into the SBLG samples were compressed and were no good for property testing.

B.5.3 Fixed Piston Samples

Samples taken with the fixed piston were not compressed, but the horizontal stress in the grout caused by expansive cement was relieved. The samples were good for strength testing but not for uniaxial strain testing.

B.5.4 Molded Samples

Small samples molded on the side from pours of the SBLG sample may not cure in the same way as do samples in the large mass. There is a

possiblity that more heat is built up in the large mass and maintained for a longer time, resulting in a drier, stiffer, higher strength material in the large mass than in the small samples.

It appears that the best way to take representative samples of the material from large samples is to pour small samples in a separate sample container; therefore, the curing environment of the small samples must be controlled in the same way as that of the large sample. One possible way to do this is to place the small-diameter samples in a large container, pour it full of grout, and after curing has taken place, dig out the small samples.

B.5.5 Uncertainties Associated with Artificial Soils (Grouts)

One important factor that must be recognized is that very little is known about material properties of artificial soils (grouts) and factors that affect these properties. Preparation and placement of various grouts to achieve consistent stress-strain properties for all batches necessitates much more care than in preparing and placing grouts for general-purpose uses. Since very little is known about factors that affect the stress-strain properties of grout, quality control must be stringent. It cannot be assumed that small changes in constituents, preparation methods, and placement methods will not affect the properties of the grout.

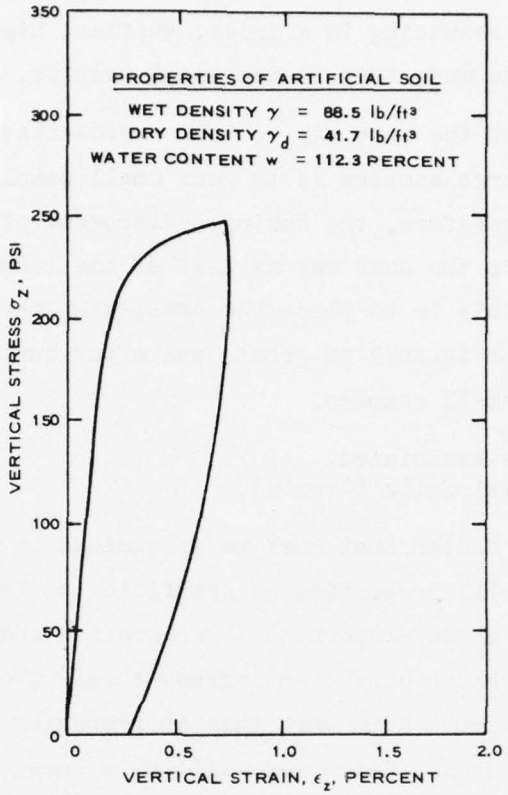

a. SELECTED DYNAMIC UNIAXIAL-STRAIN/STRESS-STRAIN RELATION

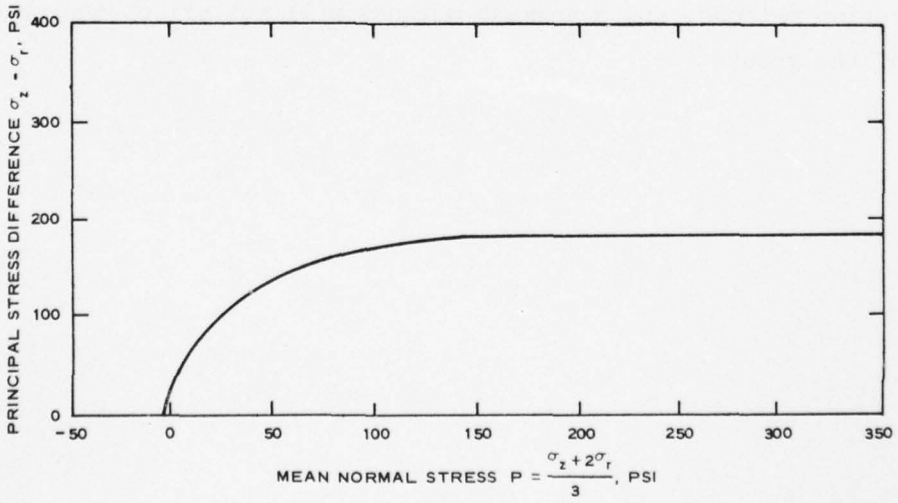

b. SELECTED DYNAMIC FAILURE RELATION

Figure B.1 Selected properties for free-field matrix, CBMI-5.

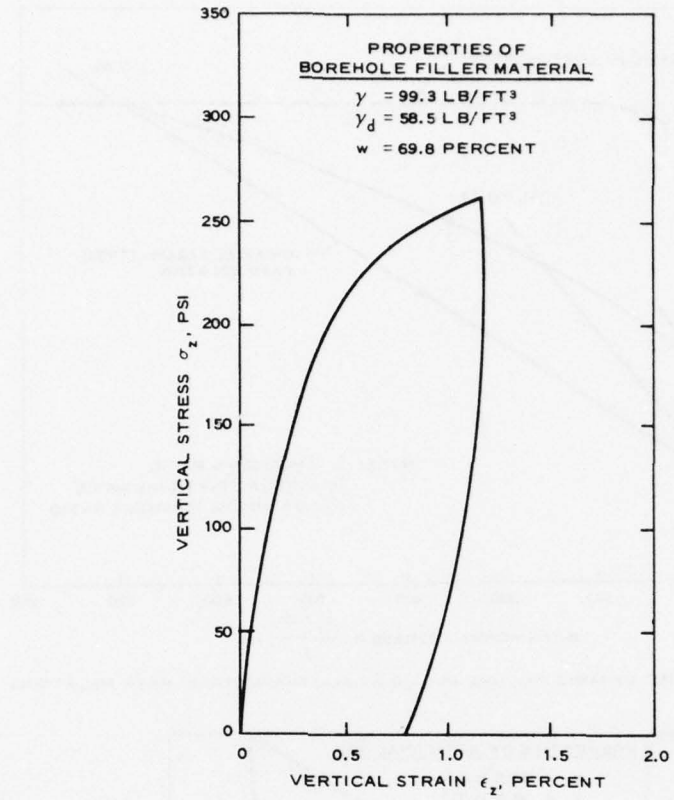

a. SELECTED DYNAMIC UNIAXIAL-STRAIN/STRESS-STRAIN RELATION

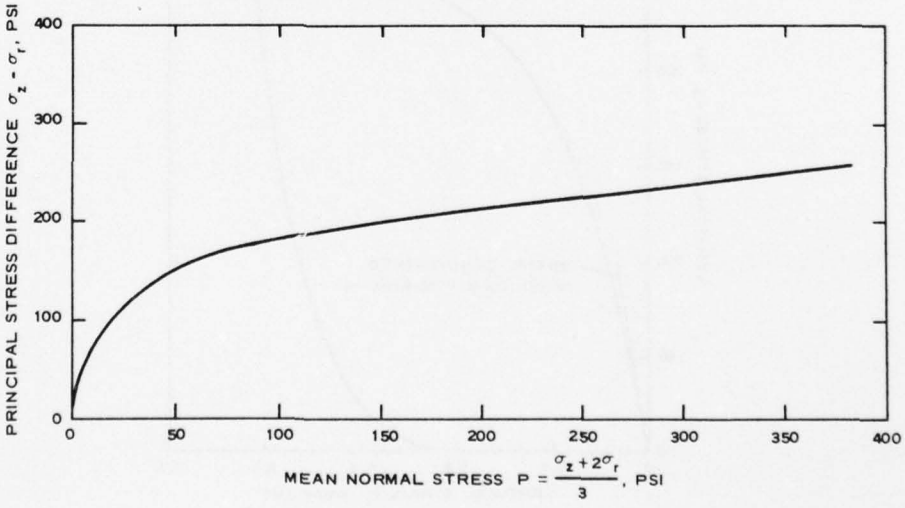

b. SELECTED DYNAMIC FAILURE RELATION

Figure B.2 Selected properties for borehole filler material, CBMI-5.

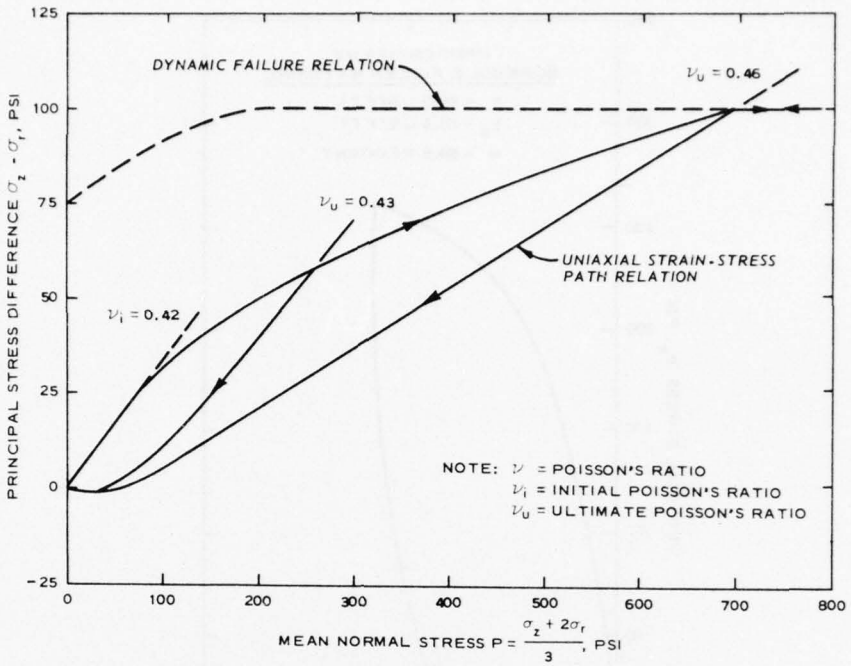

a. RECOMMENDED DYNAMIC FAILURE AND UNIAXIAL-STRAIN/STRESS PATH RELATIONS

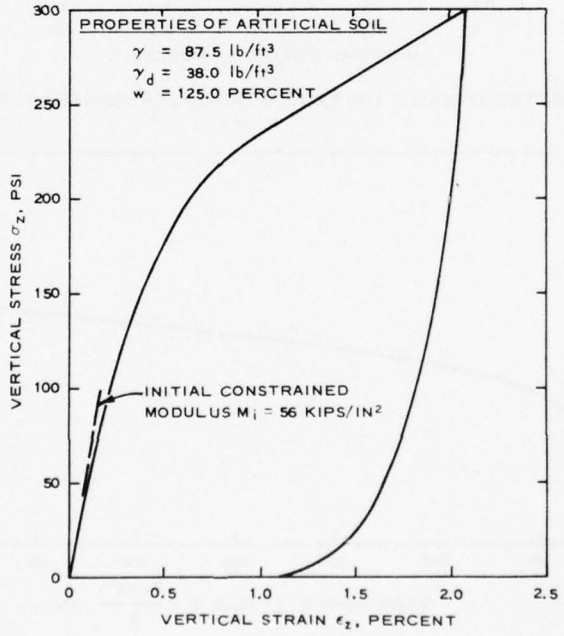

b. RECOMMENDED (REVISED) DYNAMIC UNIAXIAL-STRAIN/STRESS-STRAIN RELATION

Figure B.3 Recommended calculational properties for CBMI-10 artificial soil.

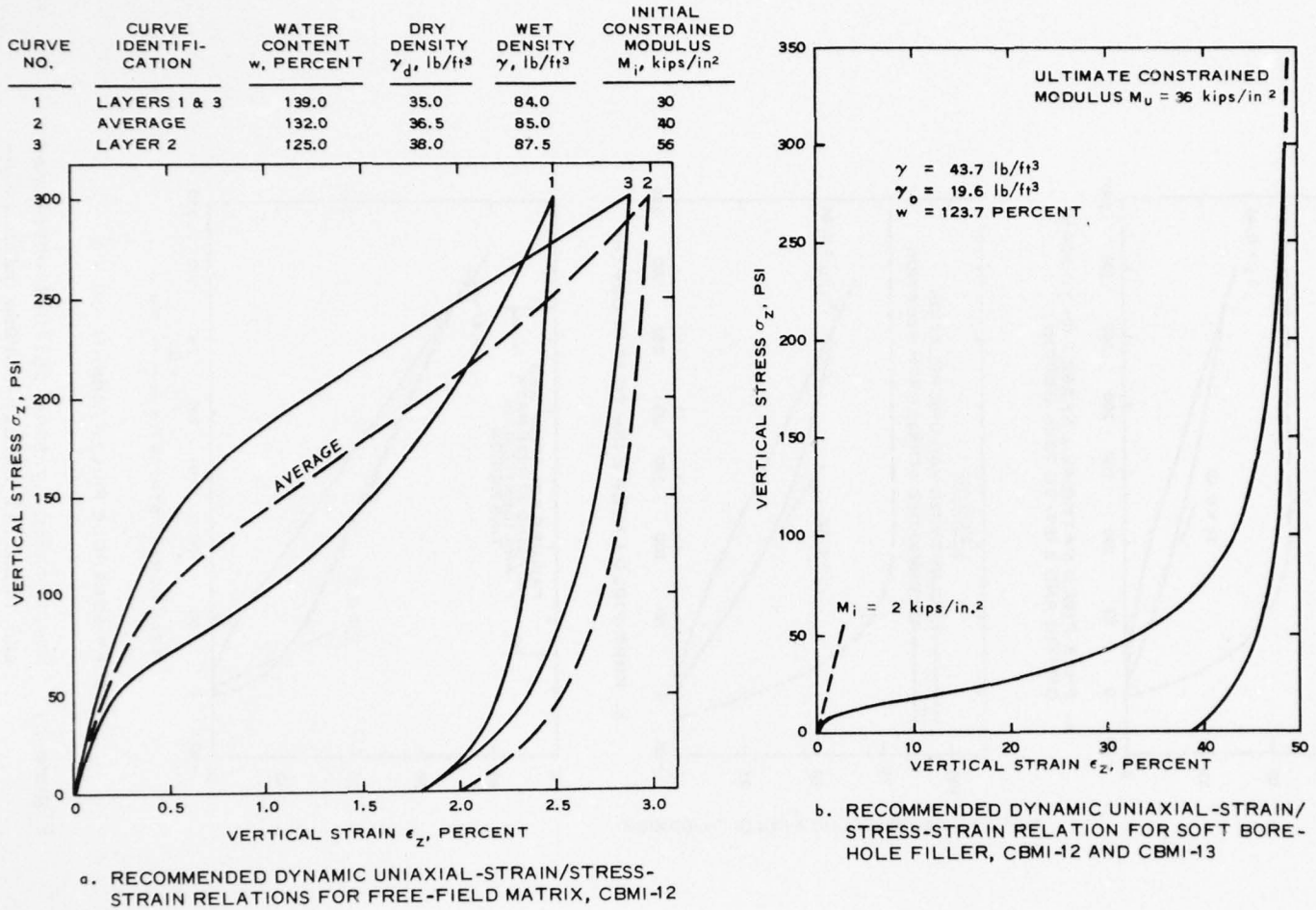

a. RECOMMENDED DYNAMIC UNIAXIAL-STRAIN/STRESS-STRAIN RELATIONS FOR FREE-FIELD MATRIX, CBMI-12

b. RECOMMENDED DYNAMIC UNIAXIAL-STRAIN/STRESS-STRAIN RELATION FOR SOFT BOREHOLE FILLER, CBMI-12 AND CBMI-13

Figure B.4 Recommended calculational properties for CBMI-12 matrix and borehole filler materials.

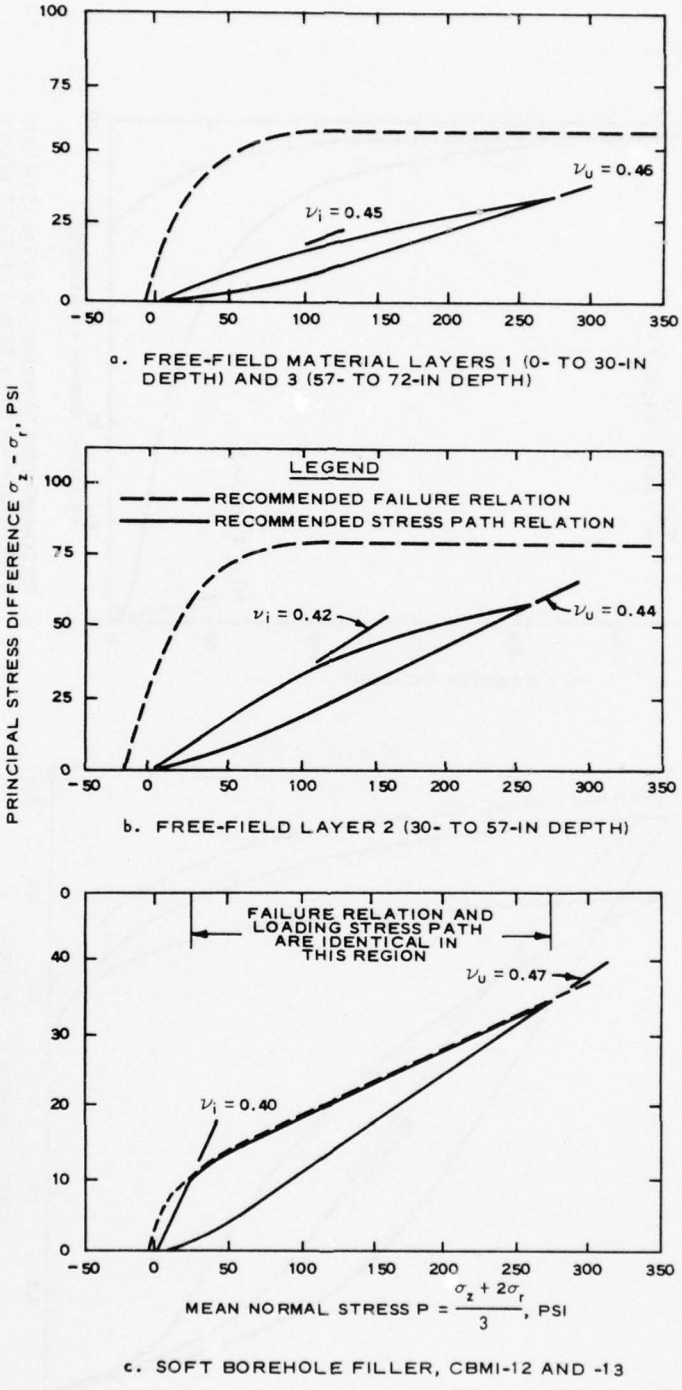

Figure B.5 Recommended dynamic failure envelopes and uniaxial strain-stress path relations for modeling CBMI-12 matrix and borehole filler materials.

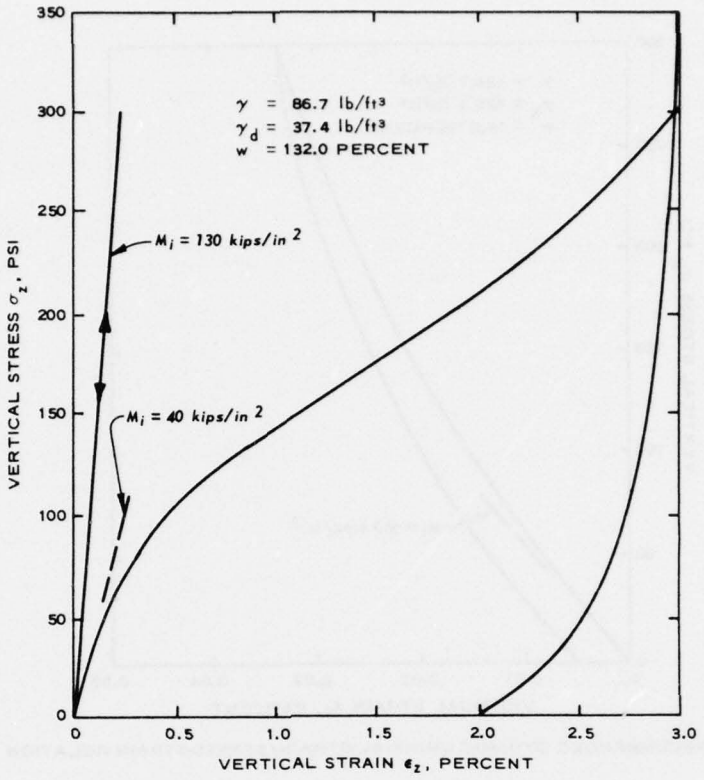

a. RECOMMENDED UPPER AND LOWER BOUND DYNAMIC UNIAXIAL-STRAIN/STRESS-STRAIN RELATIONS

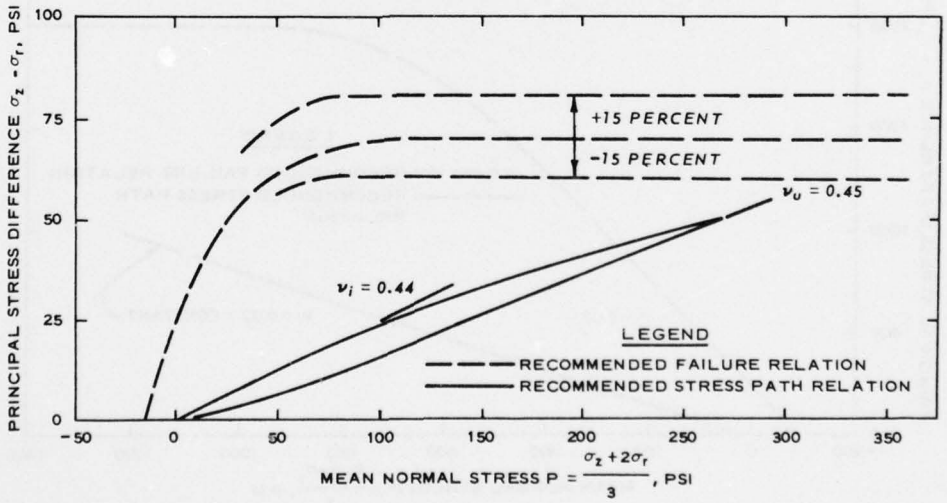

b. RECOMMENDED AVERAGE DYNAMIC FAILURE AND UNIAXIAL STRAIN-STRESS PATH RELATIONS (WITH ±15 PERCENT UNCERTAINTY) FOR CBMI-13 AND -14

Figure B.6 Recommended free-field calculational properties, CBMI-13 and -14.

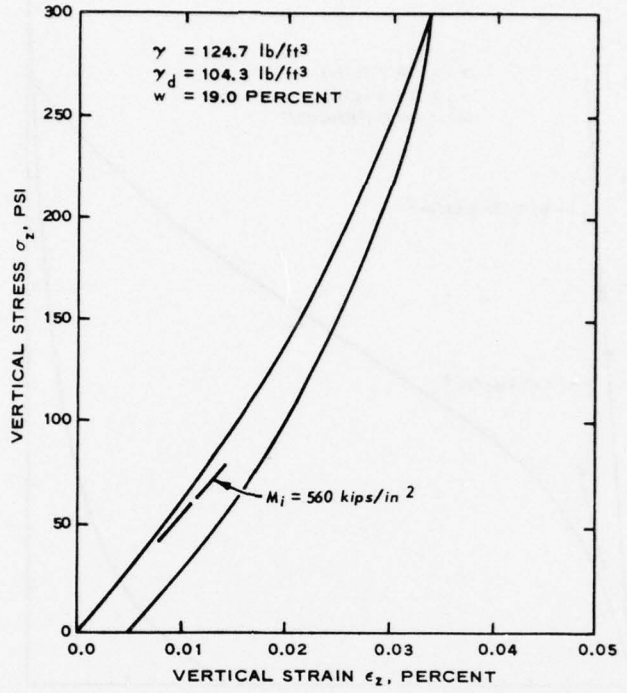

a. RECOMMENDED DYNAMIC UNIAXIAL-STRAIN/STRESS-STRAIN RELATION

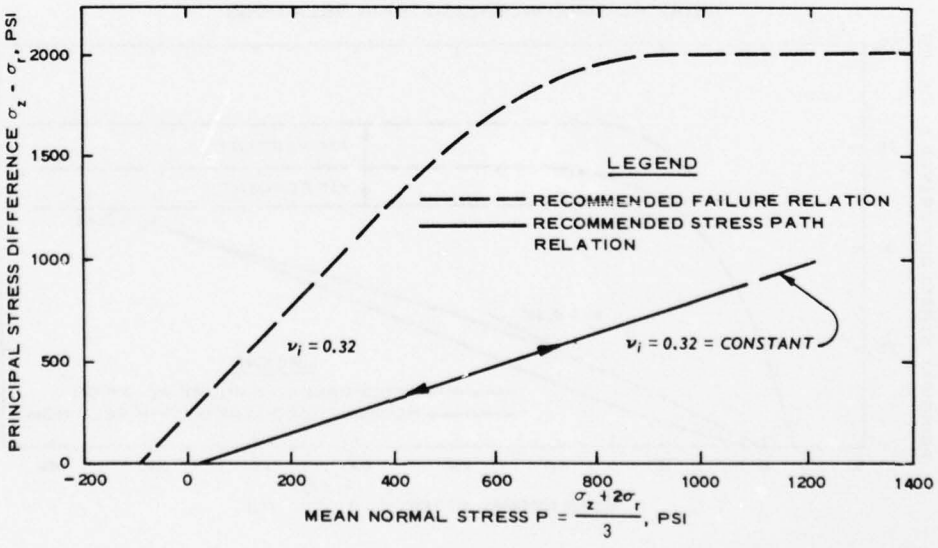

b. RECOMMENDED DYNAMIC FAILURE AND UNIAXIAL STRAIN-STRESS PATH RELATIONS

Figure B.7 Recommended calculational properties for canister-locking grout, CBMI-13.

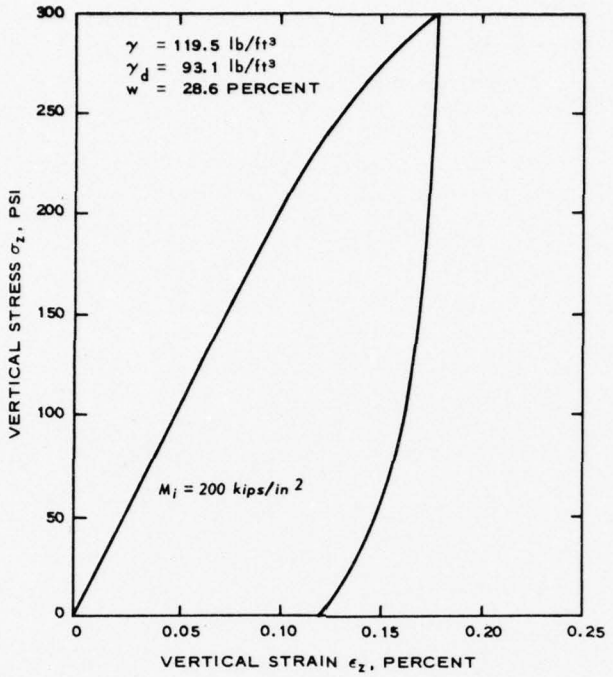

a. RECOMMENDED DYNAMIC UNIAXIAL-STRAIN/STRESS-STRAIN RELATION

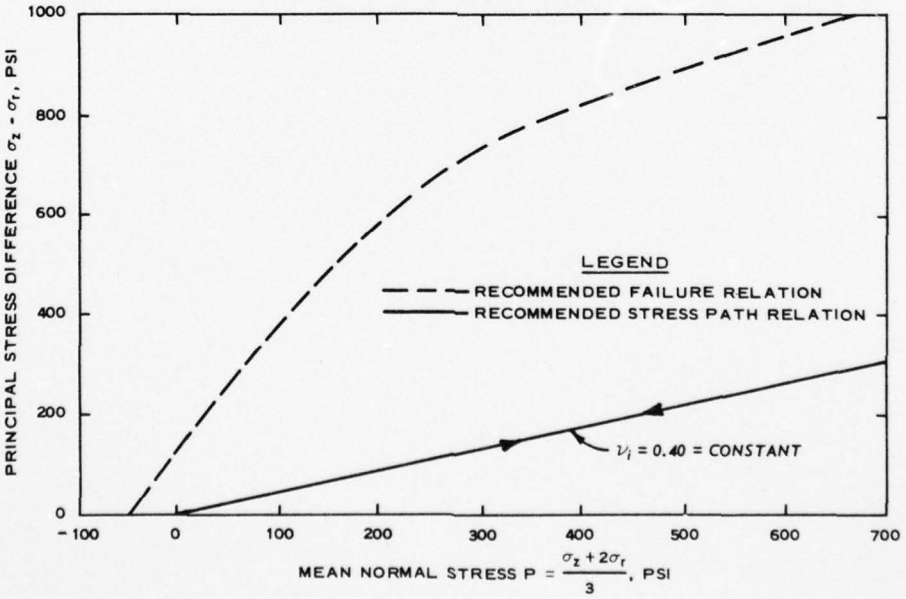

b. RECOMMENDED DYNAMIC FAILURE AND UNIAXIAL STRAIN-STRESS PATH RELATIONS

Figure B.8 Recommended calculational properties for stiff borehole filler material, CBMI-14.

APPENDIX C

CBMI INSTRUMENTATION

C.1 CBMI INSTRUMENTS

Standard instruments (Figure C.1), signal conditioners, and recording systems were used for the CBMI tests.

C.1.1 Airblast

Norwood diaphragm-type resistive gages were used to monitor detonation chamber blast pressures (Reference 10[1]). The gage consists of a force-sensitive member loaded by the diaphragm and mounted in a stainless steel case.

C.1.2 Stress

WES-developed SE stress gages were used. This gage is wafer shaped with an active diaphragm in both top and bottom surfaces (References 7 and 11). Piezoresistive strain gages are bonded directly to the diaphragms.

C.1.3 Acceleration

Endevco 2264 piezoresistive accelerometers (Reference 12) were used. This gage is similar to the models used in the background study but has a much smaller profile and mass and higher frequency response.

C.1.4 Velocity

Bell and Howell/CEC Model 4-155-0111 velocity gages (Reference 13) were used in the CBMI tests. This gage is basically a piezoelectric accelerometer with an integral electronic integrator and signal conditioner.

C.2 INSTRUMENT CANISTER

Motion instruments used in the CBMI tests were mounted in

---

[1] References mentioned in this appendix are listed in the References at the end of the main text.

cylindrical aluminum canisters (Figures C.1 and C.2). Each canister normally contained both a Bell and Howell 4-155 velocity gage and an Endevco 2264A piezoresistive accelerometer. The canister density was approximately 100 lb/ft^3.

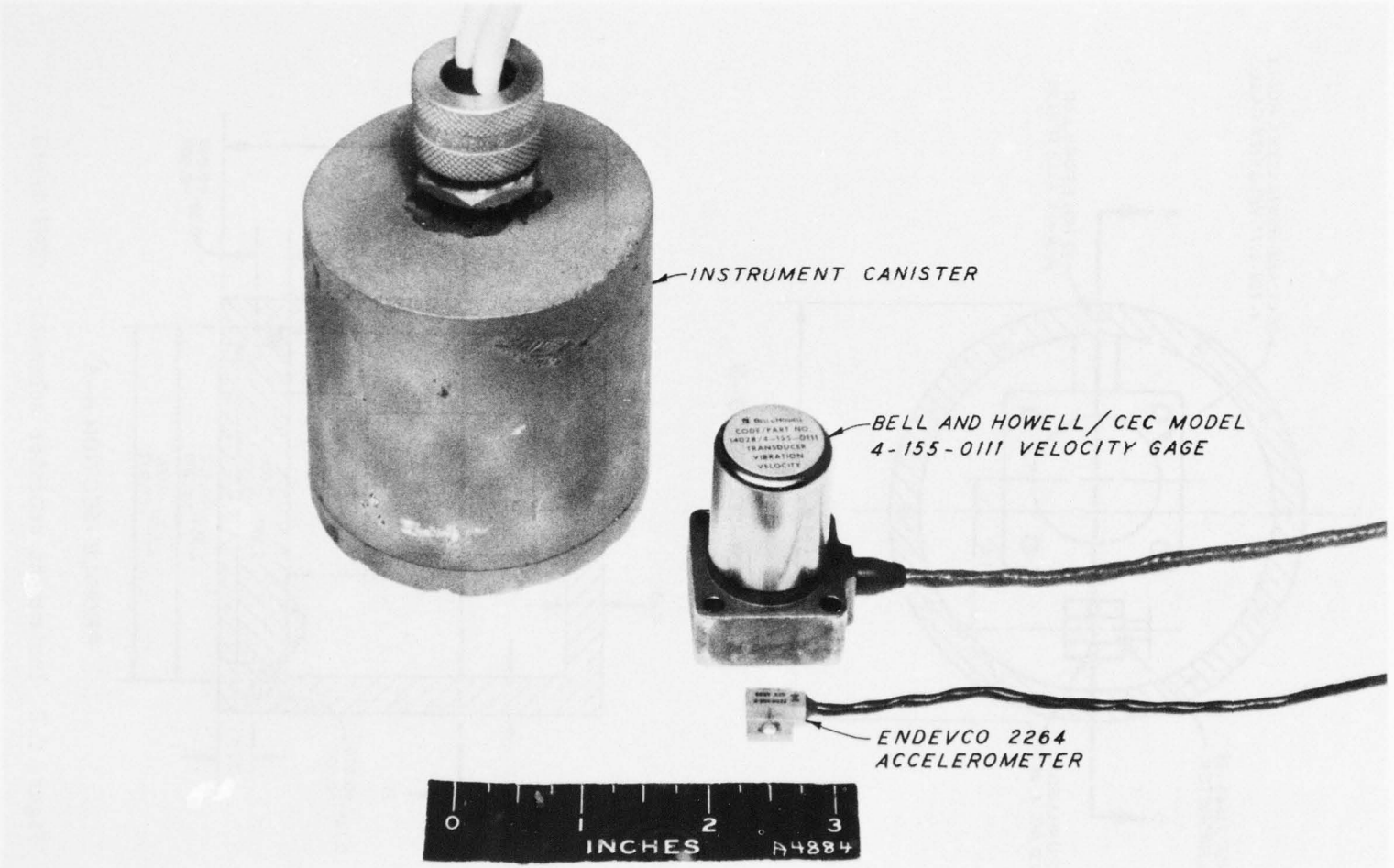

Figure C.1 CBMI instruments.

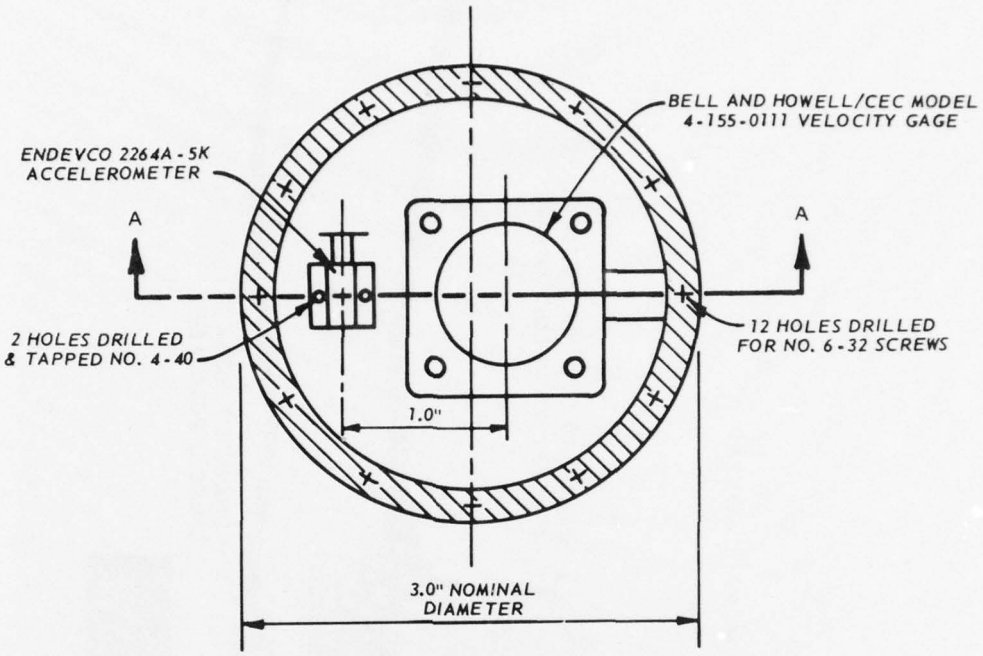

TOP VIEW–SECTION B–B

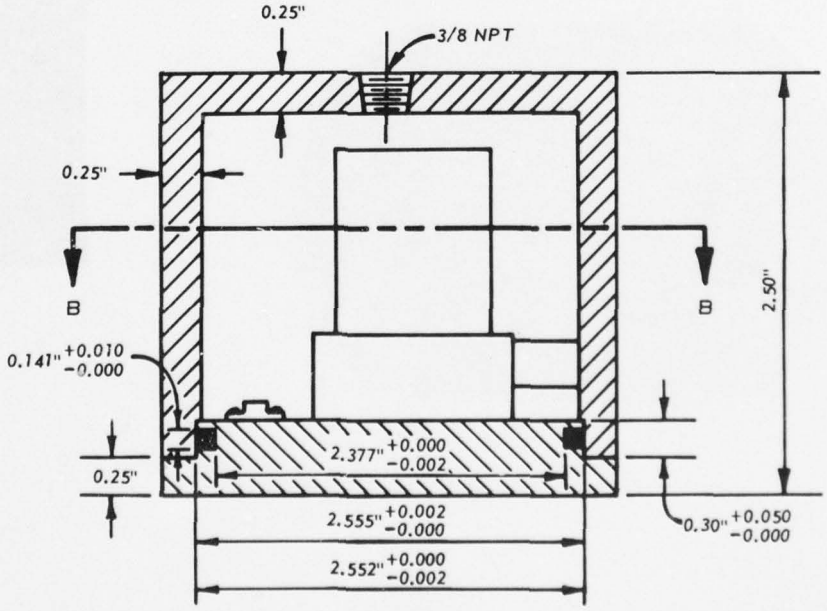

PROFILE–SECTION A–A

Figure C.2 Instrument canister schematic, CBMI tests.

APPENDIX D

ARTIFICIAL SOILS

D.1 PHILOSOPHY

In order to meet basic material properties matching requirements and handling restrictions, the development of an artificial soil for use as an instrumentation borehole backfill material was pursued. Experience had shown that naturally occurring earth materials were generally not suitable for this purpose, particularly at wet cohesive-type soil sites. A number of criteria were set up for evaluating practical borehole filler materials:

1. Readily available components.
2. Pumpable, i.e., can be mixed into a controlled slurry form.
3. Rapid setup time.
4. Nonhygroscopic when cured.
5. Ability to set up under water.
6. Nonshrinking, slight expansion upon curing.
7. Dynamic stress-strain and strength response characteristics tailorable to those of a variety of natural earth materials.
8. Density approximately that of active earth materials.
9. Economical.

A survey was made of readily available materials that might be adaptable to this purpose. Several materials had already seen much service in grouting and earth-drilling operation, e.g., bentonite, gypsum cement, and portland cement. These materials were investigated further and appeared to be likely candidates for the proposed pseudo-soil. Bentonite is a platy, relatively uniform, fine-grained montmorillonitic clay used to hold drill holes open and to seal their sidewalls. It swells when wet. Gypsum cement has often been used in conjunction with bentonite as a quick-setting binder. The addition of portland cement to such a binder would give predictable long-term strength to the admixture. Substitution of Chem-Stress, a highly expansive cement, for Type I or II portland cement would help ensure a firm bond of the

AD-A045 999 ARMY ENGINEER WATERWAYS EXPERIMENT STATION VICKSBURG MISS F/G 19/4
EFFECTS OF INSTRUMENT CANISTER PLACEMENT CONDITIONS ON GROUND S--ETC(U)
SEP 77 J K INGRAM, M B FORD

UNCLASSIFIED WES-TR-N-77-5 NL

2 OF 2
AD
A045999

END
DATE
FILMED
11-77
DDC

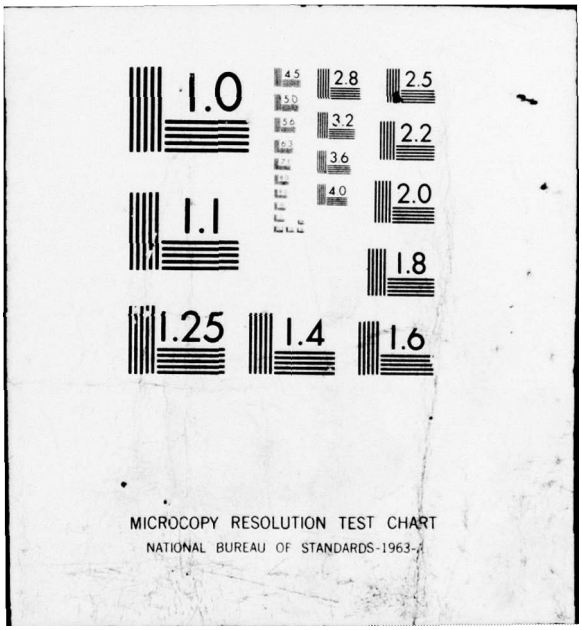
1.0
1.1
1.25
1.4
1.6
1.8
2.0
2.2
2.5
2.8
3.2
3.6
4.0
4.5
5.0
5.6
6.3
7.1
MICROCOPY RESOLUTION TEST CHART
NATIONAL BUREAU OF STANDARDS-1963-A

grout to the borehole walls (free field).

D.2 CBMI ARTIFICIAL SOIL FORMULAS

Formulas for the various artificial soils used in the CBMI study are given in Tables D.1 and D.2. The basic constituents used in all mixes were portland cement (and/or expanding Chem-Stress cement), bentonite clay, gypsum cement, and water. An air-entrainment additive was used for Tests CBMI-12 and -13 to obtain a low-stiffness borehole filler material. The use of entrained air simultaneously produced the somewhat undesirable side effect of a significant reduction in material density.

Laboratory sonic wave velocities for the artificial soils used in the background study were found to be proportional to the portland cement content (Figure D.1). No laboratory wave velocity tests were conducted for the CBMI materials.

TABLE D.1 ARTIFICIAL SOIL FORMULAS FOR BACKGROUND STUDY

Material	Percent by Weight		
	Test GPS-3	Tests GPS-5 and GPS-6	
	Borehole	Free Field	Borehole
Gypsum cement (Cal-Seal)[a]	30	30	30
Bentonite clay (Aquagel)[b]	15	15	15
Portland cement (Type III)	3	10	3
Water	52	45	52

[a] Cal-Seal, trade name, United States Gypsum Company.
[b] Aquagel, trade name, Baroid Division, National Lead Company.

TABLE D.2 ARTIFICIAL SOIL FORMULAS FOR CBMI STUDY

	Free Field					Borehole Filler							Canister Locking-Grout
	Test No.					Test No.							Test No.
Material	P2-1	P2-2	P2-3	P2-4	P2-5	CBMI 1,2	CBMI 3,4	CBMI 5-7	CBMI 8,9	CBMI 10,11	CBMI[a] 12,13	CBMI 14	CBMI 8,9,13
Gypsum cement (Cal-Seal)	23.3	26.0	20.0	20.0	20.0	--	23.0	23.7	24.3	--	20	24.0	31.6
Bentonite clay (Aquagel)	13.0	14.0	10.0	14.0	14.0	--	12.0	9.1	14.5	--	14	4.0	--
Portland cement Type I	--	--	--	5.0	--	--	--	--	--	--	--	--	--
Chem-Stress II[b]	14.5	9.0	10.0	5.0	10.0	--	15.0	9.1	9.7	--	10.0	10.0	10.5
Sand	--	--	20.0	--	--	--	--	18.1	--	--	--	39.0	42.1
Water	49.2	51.0	40.0	56.0	56.0	--	50.0	40.0	51.0	--	56.0	23.0	15.8
CFR-2[c]	--	0.004	--	--	--	--	--	0.004	--	--	--	--	--

[a] An air-entraining agent was used to add 50 percent air by volume to this mix.
[b] Chem-Stress II, Type K, self-straining, highly expansive cement. Proprietary product of Southwestern Portland Cement Company, Victorville, California.
[c] CFR-2 is a wetting agent added as a small percentage of the cementitious materials.

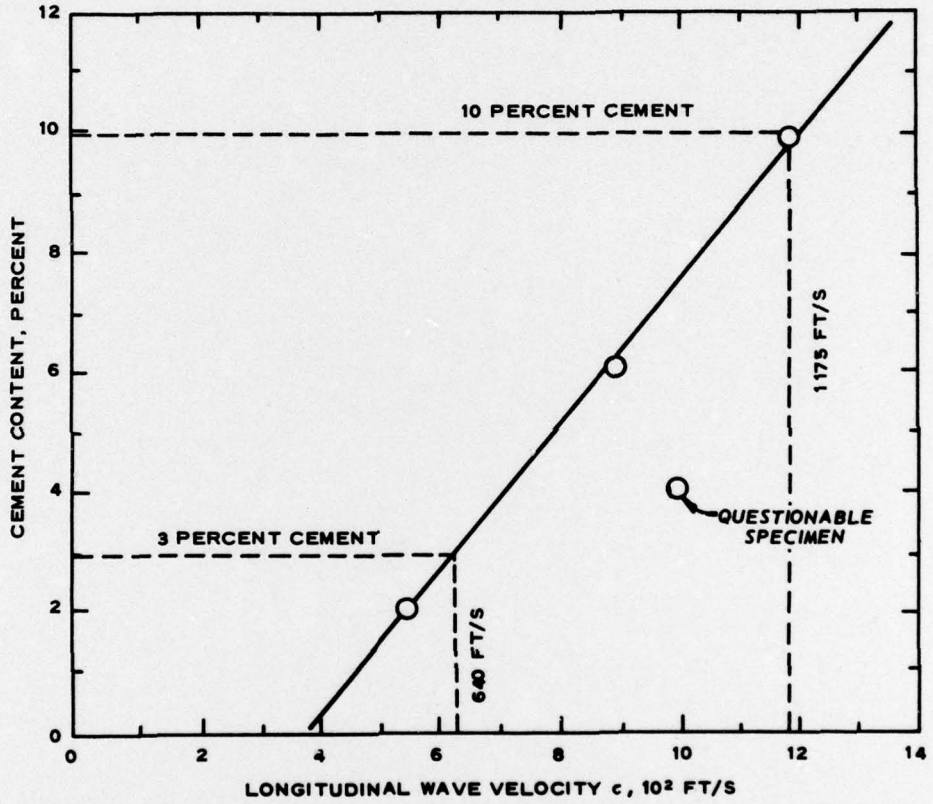

Figure D.1 Empirical relation between wave velocity and cement (portland or Chem-Stress) content for artificial soils of background study.

DEPARTMENT OF DEFENSE

Assistant to the Secretary of Defense
Atomic Energy
46886 ATTN: Donald R. Cotter

Director
Defense Advanced Research Project Agency
46044 ATTN: PMO
46047 Technical Library
46045 STO
46018 NMRO

Defense Documentation Center
12149 2 cy ATTN: TC/Mr. Meyer B. Kahn

Director
Defense Nuclear Agency
46753 ATTN: STSI, Archives
46884 DDST
46755 2 cy SPSS
46754 3 cy STTL, Technical Library

Chairman
Department of Defense Explosives Safety Board
46797 ATTN: Thomas Zaker

Director of Defense Research and Engineering
Type ATTN: Dep. Dir. Info. & Space Sys.
46717 Asst. Dir. Nuc. Prgms.
46718 Dep. Dir. Strat. Sys.

Commander
Field Command, Defense Nuclear Agency
40713 ATTN: FCPR
Type FCT

Chief
Livermore Division, Field Command DNA
30998 ATTN: FCPRL

DEPARTMENT OF THE ARMY

Assistant Chief of Staff for Ops. and Plans
Type ATTN: Technical Library

Office, Chief of Engineers
00041 ATTN: DAEN-MCE-D
Type 2 cy DAEN-RDM
00055 DAEN-RDL
00011 DAEN-ASI-L

Commander
Type ATTN: Rolland J. Tuttle

Commander
Harry Diamond Laboratories
Type ATTN: DRXDO-NP
Type Frank Wiesenitz, L. J. Belliveau
15758 Technical Library

Commander
U. S. Army Engineer School
12551 ATTN: ATSEN-SY-L

Division Engineer
U. S. Army Engineer Division, Ohio River
04767 ATTN: Technical Library/ORDAS-L

DEPARTMENT OF THE ARMY (Continued)

Commander
U. S. Army Nuclear Agency
Type ATTN: ATCA-NAW
17047 Technical Library

DEPARTMENT OF THE NAVY

Officer-in-Charge
Civil Engineering Laboratory
Type ATTN: R. J. Odello, Stan Takahashi
17528 Technical Library

Commander
Naval Surface Weapons Center
17880 ATTN: Code 240
17827 Code 1224, Navy Nuclear Programs Office
17890 241, J. Petes
17826 Code 730, Technical Library

Commander
Naval Surface Weapons Center
18107 ATTN: Technical Library

Commander
17524 ATTN: Technical Library/Code 533

Commanding Officer
Naval Weapons Evaluation Facility
17952 ATTN: R. Hughes
17951 Technical Library

DEPARTMENT OF THE AIR FORCE

Commander
AF Armament and Testing Laboratory, AFSC
19938 ATTN: Technical Library

Commander
AF Weapons Laboratory, AFSC,
Type ATTN: DED-I
Type DES-G
Type DE
Type DES-S
20260 SUL, Technical Library

Headquarters
Air Force Systems Command
Type ATTN: DLCAW
20705 Technical Library

Commander
Armament Development and Test Center
19931 ATTN: Technical Library/ADTC/DLODL

SAMSO/MN
Type ATTN: MNN, Engr. Division
19970 MNNH
Type MMI

ENERGY RESEARCH & DEVELOPMENT ADMINISTRATION

Director
Los Alamos Scientific Laboratory
Type ATTN: Technical Library

ENERGY RESEARCH & DEVELOPMENT ADMINISTRATION (Continued)

Sandia Laboratories
40715 ATTN: Technical Library

Sandia Laboratories
40718 ATTN: L. J. Vortman
Type Technical Library

Director
Lawrence Livermore Laboratory
30922 ATTN: Technical Library

OTHER GOVERNMENT AGENCIES

Department of the Interior
Type ATTN: Technical Library
Type Leonard A. Obert

DEPARTMENT OF DEFENSE CONTRACTORS

Aerospace Corporation
62502 ATTN: Technical Information Services

Agbabian Associates
62504 ATTN: M. Agbabian
Type M. B. Balachandra
Type J. A. Malthan

The Boeing Company
63011 ATTN: Technical Library

California Research and Technology, Inc.
63442 ATTN: Technical Library

EG&G, Inc., Albuquerque Division
64330 ATTN: Technical Library

Electromechanical Systems of New Mexico, Inc.
64361 ATTN: R. A. Shunk

General Electric Company
TEMPO-Center for Advanced Studies
65337 ATTN: DASIAC

J. L. Merritt
Consulting & Special Engr. Svs., Inc.
63443 ATTN: Technical Library

Kaman Sciences Corporation
67016 ATTN: Technical Library

DEPARTMENT OF DEFENSE CONTRACTORS (Continued)

University of Illinois
54069 ATTN: N. M. Newmark
54067 Prof. W. J. Hall

Physics International Company
Type ATTN: C. Godfrey
Type Coye Vincent, Dennis Orphal
69722 Technical Library
69704 Fred M. Sauer

R & D associates
70635 ATTN: C. P. Knowles
70603 Dr. Henry Cooper
70636 J. G. Lewis
70616 Technical Library

Science Applications, Inc.
Type ATTN: Mr. J. L. Bratton

Stanford Research Institute
71275 ATTN: G. Abrahamson
Type Technical Library
71282 Dr. Carl W. Smith

Systems, Science and Software, Inc.
71233 ATTN: Dr. Donald R. Grine
71217 Technical Library

Terra Tek, Inc.
71614 ATTN: Sidney J. Green
71646 Technical Library

TRW Defense and Space Systems Group
Type ATTN: Paul Lieberman
71647 Technical Info Center S-1930

Wang, The Eric H. Civil Engineering Research Facility
Type ATTN: Library

Weidlinger Associates, Consulting Engineers
72339 ATTN: Dr. J. Isenberg

Weidlinger Associates, Consulting Engineers
72303 ATTN: Dr. Melvin L. Baron

In accordance with letter from DAEN-RDC, DAEN-ASI dated 22 July 1977, Subject: Facsimile Catalog Cards for Laboratory Technical Publications, a facsimile catalog card in Library of Congress MARC format is reproduced below.

Ingram, James K
  Effects of instrument canister placement conditions on ground shock measurements / J. K. Ingram, M. B. Ford. Vicksburg, Miss. : U. S. Waterways Experiment Station, 1977.
  104 p. : ill. ; 27 cm. (Technical report - U. S. Army Engineer Waterways Experiment Station ; N-77-5)
  Work sponsored by the Defense Nuclear Agency under DNA Subtask L11CAXSX352, Work Unit 50.
  Prepared for Director, Defense Nuclear Agency, Washington, D. C.
  References: p. 64-65.

1. Backfills. 2. Ground shock measurement. 3. Measuring instruments. 4. Wave propagation. I. Ford, Max B., joint author. II. Defense Nuclear Agency. III. Series: United States. Waterways Experiment Station, Vicksburg, Miss. Technical report ; N-77-5.
TA7.W34 no.N-77-5